



**CRCLEME**

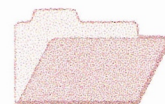
Cooperative Research Centre for  
Landscape Evolution & Mineral Exploration



**CSIRO**  
EXPLORATION  
AND MINING



Australian Mineral Industries Research Association Limited ACN 004 448 266



**OPEN FILE  
REPORT  
SERIES**

# **GEOCHEMICAL AND HYDROGEOCHEMICAL INVESTIGATIONS OF ALLUVIUM AT MULGARRIE, WESTERN AUSTRALIA**

*D.J. Gray*

**CRC LEME OPEN FILE REPORT 32**

September 1998

(CSIRO Division of Exploration Geoscience Report 339R, 1992.  
Second impression 1998)

CRC LEME is an unincorporated joint venture between The Australian National University, University of Canberra, Australian Geological Survey Organisation and CSIRO Exploration and Mining, established and supported under the Australian Government's Cooperative Research Centres Program.



# **GEOCHEMICAL AND HYDROGEOCHEMICAL INVESTIGATIONS OF ALLUVIUM AT MULGARRIE, WESTERN AUSTRALIA**

*D.J. Gray*

**CRC LEME OPEN FILE REPORT 32**

September 1998

(CSIRO Division of Exploration Geoscience Report 339R, 1992.  
Second impression 1998)

© CSIRO 1992

## RESEARCH ARISING FROM CSIRO/AMIRA REGOLITH GEOCHEMISTRY PROJECTS 1987-1993

In 1987, CSIRO commenced a series of multi-client research projects in regolith geology and geochemistry which were sponsored by companies in the Australian mining industry, through the Australian Mineral Industries Research Association Limited (AMIRA). The initial research program, "Exploration for concealed gold deposits, Yilgarn Block, Western Australia" (1987-1993) had the aim of developing improved geological, geochemical and geophysical methods for mineral exploration that would facilitate the location of blind, buried or deeply weathered gold deposits. The program included the following projects:

**P240: Laterite geochemistry for detecting concealed mineral deposits (1987-1991).** Leader: Dr R.E. Smith.  
Its scope was development of methods for sampling and interpretation of multi-element laterite geochemistry data and application of multi-element techniques to gold and polymetallic mineral exploration in weathered terrain. The project emphasised viewing laterite geochemical dispersion patterns in their regolith-landform context at local and district scales. It was supported by 30 companies.

**P241: Gold and associated elements in the regolith - dispersion processes and implications for exploration (1987-1991).** Leader: Dr C.R.M. Butt.

The project investigated the distribution of ore and indicator elements in the regolith. It included studies of the mineralogical and geochemical characteristics of weathered ore deposits and wall rocks, and the chemical controls on element dispersion and concentration during regolith evolution. This was to increase the effectiveness of geochemical exploration in weathered terrain through improved understanding of weathering processes. It was supported by 26 companies.

These projects represented "an opportunity for the mineral industry to participate in a multi-disciplinary program of geoscience research aimed at developing new geological, geochemical and geophysical methods for exploration in deeply weathered Archaean terrains". This initiative recognised the unique opportunities, created by exploration and open-cut mining, to conduct detailed studies of the weathered zone, with particular emphasis on the near-surface expression of gold mineralisation. The skills of existing and specially recruited research staff from the Floreat Park and North Ryde laboratories (of the then Divisions of Minerals and Geochemistry, and Mineral Physics and Mineralogy, subsequently Exploration Geoscience and later Exploration and Mining) were integrated to form a task force with expertise in geology, mineralogy, geochemistry and geophysics. Several staff participated in more than one project. Following completion of the original projects, two continuation projects were developed.

**P240A: Geochemical exploration in complex lateritic environments of the Yilgarn Craton, Western Australia (1991-1993).** Leaders: Drs R.E. Smith and R.R. Anand.

The approach of viewing geochemical dispersion within a well-controlled and well-understood regolith-landform and bedrock framework at detailed and district scales continued. In this extension, focus was particularly on areas of transported cover and on more complex lateritic environments typified by the Kalgoorlie regional study. This was supported by 17 companies.

**P241A: Gold and associated elements in the regolith - dispersion processes and implications for exploration.** Leader: Dr. C.R.M. Butt.

The significance of gold mobilisation under present-day conditions, particularly the important relationship with pedogenic carbonate, was investigated further. In addition, attention was focussed on the recognition of primary lithologies from their weathered equivalents. This project was supported by 14 companies.

Although the confidentiality periods of the research reports have expired, the last in December 1994, they have not been made public until now. Publishing the reports through the CRC LEME Report Series is seen as an appropriate means of doing this. By making available the results of the research and the authors' interpretations, it is hoped that the reports will provide source data for future research and be useful for teaching. CRC LEME acknowledges the Australian Mineral Industries Research Association and CSIRO Division of Exploration and Mining for authorisation to publish these reports. It is intended that publication of the reports will be a substantial additional factor in transferring technology to aid the Australian Mineral Industry.

This report (CRC LEME Open File Report 32) is a first revision of CSIRO, Division of Exploration Geoscience Restricted Report 339R, first issued in 1992, which formed part of the CSIRO/AMIRA Project P241A.

**Copies of this publication can be obtained from:**

The Publication Officer, CRC LEME, CSIRO Exploration and Mining, PMB, Wembley, WA 6014, Australia. Information on other publications in this series may be obtained from the above or from <http://leme.anu.edu.au/>

**Bibliographic reference:**

This publication should be referred to as Gray, D.J., 1998. Geochemical and hydrogeochemical investigations of alluvium at Mulgarrie, Western Australia. Open File Report 32, Cooperative Research Centre for Landscape Evolution and Mineral Exploration, Perth, Australia.

**Cataloguing-in-Publication:**

Gray, D.J.

Geochemical and hydrogeochemical investigations of alluvium at Mulgarrie, Western Australia

ISBN 0 642 28227 7

1. Geochemistry 2. Alluvium - Western Australia.

I. Title

CRC LEME Open File Report 32.

ISSN 1329-4768

## PREFACE

The continuation of AMIRA Project 241 (Gold and associated elements in the regolith - dispersion processes and implications for exploration) has as an objective further investigations of the geochemistry, surface expression and hydrogeochemistry of gold and the determination of characteristics useful for exploration for supergene and primary gold deposits.

Geochemical, chemical and hydrogeochemical investigations of the Mulgarrie study area detailed in this report have advanced our understanding of areas under transported overburden. Specifically, the study:

- (i) demonstrates the usefulness of geochemistry in determining boundaries between alluvium and basement and in determining the original lithology of highly weathered material;
- (ii) demonstrates that surface carbonates accumulate Au, possibly through tens of metres of barren alluvium;
- (iii) discusses a potentially critical role of Mn oxides in the mobility of Au in the regolith;
- (iv) shows that mineralized waters at Mulgarrie may have important similarities with mineralized waters at other sites;
- (v) supports previous work indicating a role for major and minor ion hydrogeochemistry in determining gross regional differences and in lithological discrimination;
- (vi) indicates that groundwaters at Mulgarrie are not transporting Au, and are not able to "see through" barren alluvium, unlike other sites, and offers reasons for this difference.

This study has sought to provide an integrated approach to understanding the characteristics of Au mobility and expression at this site, and the implications for exploration. As such, this investigation addresses many of the principal objectives of the Project.

C.R.M. Butt,  
Project Leader.  
December, 1992

## ABSTRACT

An integrated geochemical, chemical and hydrogeochemical survey of the Mulgarrie gold deposit was conducted by sampling RAB material, pit samples and groundwaters in the south-east margin of a palaeodrainage which overlies Au mineralization. The boundary between basement and alluvium is marked by decreased Mg, Zn, Ni and Au in the alluvium. Both basement and alluvium were identified as ultramafic by examining Ti/Zr and Cr/Fe ratios. Close to the surface, samples appeared to be depleted in Ti, relative to Zr, possibly due to organic acids dissolving Ti.

Elements associated with the surface carbonates are Au, which has been correlated with surface carbonates throughout the southern Yilgarn, and Th. These two metals are similar in that they are ordinarily highly insoluble but have enhanced mobilities in organic-rich horizons. Gold associated with carbonate is highly soluble and would be expected to have a high mobility in soil horizons. The soil enhancement could be caused by the metals been taken up by deeply rooting plants and then deposited on the soil surface.

There is a reduction in the magnitude of the surface Au anomaly from outcropping mineralization towards the middle of the drainage. This could be explained in terms of a lateral transport of Au, with dilution with distance, or by a upward movement of Au from the buried mineralization, with the magnitude of the soil Au anomaly being lesser with greater depth to mineralization. Iodide extraction has shown that surface Au close to the outcropping mineralization has a lower solubility than surface Au near the centre of the palaeodrainage (which has a similar extraction behaviour to Au in carbonate soils at other sites in the Yilgarn). Such distinctions may well be significant in understanding and utilizing exploration data.

Iron oxides control the geochemistry of a number of elements, particularly V, Cr, As and to a lesser extent, Sb, and Mn oxides have a critical role in the accumulation of Co, Ba and the REEs, and possibly Cu, Mg, Ca, Zn, Ni and S. In addition, Au in Mn-rich zones appears to be highly mobile, with only that Au which has been totally occluded by other phases being retained. Gold mobilized from such Mn-rich zones, either at Mulgarrie or at other sites, could be a source for secondary deposits.

Present-day groundwaters at this site are very unreactive, possibly because of low rates of sulphide oxidation. However, there are still several elements which have anomalous concentrations, due either to significant lithological enhancement (*e.g.*, Ni and Cr with ultramafics) or to enhancements related to mineralization (*e.g.*, Mn, Co, Ba, I and Ni), which are similar to groundwater enhancements observed at other sites. In addition, Mulgarrie groundwaters have specific depletions (K) or enrichments (Mg and  $\text{SO}_4^{2-}$ ) of some of the major ions, which vary at a regional level, and may be useful in distinguishing different lithological regions. These data suggest the potential usefulness of groundwaters at a regional, lithological and exploration scale.

At this site (contrary to observations elsewhere) groundwater geochemistry did not "see through" the alluvium. This may be a consequence of the low activity of the groundwater and/or the presence of adsorptive phases such as Mn and Fe oxides. Additionally, groundwater at Mulgarrie has very low concentrations of Au, probably due to the lack of a means for Au mobilization, which at other sites involves either acid/oxidizing conditions (Au chloride) or neutral sulphide weathering (Au thiosulphate). The Au contents of Mulgarrie groundwater would be classified as background at these other sites.

## TABLE OF CONTENTS

	Page No
1 INTRODUCTION .....	1
2 STUDY SITE AND METHODS .....	1
2.1 Site characteristics .....	1
2.2 Sampling and analysis .....	3
2.2.1 Alluvium and saprolite sampling .....	3
2.2.2 Iodide extraction .....	5
2.2.3 Water sampling .....	6
3 RESULTS AND DISCUSSION .....	6
3.1 Solid samples .....	6
3.1.1 Mineralogy .....	6
3.1.2 Lithological boundaries .....	8
3.1.3 Group 3 elements (Al, Ga, Sc) .....	9
3.1.4 Iron oxide related elements (Fe, V, Cr, As, Sb) .....	9
3.1.5 Manganese oxide related elements (Mn, S, Co, Ni, Cu, Zn, Y, Ba, rare earth elements) .....	9
3.1.6 Mica elements (K, Rb, Cs) .....	10
3.1.7 Evaporites (Na, Cl, Br) .....	10
3.1.8 Carbonate elements (Mg, Ca, Sr, Th) .....	11
3.1.9 Gold geochemistry .....	12
3.2 Iodide extractions of Mulgarrie samples .....	13
3.3 Hydrogeochemistry .....	16
3.3.1 Compilation of results .....	16
3.3.2 Acidity and oxidation potential .....	16
3.3.3 Major ion chemistry .....	18
3.3.4 Minor ion chemistry .....	20
3.3.5 Gold chemistry .....	23
3.3.6 Hydrogeochemical changes between Palm and Trial Pit .....	24
4 GENERAL DISCUSSION .....	26
4.1 Processes at Mulgarrie and comparisons with other Sites .....	26
4.2 Exploration implications .....	27
Acknowledgments .....	28
References .....	29
Appendices .....	32
Appendix 1: Geochemical Data .....	33
Appendix 2: X-ray Diffraction Data .....	43
Appendix 3: X-ray Diffraction of Sedimented Aggregates .....	44
Appendix 4: Correlation Coefficient Tables for Mulgarrie solids .....	53
Appendix 5: Mulgarrie Groundwater Data .....	66

## **1 INTRODUCTION**

This report describes the results of water and regolith sampling at Mulgarrie. Specific fields of interest are:

- (i) geochemical and mineralogical properties of alluvium and potential for exploration for buried mineralization;
- (ii) association of Au with carbonate in soils and its use for exploration;
- (iii) use of Au and other pathfinder elements in water as an exploration tool;
- (iv) what ions cause mobility of Au, and how these ions are influenced by groundwater chemistry and water-rock interactions;
- (v) further understanding of the chemical and geological factors influencing the chemistry of waters in the Yilgarn Block;
- (vi) development of techniques for analysis of groundwater data from mineralized areas;
- (vii) interaction with laboratory investigations and other site studies;

This work was compared with investigations of the geochemistry and hydrogeochemistry of other Au-rich areas in the Yilgarn Block. The results contribute to a compilation of data for mineralized and unmineralized regions in the Yilgarn Block. This compilation will advance our knowledge of groundwater characteristics, particularly in reference to the formation of geochemical haloes in the regolith and the use of groundwaters in exploration.

## **2 STUDY SITE AND METHODS**

### **2.1 Site characteristics**

The Mulgarrie gold deposit is located 40 km north of Kalgoorlie at longitude 121° 30'E and latitude 30° 22'S (Figure 1), with the area investigated primarily consisting of the Palm Pit, with outcropping Au mineralization, and the Trial Pit excavated into a palaeochannel about 200 m to the north-west (Figure 2). The site occurs within mafic and ultramafic rocks of the Mulgarrie - Gordons greenstone belt on the east side of a granitic batholith. The regional strike is north-west, dips are steeply east and metamorphic grade is lower greenschist facies. Locally, the stratigraphic succession consists of massive blocky tholeiitic basalts, overlain by a thinner pile of komatiites whose mineralogy is highly variable both laterally and vertically within the pile. South of Palm Pit, strong serpentinization of the ultramafic komatiites has occurred whereas the upper, more mafic, komatiites have been intensely carbonated.

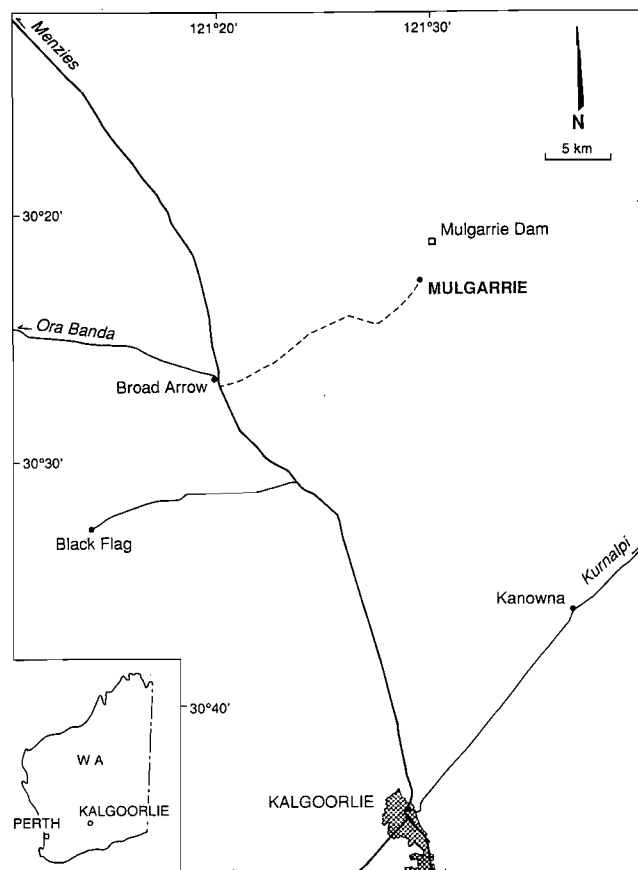


Figure 1: Regional map, showing location of the Mulgarrie study area.

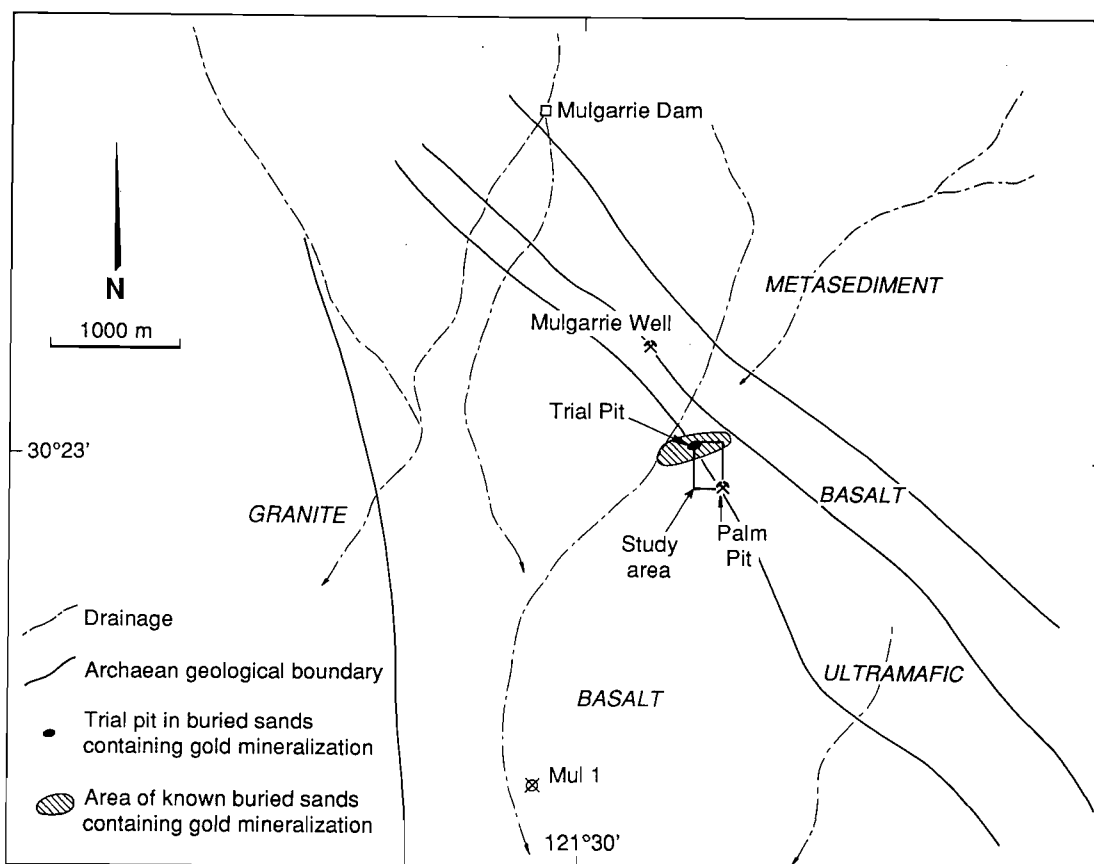


Figure 2: Regional geology, major drainage channels and mineralized zones at Mulgarrie.

At Palm Pit, high grade Au mineralization (5-100 ppm) is associated with quartz vein sets trending north-east and dipping between 40-70° north-west. The quartz sets consist of a high density of narrow, 1-10 cm subparallel quartz veins and stringers hosted by an intensely carbonated talcose ultramafic. Other quartz veins trending east and dipping subvertically are noted and are weakly mineralized. The host rock is also weakly mineralized, but Au levels rarely exceed 1 ppm.

The Trial Pit is located 200 m north-west of the Palm Pit. *In situ* weathered ultramafics are covered with about 35 m of drainage sediments. A diagrammatic pit section of the eastern face of the Trial Pit, as exposed in early 1991, is shown in Figure 3. The base of the transported cover consists of 3 - 4 m of permeable sand and conglomerate horizons, which is overlain with other, finer textured, materials. The alluvium appears to be lateritized, with various mottled and Fe-rich horizons. Of particular note is a black Mn-rich zone at 22 m. Gold is observed by Newcrest to be located within buried sands, in horizontal or sub-horizontal enrichment zones.

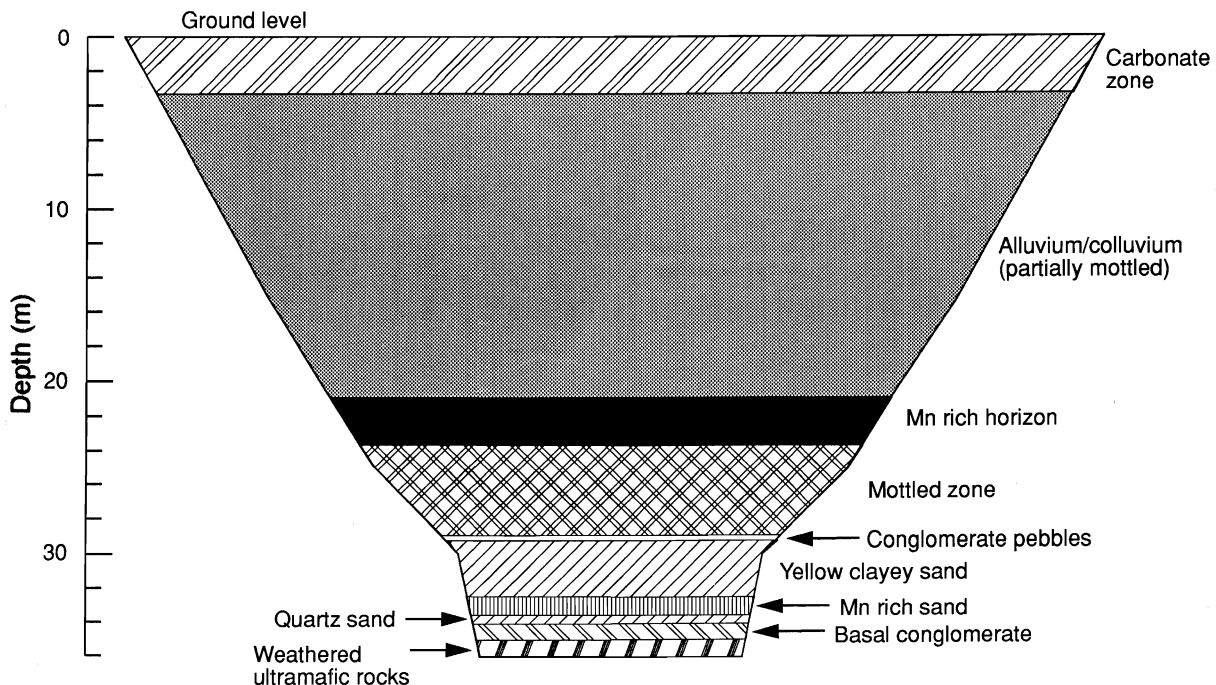


Figure 3: Diagrammatic Trial Pit Section - Eastern Face (at 10000m E).

The area has a semi-arid climate, with an annual rainfall of about 250 mm, most of which falls during the cooler months of May to August (Figure 4). However, there is a significant component of summer rainfall from erratic thunderstorms. Pan-evaporation, at 2700 mm, is well in excess of rainfall, leading to highly saline conditions due to evaporation of groundwater.

## 2.2 Sampling And Analysis

### 2.2.1 Alluvium and saprolite sampling

Solid samples were taken from RAB sample bags from drill holes MC500, MC505 and MC529 (Figure 5; filled circles). Additional samples were also taken for study, as listed in Table 1. The context of the sampling depth at the Trial Pit Eastern Face can be obtained from Figure 3.

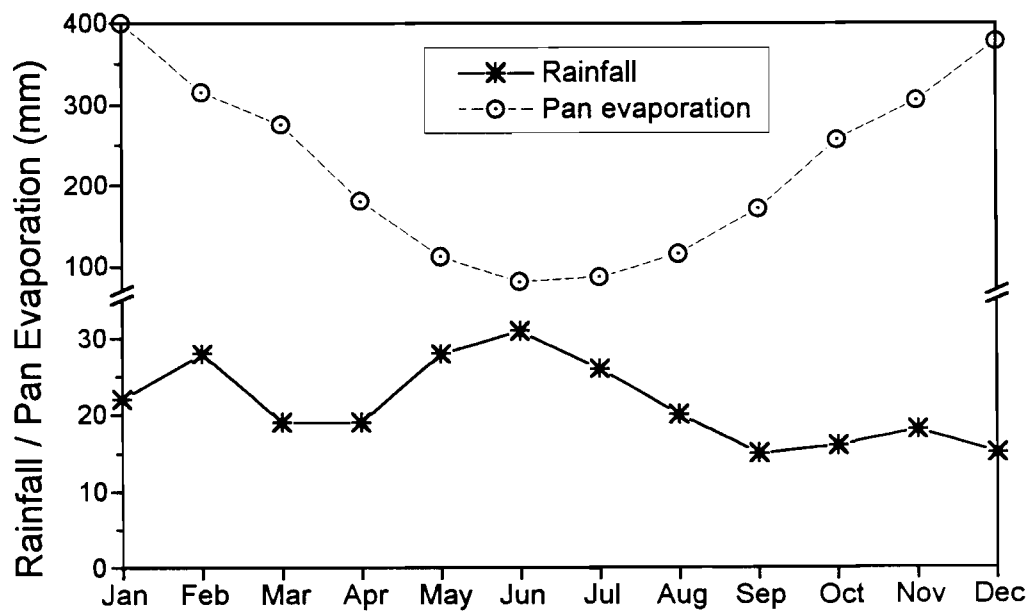


Figure 4: Average rainfall and pan-evaporation, as measured at Kalgoorlie.

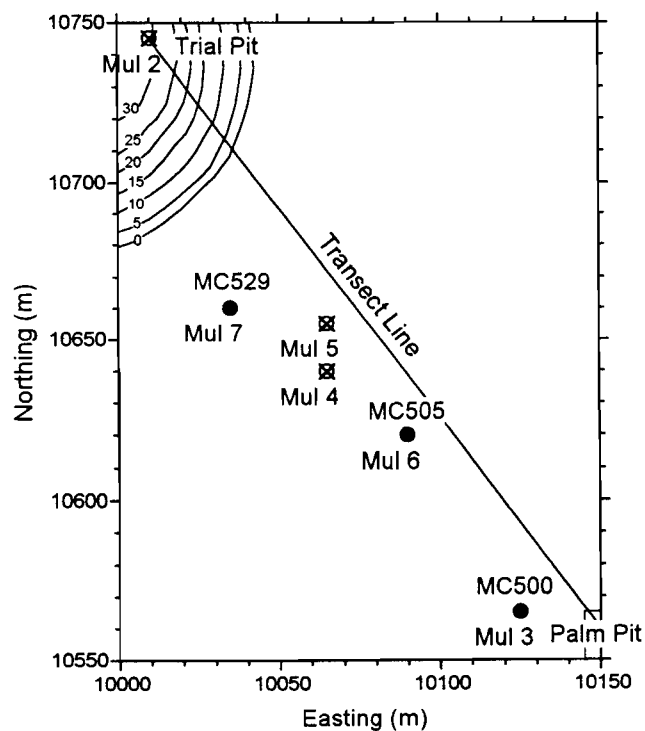


Figure 5: Location of sampled drill holes, with Trial Pit depth contours given in metres. All holes shown were sampled for groundwater, with the filled circles denoting drill holes used for alluvium sampling.

Samples were crushed to  $< 75 \mu\text{m}$  using a hardened steel mill. In addition, samples 04-4165 and 04-4167 were separated into 4 fractions: namely (A)  $> 2000 \mu\text{m}$ , (B)  $180 - 2000 \mu\text{m}$ , (C)  $20 - 180 \mu\text{m}$ , and (D)  $< 20 \mu\text{m}$  diameter, by a combination of sieving and sedimentation in water. These fractions were then crushed for analysis. Samples were analysed for Ag, As, Au, Br, Co, Cr, Cs, Eu, Hf, Ir, La, Lu, Mo, Sb, Sc, Se, Sm, Ta, Th, U and Yb by neutron activation analysis (NAA) and for  $\text{SiO}_2$ ,  $\text{Al}_2\text{O}_3$ ,  $\text{Fe}_2\text{O}_3$ , MnO, MgO, CaO,  $\text{Na}_2\text{O}$ ,  $\text{K}_2\text{O}$ ,  $\text{TiO}_2$ ,  $\text{P}_2\text{O}_5$ , Ba, Ce, Cl, Cu, Ga, Nb, Ni, Pb, Rb, S, Sr, V, Y, Zn and Zr by X-ray fluorescence (XRF). Selected samples were also analysed by random powder X-ray diffraction (XRD). The  $< 2 \mu\text{m}$  fractions of 6 samples (04-4003, 04-4075, 04-4133, 04-4137, 04-4166, 04-4184) were investigated by XRD, using material that was sedimented onto ceramic tiles (Appendix 3).

Table 1: Additional grab samples taken from the Mulgarrie study area.

Sample No.	Description
04-4159	Ultramafic rock sample
04-4160	Basalt rock sample
04-4161	Sheared basalt / ultramafic rock sample
04-4162	Basalt rock sample
04-4163	Manganiferrous horizon - taken from Trial Pit eastern face at 28 m depth
04-4164	Mn sand - taken from Trial Pit eastern face at 33 m depth
04-4165	Conglomerate - taken from Trial Pit eastern face at 34.5 m depth
04-4166	Weathered ultramafic - taken from Trial Pit eastern face at 36 m depth
04-4167	Thin conglomerate horizon - taken from Trial Pit eastern face at 29 m depth
04-4191	Crystalline calcite rich material
04-4192	Mn oxide cemented material
04-4193	Mn-rich material with calcrete
04-4194	Mn oxide rich sand
04-4195	Massive clay

### 2.2.2 Iodide extraction

The solution used for these extractions was 0.1 M potassium iodide / 1 M sodium hydrogen carbonate, saturated with  $\text{CO}_2$  via bubbling and taken to pH 7.4 with hydrochloric acid. The reagent was shaken with 25 g of sample (pulverized to  $< 75 \mu\text{m}$ ) for one day, at a soil:solution ratio of 1:2. Following this, the suspension was centrifuged (3000 revolutions per minute for 15 minutes) and the solution decanted and analysed for Au by ICP-MS. An additional experiment was conducted on the same sample sets, using the same reagent conditions, except that samples were as taken from the sample bags, without pulverization, in order to test for any inclusion effects. The two different sample types are denoted here as fine ( $< 75 \mu\text{m}$ ) and coarse (unpulverized).

### 2.2.3 Water sampling

Sampling was done in early 1991. Seven water samples were taken: Mul 1 was sampled along the major drainage approximately 2 km south of the Mulgarrie site (Figure 2), and Mul 2 - 7 were sampled between Palm Pit and the Trial Pit (Figure 5, crossed and filled circles), using a pump-sampler.

Waters were analysed for pH, temperature, conductivity, and oxidation potential (Eh) at the time of sampling. A 125 mL water sample was collected in a polyethylene bottle (with overfilling to remove all air) for later  $\text{HCO}_3^-$  analysis by alkalinity titration in the laboratory. About 2.5 L of water was filtered through a 0.45  $\mu\text{m}$  membrane filter in the field. About 100 mL of the filtered solution was acidified [0.1 mL 15 moles/litre (M) nitric acid ( $\text{HNO}_3$ )], and analysed for Na, Mg, Ca and K by Atomic Absorption Spectrometry and for Cu, Zn, Pb and Cd by Anodic Stripping Voltammetry, and for Co, Al, Fe, Mn, Ba, Cr, Ni, Sr and Si by Inductively Coupled Plasma - Atomic Emission Spectroscopy.

In addition, about 50 mL of the filtered water was collected separately, and analysed by Ion Chromatography, for  $\text{Cl}^-$ ,  $\text{Br}^-$  and  $\text{SO}_4^{2-}$ , using a DIONEX AS4A column under standard eluent conditions (Dionex, 1985) with a conductivity detector, and for  $\text{I}^-$  using a DIONEX AS5 column under standard eluent conditions with an electrochemical detector.

Two 1 L sub-samples of the filtered water were acidified with 1 mL 15 M  $\text{HNO}_3$  with addition of a one gram sachet of activated carbon. The bottles were rolled for eight days in the laboratory and the water then discarded. The carbon was then analysed for Sb and Au by NAA and for As by XRF. Laboratory investigations have indicated that using this pre-concentration system permits successful analyses of waters for these elements at low concentrations and high salinities. Calibration of the method was obtained by shaking standards of varying concentrations, and in varying salinities, with activated carbon.

The accuracies of the total analyses were confirmed by measuring the cation/anion balance (*i.e.*, total cationic charge less total anionic charge, all divided by total charge). The balances were better than 2%, indicating good analytical accuracy for the major elements.

## 3 RESULTS AND DISCUSSION

### 3.1 Solid samples

Geochemical data are listed in full in Appendix 1, with results for RAB holes MC500, MC505 and MC529 shown as a traverse between the Palm Pit and the Trial Pit (Figure 5) in Figures A1.1 - A1.20. The position of the unconformity between alluvium and the *in situ* Archaean basement (as based on company drill logs and assumed to be linear) is shown for MC505 and MC529. X-ray diffraction data are given in Appendix 2. Sedimented aggregate XRD was performed on selected < 2  $\mu\text{m}$  fractions, in order to facilitate identification, with results and interpretations given in Appendix 3. Correlation coefficient tables for particular data-sets are shown in Appendix 4.

#### 3.1.1 Mineralogy

The XRD results are listed in full in Appendix 3, with the significant minerals observed in drill holes MC500, MC505 and MC529 listed in Table 2. Secondary and resistant primary minerals such as kaolinite, and quartz are the major constituents of the deeper MC529 samples, matching the coarse

horizon observed at about 34 m in the eastern face of the Trial Pit (Figure 3), indicating deposition of conglomerate and sand at the base of the channel under quickly flowing conditions. This coarse zone has subsequently been overlain by finer material, though some additional thin conglomerate horizons are observed.

Table 2: Qualitative mineralogy of drill holes MC500, MC505 and MC529.

Profile	Depth (m)	Chlorite/Smectite	Talc	Mica	Quartz	Anatase - Rutile	Kaolin	Goe-thite	Hema-tite	Palygor-skite	Cal-cite	Dolo-mite	Magne-site
MC-500	0.5	?			X	XX	XX	XX	XXX	XX	XXX		
"	2.5	X		X	XX	X	XXX	XX	XXX		X	XXX	
"	4.5	?			XX	X	XXX	XXX				X	
"	17.5			XXX	XX	X	XXX	XX				X	
"	21.5			XXX	XXX	X	XXX	XXX					
"	24.5		XX	XXX	XXX	X	XXX	XX	?			XXX	
"	27.5	XX		XXX	XXX	X	XXX	XX				X	
"	31.5	XXX		XXX	XXX	X	XXX	XXX					
"	36.5	XXX		XXX	XXX	X		X	?				
"	38.5	XXX		XXX	XXX	X		X	X				
"	40.5	XXX		XX	XXX	X		X	X			X	
"	45.5	XXX		XXX	XX							XXX	XXX
MC-505	0.5	XX	X		XXX		XX	X	X		XXX	XX	
"	1.5	X	X		X		XX	X	X		X	XX	
"	2.5	X	XX		X		XXX	XX	XXX			X	
"	3.5	X	XX		X		XXX	XXX	X				
"	4.5	X	XX		X		XXX	XXX	XX				
"	14.5				XX	XX	XXX	XXX	XXX				
"	22.5			XX	XX	X	XXX	XXX	XXX		X		
"	30.5			XX	XX	XX	XXX	XXX	XX		X	X	
"	38.5	XXX		XXX	XXX	XX	?	XX	XX		X	X	
"	46.5	XXX		XX	XXX	X	?	XX				X	
MC-529	0.5	XXX	X		XX	XX	XXX	XX			XX	XXX	
"	1.5	XX	XX		XX		XX	X				XXX	
"	2.5	XX	XX		XX		XX	X				XXX	
"	3.5	XX	XX		XX		XXX	X	X	X		XX	X
"	4.5	XX	XX		XX		XXX	X	XX	XX			XXX
"	8.5		XXX		X		XXX	XXX	XX				X
"	14.5				XX		XXX	XXX	XXX				
"	20.5				XX		XXX	XXX	XX				
"	26.5				X		XXXX	XX					
"	28.5			XXX	X		XXXX	XXX					
"	30.5				XX		XXX	XXX					
"	34.5				XXX		XXX	XXX				X	
"	40.5				XXX		XXXX	X				X	

#### Key

- ? Presence uncertain (due to interference from other reflections)  
X Trace  
XX Minor  
XXX Major  
XXXX Dominant

Significant amounts of weatherable minerals such as talc, chlorite and magnesite, which are presumably of primary origin, are observed close to the surface in both MC505 and MC529. Given the highly weatherable nature of magnesite in particular, this may derive from recent physical transport of rock fragments onto the palaeochannel surface.

### 3.1.2 Lithological Boundaries

Significant increases in Mg (Figure A1.3), Zn, Ni (Figure A1.11), and Au (Figure A1.21) occur at or below the observed unconformity between the alluvium and Archaean bedrock. With the exception of the sand/conglomerate layer at the base of the drainage (see below), the alluvium is geochemically and mineralogically (Appendices 1 and 2) similar to the weathered Archaean basement, with the minor differences representing weathering changes, or spatial heterogeneity. In particular, the overlying alluvium commonly contains less than 50 ppb Au, and is effectively a barren cover over the mineralized Archaean.

The high Cr and Ni contents (Appendix 1; Figures A1.9 and A1.11) indicate that both the basement and the alluvial clays are ultramafic in origin. The Ni concentration increases with depth, suggesting that it is being depleted during weathering or was originally less abundant in the alluvium than in the basement, whereas Cr is strongly correlated with Fe (Appendix 4), indicating that Cr is associated with Fe in the weathered material. Chromium abundances, along with Zr/Ti ratios are used to distinguish various rock types (Hallberg, 1984). This methodology is used here, except that Cr/Fe ratios are used rather than Cr, in order to correct for the effect on Fe oxide content. Plotting Cr/Fe vs. Zr/Ti (Figure 6) indicates that virtually all of the basement and alluvium samples plot in the ultramafic field. The one major exception is MC529 28.5m, near the base of the alluvium, which is lower in Cr and Ni and higher in K, Rb, Ba, Sr and Th (Appendix 1C), with a high mica content (Appendix 2). This sample is presumably indicative of coarse material deposited at the base of the palaeodrainage under higher flow conditions than those of the present day.

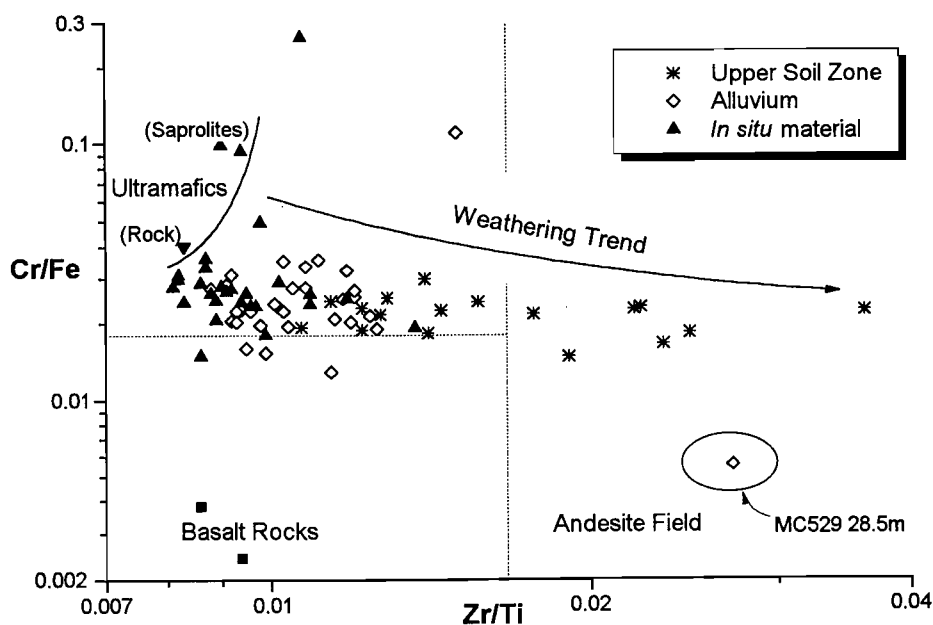


Figure 6: Cr/Fe vs. Zr/Ti for Mulgarrie Samples.

The basement material and the lower alluvium show similar Zr/Ti ratios. However, the soils of the top 5 m are strongly depleted in Ti relative to Zr (Figure 6 - Upper Soil Zone samples). This is possibly due to weathering, and in particular, to the effect of organic acids dissolving Ti (Bonneau and Souchier,

1982) during humid conditions, and has been observed in some other profiles in the Yilgarn (Robertson, 1991).

Thus, the geochemical and mineralogical data are consistent with the following sequence:

- (i) incision of the channel;
- (ii) rapid sedimentation of coarse material at the base of the channel, followed by slower deposition of finer sediments;
- (iii) deep weathering, with continuing slow sedimentation;
- (iv) erosion, with dispersion of chlorite and magnesite from rocks onto the surface of the channel;
- (v) precipitation of Mn in specific channel horizons.

The final two processes are possibly contemporaneous and may still be continuing.

### 3.1.3 Group 3 elements (Al, Ga, Sc)

The highest Al contents generally occur between 5 and 30 m depth (Figure A1.1), broadly reflecting the kaolinite distribution (Appendix 2). Gallium (Figure A1.16) has, as expected, a similar distribution to Al and the two elements are highly correlated (Appendix 4). Scandium (Figure A1.8), like Al, occurs as a 3+ ion, though with a significantly higher ionic radius (81 pm compared with 51 pm for  $\text{Al}^{3+}$  and 62 pm for  $\text{Ga}^{3+}$ ), and shows correlations (Appendix 4) both with Al and with Fe (ionic radius of  $\text{Fe}^{3+}$  is 64 pm), suggesting that Sc distribution may be controlled by both Al and Fe minerals.

### 3.1.4 Iron oxide related elements (Fe, V, Cr, As, Sb)

Iron oxides are a major constituent of the Mulgarrie samples, with  $\text{Fe}_2\text{O}_3$  contents at this site up to 42% (Figure A1.2). Iron is strongly correlated with V (Figure A1.9), moderately correlated with Cr (Figure A1.9) and As (Figure A1.16), and more weakly correlated with Sb (Figure A1.18; Appendix 4). Iron does not correlate with the other base metals Co, Ni, Cu and Zn (Figures A1.10 and A1.11).

### 3.1.5 Manganese oxide related elements (Mn, S, Co, Ni, Cu, Zn, Y, Ba, rare earth elements)

Based on observations of drill core, separate phase manganese oxides (hereafter abbreviated as Mn oxides) occur at about 20 - 30 m depth in the north-east part of the study area (Figure 5). These Mn oxides are observed in MC500 (Figure A1.2) and on the eastern face of the Trial Pit (Figure 3), but not in MC505 and MC529, and may be related the large concentrations of Mn being released from the *in situ* mineralized material, and then precipitated as Mn oxide minerals (Section 3.3.6; Table 5). Mn oxides have accumulated Co, Cu, La, Ce, Sm, Eu, Yb, La, Ba and Y (Figures A1.10, A1.12 - A1.15) and possibly Mg, Ca (Figure A1.3), Zn, Ni (Figure A1.11) and S (Figure A1.6). There are some differences in the mode of the correlation of these elements with Mn. Cobalt, La, Ce and Ba tend to be observed in the Mn oxides in MC500 and are very low elsewhere, whereas the other elements are concentrated with Mn in MC500, but have significant concentrations in the other profiles. Two possible explanations for this observations are that:

- (i) Co, La, Ce and Ba are all released into solution with Mn during weathering, and are co-precipitated in the Mn oxides;

and/or

- (ii) Co, La, Ce and Ba are generally highly mobile in this environment, and are fixed from solution only by the presence of Mn oxides.

The rare earth elements (REE) show systematic changes in their geochemical behaviour going across the Periodic Table. The light REEs La and Ce (Figure A1.12) show very strong accumulations in the Mn oxides in MC500, with low concentrations in the other drill holes; the heavy REEs Yb and Lu (Figure A1.14) show only weak concentration in the Mn oxides and similar abundances in the other holes; and the mid-range REEs Sm and Eu (Figure A1.13) show intermediate behaviour.

Such changes in REE behaviour are generally related to the lanthanide contraction, whereby the heavier REEs have progressively smaller ionic radii and therefore changes in chemistry. Yttrium, which has a similar ionic radii to the heavy REEs, also has a similar geochemical distribution (Figure A1.15). However, on ionic radii grounds, the heavier REEs would be expected to have a greater affinity for Mn oxides than the light REEs, rather than the converse, as observed here. It may be that the lesser accumulation of the heavy REEs in Mn oxides may represent a greater tendency to occur in resistate minerals and therefore not dispersed into secondary phases. Indeed, with the exception of the modest accumulation in the Mn oxide zone in MC500, the distributions of Yb, Lu and Y (Figures A1.14 and A1.15) are similar to those of Zr and Hf (Figure A1.20).

These results are also consistent with groundwater investigations in an area south of New Celebration, which showed that high concentrations of light REEs (in both absolute terms, and in terms of the expected ratios to the heavy REE concentrations) were dissolved in mineralized waters.

#### 3.1.6 Mica elements (K, Rb, Cs)

Potassium is generally found in micas, and in these profiles K distribution (Appendix 1; Figure A1.4) matches the observed mica abundances (Appendix 2). Rubidium (Figure A1.5) is highly correlated with K (Appendix 4), with the weaker Cs correlation presumably a function of the Cs concentrations being below detection for a number of samples.

There is a minor enrichment of K in the upper soil, which matches that of the carbonates (Section 3.1.8). This is consistent with chemical investigations of soils at Mt. Hope in the southern Yilgarn (Gray *et al.*, 1990), which indicated that carbonates in soils were commonly K-rich.

#### 3.1.7 Evaporites (Na, Cl, Br)

The saline groundwater observed here (Section 3.3) is enriched in ions of high solubility, such as Na, Cl, Br and S (as  $\text{SO}_4^{2-}$ ), which will cause measured enrichment of these elements in samples which had significant water contents, as the samples were oven-dried for geochemical analysis. For the solid samples tested from Mulgarrie, Na and Cl are correlated to a 99.9% significance level (Appendix 4A), consistent with precipitation of these elements as halite (NaCl). However, the correlation between Na or Cl with Br (Appendix 4) is much weaker, despite the high correlation between these elements in the groundwater (Section 3.3). This appears to be due to the presence of Br in the ultramafic material itself. This is demonstrated in Figure 7, in which the Br and Cl data for the solid samples could be modelled by assuming mixing of a solid material containing 4 mg/kg Br and 200 mg/kg Cl (*i.e.*, with 7 times more Br, relative to Cl, in the solid compared to the groundwater; Section 3.3) with evaporated groundwater. *I.e.*, samples with low Cl concentrations, which therefore had smaller amounts of

groundwater evaporated on the solid, the Cl/Br ratio decreases from that of the groundwater (about 290) to that of the original solid (about 50). The implication of this observation is that at this site, and presumably elsewhere, Br contents cannot be used as an indicator of water-rich materials (such as clays) due to high background concentrations in some rocks, and Na (assuming absence of feldspars or other Na-containing minerals) or Cl should be used for this purpose.

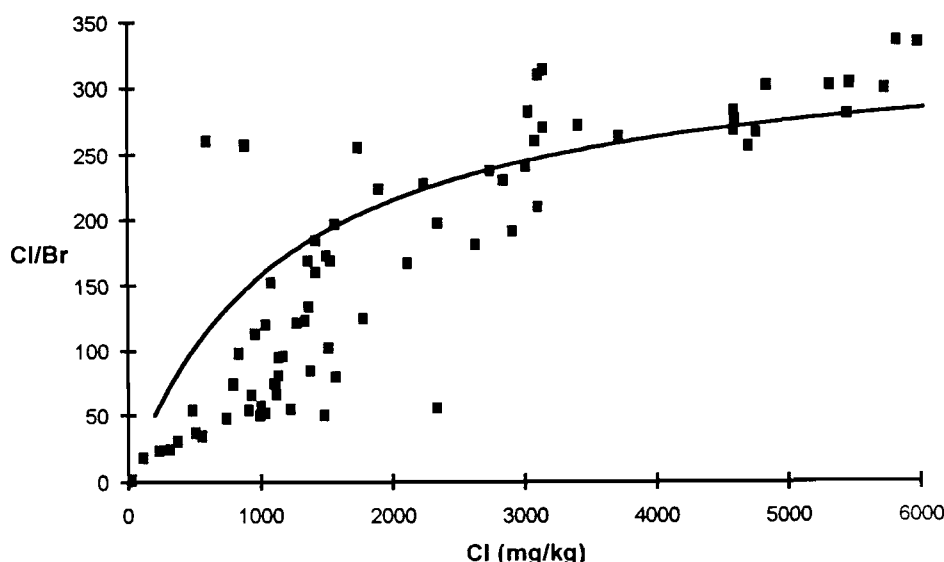


Figure 7: Cl/Br vs. Cl for Mulgarrie solid samples, with a mixing line calculated by assuming mixing between groundwater (composition as given in Appendix 5) and solid material with 4 mg/kg Br and 200 mg/kg Cl.

### 3.1.8 Carbonate elements (Mg, Ca, Sr, Th)

The enrichment of Ca in the top 5 m of the Mulgarrie alluvium is similar to that observed throughout the southern Yilgarn (Lintern, 1989; Scott, 1989; Lintern *et al.*, 1990; Lintern and Scott, 1990; Butt, 1991; Lintern and Butt, 1991, 1992), and represents accumulation of secondary carbonates such as calcite ( $\text{CaCO}_3$ ) or dolomite [ $\text{CaMg}(\text{CO}_3)_2$ ] during the present arid period. At this site, the high Mg abundances at surface, particularly in MC529 (Figure A1.3), in which magnesite ( $\text{MgCO}_3$ ) was observed within 2 m of the surface (Appendix 2), probably represent an additional contribution of Mg eroded from the ultramafic outcrop upslope (Section 3.1.1). This is corroborated by the poor correlation between Ca and Mg, even when only the top 5 m samples were used (Appendix 4B), in comparison with other sites in which Ca and Mg distributions in soil profiles were very similar (Lintern, 1989; Lintern and Scott, 1990).

As expected, Sr was also highly correlated with Ca, and the two ions are presumably co-precipitated. More surprising is the correlation of the alkaline earth ions with Th (Appendix 4A), due to an enrichment of Th in the surface zone matching the zone of high Ca, Mg and Sr (Figures A1.3 and A1.17). Under most conditions Th is highly insoluble (Langmuir and Herman, 1980). However, various workers (Hansen and Stout, 1968; Hansen and Huntington, 1969; Rubtsov, 1972; Miekeley *et al.*, 1985) have demonstrated that Th may be mobilized in organic-rich soil horizons via Th-organic complexes. This mechanism could lead to Th been mobilized by organic ligands and then precipitated

with Ca and Mg carbonates in evaporitic zones, in a similar manner to that postulated for Au (Gray *et al.*, 1990; Section 3.1.9).

### 3.1.9 Gold geochemistry

Plots of Au and CaO abundances (shown separately in Figures A1.3 and A1.21) are repeated in Figure 8, in which a lower scale is used for Au, in order to discuss specific geochemical effects. Data for MC505 and MC529 indicate major Au enrichment in the basement, but with an essentially barren alluvial cover (Figure 8). This is possibly because the alluvium was primarily deposited in the direction of the drainage flow: *i.e.*, from north-east of the study area (Figure 2). The alluvial cover in MC500 has higher concentrations of Au than MC505 and MC529, possibly due to the close proximity to out-cropping mineralization at Palm (Figure 5).

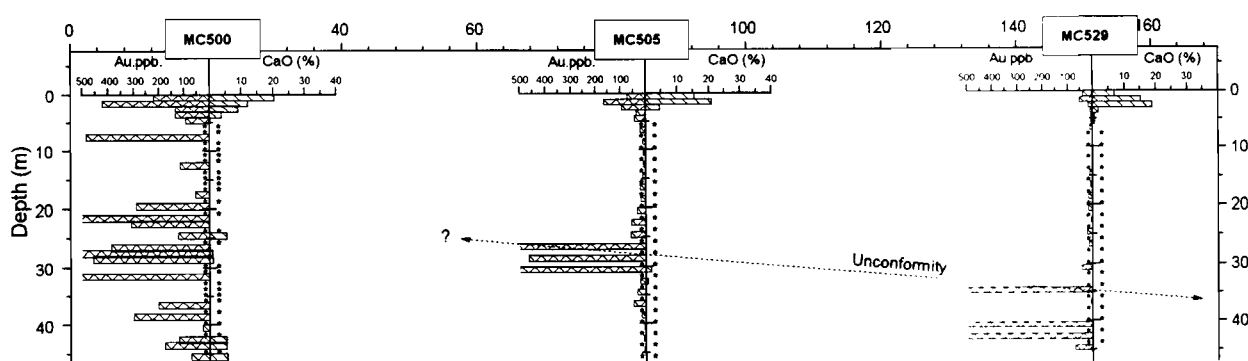


Figure 8: Au and CaO for section from Palm to Trial pits.

Mulgarrie was initially considered to be of interest due to a suggested correlation of Au with Mn oxides. However, it was later indicated that this association occurred in only about 10% of the ore material, and therefore could be wholly coincidental. No significant correlations were observed between Au and Mn for MC500 (Appendix 4) and geochemical data for Mn-rich samples 04-4163, 04-4164, 04-4192, 04-4193 and 04-4194 indicated that none of these samples contained high levels of Au (Appendix 1D). Thus, the elemental composition data available in this report do not indicate any Au - Mn association. However, extraction work (Section 3.2) does indicate that Mn oxides may play a significant role in the mobilization of Au, though not in a manner that would cause elemental correlations.

Whereas the alluvial cover in holes MC500, MC505 and MC529 is generally barren, there is a clear concentration of Au in the uppermost 5 m, closely correlated with the Ca and Mg rich carbonate layer (Figure 8). Such associations of Au with carbonate is ubiquitous throughout the southern Yilgarn (Lintern, 1989; Lintern and Scott, 1990; Butt, 1991; Lintern and Butt, 1991, 1992), and continues to be studied as part of AMIRA Project 241A due to its exploration significance. In the case of these holes, the Au anomaly occurs over barren cover, and decreases in magnitude across the transect from MC500 to MC529 (Figure 8). The Au could have travelled either laterally from Palm (Figure 9a) or upwards from the underlying basement (Figure 9b). In terms of our present understanding of the processes of Au - carbonate association, the later postulate seems more likely, but cannot be proved at this site.

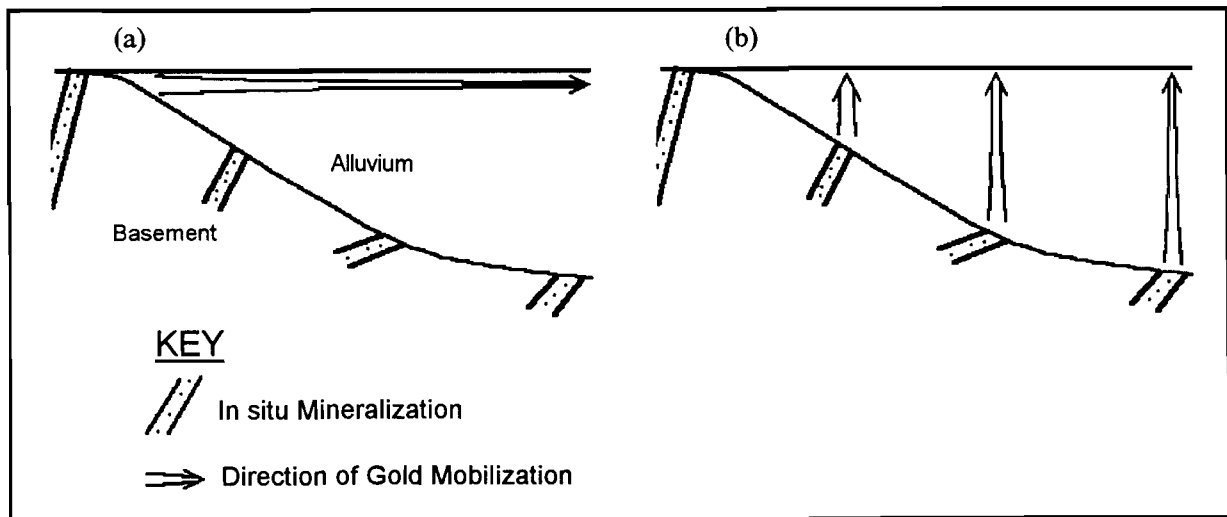


Figure 9: Model of two potential modes for mobilization and secondary precipitation of Au: (a) via horizontal (chemical and/or physical) transport from Palm outcrop, with diminution of secondary Au concentration with distance; and (b) via upward (chemical) transport, with diminution of secondary Au concentration with increasing depth to the primary mineralization.

The, Au is clearly associated with carbonate at this site, and this Au-carbonate anomaly occurs over buried mineralization. However, the presence of outcropping Au mineralization at Palm prevents an unambiguous interpretation of the mechanism for the formation of this anomaly

### 3.2 Iodide extractions of Mulgarrie samples

Iodide extractions were performed on samples from the three different drill holes, and on two of the Pit samples, with results given in Table 3. The two different sample types are denoted here as fine ( $< 75 \mu\text{m}$ ) and coarse (unpulverized). Between 20 and 60 % of the Au from the upper zone in MC529 was extracted from both coarse and fine samples, indicating that much of the Au in this zone is highly mobile and that the entire anomaly at the surface is in dynamic equilibrium with soil and biological phases. This is similar to a number of other sites south of the Menzies line, for which it was observed that about 30% of the Au could be dissolved from carbonate-rich soils.

In contrast, less than 15 % of the total Au was extracted from the upper carbonate-rich zone of MC500, consistent with the soil in that area being close to the Palm outcrop (Figure 5) and therefore likely to be enriched in primary (and poorly extractable) Au via mechanical transport.

Below the surface carbonate zone, Au has a low extractability (Table 3), consistent with observations at other sites. The major exception is a zone at about 22 - 25 m in MC500 (Figure 10a), where up to 37 % of the Au in the coarse material and 93 % of the Au (*i.e.*, virtually total extraction) in the fine material was dissolved. This zone of high Au extractability closely corresponds to the Mn oxide zone (Figure 10b), indicating that Au is highly soluble when present with Mn oxides. This hypothesis is also supported by the extraction results for the Mn horizon sample from the pit wall (04-4163; Table 3), for which 77 % of the total Au was extracted from the fine fraction.

Table 3: Iodide Extraction of Mulgarrie Samples.

Sample	Origin	Depth (m)	Fe <sub>2</sub> O <sub>3</sub> (%)	MnO (%)	MgO (%)	CaO (%)	Gold (µg/kg)	Gold extracted		Extracted/Total	
								Coarse	Fine	Coarse	Fine
04-4001	MC500	0.5	24.51	0.05	1.54	20.43	219	10	18	0.05	0.08
04-4002	"	1.5	20.80	0.03	5.62	11.92	423	18	16	0.04	0.04
04-4003	"	2.5	31.72	0.01	6.35	8.82	135	22	6	0.16	0.04
04-4004	"	3.5	24.69	0.01	3.37	3.49	135	16	8	0.12	0.06
04-4005	"	4.5	29.18	0.01	1.07	0.27	95	12	4	0.13	0.04
04-4017	"	7.5	38.91	0.02	0.57	0.02	486	10	12	0.02	0.02
04-4018	"	12.5	17.11	0.02	0.39	0.01	117	<2	4	0.00	0.03
04-4019	"	17.5	18.61	0.04	0.53	0.01	54	10	<2	0.18	0.00
04-4020	"	19.5	14.04	0.03	0.56	0.02	288	2	4	0.01	0.01
04-4021	"	21.5	13.73	0.09	0.50	0.02	3260	<2	40	0.00	0.01
04-4022	"	22.5	13.71	0.94	0.46	0.02	308	62	158	0.20	0.51
04-4023	"	24.5	12.27	3.60	3.98	5.09	125	46	116	0.37	0.93
04-4024	"	26.5	13.65	1.22	1.49	0.07	386	84	28	0.22	0.07
04-4025	"	27.5	13.77	0.46	1.62	0.58	1010	14	4	0.01	0.00
04-4026	"	28.5	10.93	0.98	1.95	1.00	458	14	<2	0.03	0.00
04-4027	"	31.5	19.58	0.32	2.73	0.23	4640	134	36	0.03	0.01
04-4028	"	36.5	15.41	0.34	5.18	0.06	204	52	4	0.25	0.02
04-4029	"	38.5	13.52	0.18	4.36	0.05	299	44	4	0.15	0.01
04-4030	"	40.5	13.02	0.23	6.68	0.08	29	7	<2	0.25	0.00
04-4031	"	42.5	10.27	0.17	15.96	5.22	121	<2	<2	0.00	0.00
04-4032	"	43.5	9.79	0.16	15.28	5.27	178	<2	<2	0.00	0.00
04-4033	"	45.5	9.04	0.15	15.36	5.35	73	<2	<2	0.00	0.00
04-4176	MC505	22.5	26.66	0.01	0.30	0.02	57	<2	<2	0.00	0.00
04-4177	"	24.5	30.29	0.01	0.29	0.02	61	6	6	0.10	0.10
04-4178	"	26.5	28.08	0.01	0.25	0.03	1290	4	8	0.00	0.01
04-4179	"	28.5	29.63	0.02	0.28	0.05	467	2	6	0.00	0.01
04-4180	"	30.5	26.73	0.03	1.42	1.64	4480	152	58	0.03	0.01
04-4133	MC529	0.5	13.21	0.32	6.78	6.69	42	14	10	0.34	0.24
04-4134	"	1.5	8.31	0.10	11.64	15.06	55	32	20	0.58	0.36
04-4135	"	2.5	6.05	0.07	15.44	18.76	19	6	6	0.32	0.32
04-4136	"	3.5	6.34	0.10	31.13	1.64	11	2	6	0.18	0.54
04-4137	"	4.5	15.41	0.19	18.63	0.50	8	<2	2	0.00	0.25
04-4153	"	34.5	22.00	0.01	0.31	0.05	642	<2	<2	0.00	0.00
04-4156	"	40.5	2.28	0.01	0.39	0.05	6540	40	34	0.01	0.01
04-4157	"	42.5	15.61	0.02	2.49	0.07	2130	8	6	0.00	0.00
04-4158	"	44.5	18.11	0.05	3.74	0.06	72	<2	<2	0.00	0.00
04-4163	Mn-rich Horizon	28	27.66	8.39	6.55	9.16	117	8	90	0.07	0.77
04-4166	Ultramafic Clay	36	8.20	0.03	16.23	0.04	6260	24	30	0.00	0.00

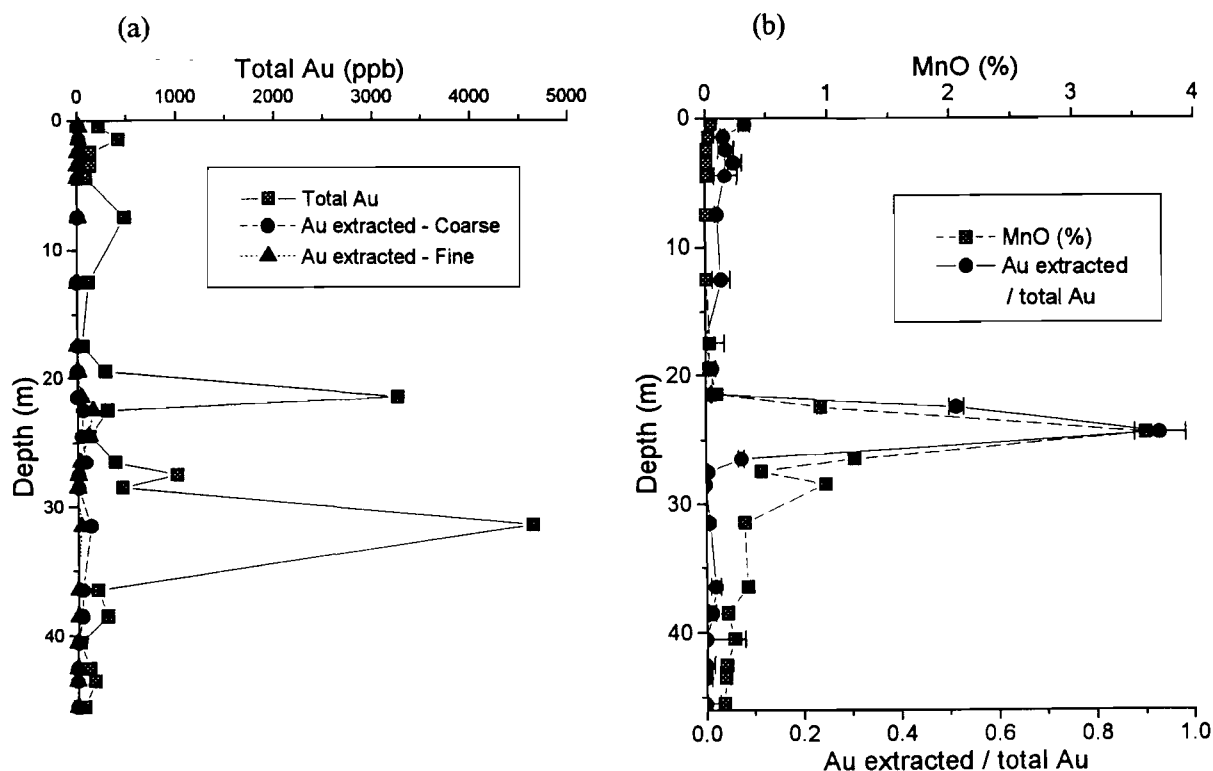


Figure 10: Iodide extraction results for MC500: (a) Total Au and Au extracted from coarse and fine samples; and (b) MnO (%) and proportion Au extracted from fine samples.

The extraction of Au from sample 04-4023 (the most Mn rich sample in Figure 10b) was further investigated by testing the proportion extracted over time (Figure 11). When the sample was pulverized to  $< 75 \mu\text{m}$  (fine), extraction was rapid, with about 90% of the total Au extracted within 1 day. For the coarse samples the extraction occurred at a similar rate, but less than half was extracted, even after 32 days. This indicates that the Au in this Mn-rich sample is highly soluble, but is (at least) partially occluded and therefore only partially dissolved from the unpulverized sample. It is possible that *in situ*, all of the Au is occluded and therefore would not be extractable. Indeed, given the high solubility of Au in this zone, any Au that was not occluded might be expected to have been leached from the Mn oxide zone by percolating groundwater.

This Mn oxide zone may represent an horizon with specific controls over Au mobility and therefore on the formation of secondary Au anomalies. Laboratory studies (summarized in Gray, 1988 - Section 4.3) have indicated a significant role for Mn oxides in raising the oxidation potential (Eh) of a system and therefore the solubility of native Au. Hydrogeochemical studies at Panglo gold deposit have supported this suggestion (Gray, 1990). Therefore, Au in contact with free Mn oxides could be expected to be oxidized and be highly solubility, as observed here, and be transported in groundwater, until being precipitated under changed solution conditions. Work is ongoing to test this hypothesis, and to investigate its exploration significance. If this is the case, then Au would not be expected to show a simple correlation with Mn. However, the presence of Mn oxides would be an important first stage for the formation of secondary deposits of Au, as they would enable the initial Au mobilization.

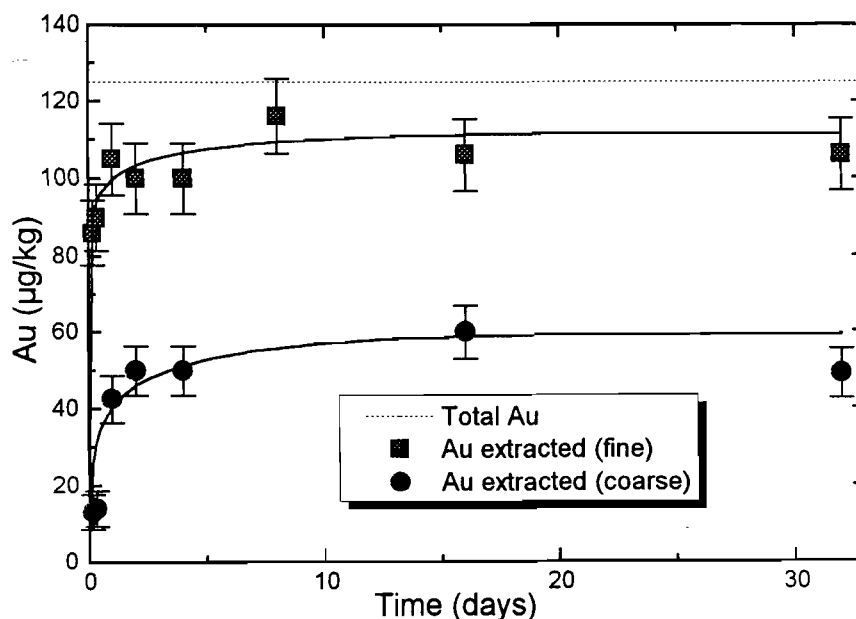


Figure 11: Gold extracted by iodide vs. time for fine and coarse samples of 04-4023.

### 3.3 Hydrogeochemistry

#### 3.3.1 Compilation of results

Elemental data for the seven samples are listed in Appendix 5, and mean compositions given in Table 4. Note that Mul 1 was sampled from about 2 km south of the Palm and Trial pits (Figure 2), under very different groundwater conditions, and is discussed separately from Mul 2 - 7. The total dissolved solids (TDS), a measure of groundwater salinity, were calculated from the major element contents. Also listed in Table 4 are data for sea water (taken from Weast *et al.*, 1984) and the averaged data for four other sites previously investigated:

- (i) Bakers Hill, a non-mineralized area which lies some 50 km east of the western edge of the Yilgarn Block;
- (ii) Boags, a gold deposit at Bottle Creek, located 210 km north north-west of Kalgoorlie (central Yilgarn; Gray, 1992);
- (iii) Mount Gibson, a gold deposit about 100 km north-east of Dalwallinu (central-west Yilgarn; Gray, 1991);
- (iv) Panglo, a gold deposit some 30 km north of Kalgoorlie (south Yilgarn; Gray, 1990).

#### 3.3.2 Acidity and oxidation potential

An Eh-pH plot of waters from Mulgarrie and other sites is shown in Figure 12. Samples Mul 2 - 7 are near neutrality, consistent with previous results for waters in contact with ultramafic lithologies, and have relatively low Eh values (Gray, 1990). Waters from Mount Gibson and Panglo that plot in the same Eh/pH zone were sampled at depth and are generally Fe rich. Soluble Fe is commonly derived from the first stage of the oxidation of pyrite and other sulphide minerals:

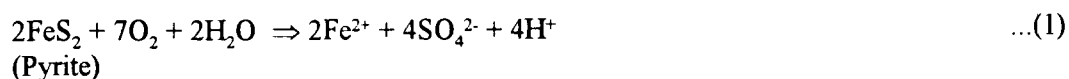


Table 4: Averaged elemental compositions of Mulgarrie waters, with results from other sites given for comparison.

Sample	Mul 1	Mul 2 - 7 (6) #		Bakers Hill (3)		Boags (2)		Mt. Gibson (50)		Panglo (50)		Sea water
		Mean	Sd Dv@	Mean	Sd Dv	Mean	Sd Dv	Mean	Sd Dv	Mean	Sd Dv	
pH	3.5	6.8	0.5	4.7	0.8	6.6	0.03	6.5	0.7	4.9	1.2	nd
Eh (mV)	325	180	50	300	50	160	30	310	100	490	180	nd
Na *	0.29	0.29	0.003	0.28	0.01	0.25	0.001	0.32	0.02	0.32	0.01	0.31
Mg *	0.054	0.052	0.001	0.057	0.002	0.052	0.002	0.033	0.007	0.032	0.003	0.040
Ca *	0.005	0.012	0.001	0.020	0.004	0.032	0.001	0.009	0.010	0.008	0.003	0.012
K *	0.0032	0.0041	0.0004	0.0030	0.0002	0.0092	0.0001	0.0112	0.0018	0.0008	0.0003	0.0112
Cl <sup>-</sup> *	0.56	0.54	0.01	0.60	0.01	0.47	0.004	0.53	0.03	0.59	0.01	0.56
SO <sub>4</sub> <sup>2-</sup> *	0.088	0.103	0.003	0.045	0.001	0.172	0.002	0.075	0.016	0.053	0.005	0.065
Br *	0.0015	0.0016	0.0001	0.0016	0.0001	0.0024	0.0000	0.0017	0.0002	0.0005	0.0001	0.0019
HCO <sub>3</sub> <sup>-</sup>	<1	398	52	nd	nd	620	50	260	240	50	60	142
TDS	46100	41800	2100	8100	2800	21000	600	24000	46000	84000	27000	34000
Al	24	0.04	0.10	1.2	1.3	0.0	0.1	0.3	2.1	8	14	0.01
Si	42	12	3	28	3	7	1	30	11	8	12	3
Cr	0.006	0.032	0.025	0.003	0.002	0.002	0.002	0.004	0.030	0.04	0.09	0.00005
Mn	3.4	4	8	1.2	0.7	0.035	0.021	1	4	3	4	0.002
Fe	0.14	0.04	0.05	0.7	0.3	0.07	0.10	3	10	0.5	1.4	0.01
Co	0.38	0.06	0.10	0.012	0.006	0.000	0.005	0.01	0.04	0.19	0.19	0.0003
Ni	0.27	0.14	0.11	0.01	0.01	0.00	0.01	0.01	0.05	0.26	0.27	0.005
Cu	0.57	0.021	0.016	nd	nd	0.007	0.009	0.01	0.03	0.08	0.06	0.003
Zn	0.81	0.033	0.012	nd	nd	0.015	0.014	0.06	0.20	0.3	0.8	0.01
As	<0.02	<0.02	-	nd	nd	0.11	0.15	nd	nd	nd	nd	0.003
Sr	8.5	8.4	0.4	1.6	0.5	5.9	0.2	2.4	2.7	7	4	8
Cd	<0.005	0.0020	0.0009	nd	nd	0.009	0.006	0.004	0.014	<0.001	-	0.0001
Sb	0.001	<0.001	-	nd	nd	0.17	0.22	nd	nd	nd	nd	0.0003
I <sup>-</sup>	0.33	0.5	0.5	0.05	0.06	2.1	0.7	0.5	0.9	0.5	0.4	0.06
Ba	0.05	0.05	0.07	0.053	0.004	0.010	0.011	0.06	0.12	<0.01	-	0.03
Pb	0.42	0.007	0.005	nd	nd	0.005	0.007	0.13	0.28	<0.05	-	0.00003
Au	0.03	0.05	0.04	nd	nd	0.5	0.7	0.13	0.21	0.3	0.6	0.01

All concentrations in mg/L, except Au in µg/L.

# Numbers in brackets denote the number of samples taken at each site.

@ Standard Deviation or detection limit (whichever is the larger).

\* For the elements Na, Mg, Ca, K, Cl<sup>-</sup>, SO<sub>4</sub><sup>2-</sup> and Br<sup>-</sup>, the ratio of the element concentration to TDS is used rather than the concentration. (See Section 3.3.3 for details.)

nd not determined

- not applicable

Although groundwaters at Mulgarrie are slightly richer in Fe than sea water (Table 4), they are Fe-poor relative to groundwaters (Figure 13) at the other sites, suggesting that sulphide oxidation is not presently occurring at an appreciable rate. As neutral sulphide oxidation is required for the production of the intermediate sulphur compounds thiosulphate (S<sub>2</sub>O<sub>3</sub><sup>2-</sup>) and sulphite (SO<sub>3</sub><sup>2-</sup>; Granger and Warren, 1969; Goldhaber, 1983; Webster, 1984), these compounds are not expected in this environment. This will have significant consequences for the groundwater mobility of Au, as discussed later (Section 3.3.5).

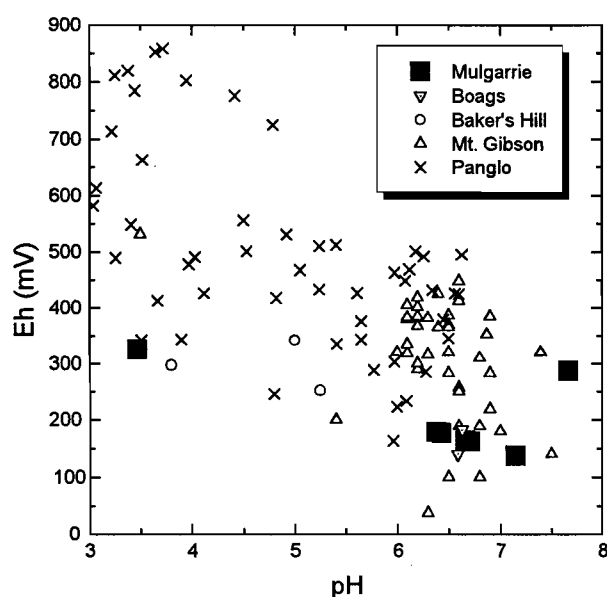


Figure 12: Eh vs. pH for groundwaters from Mulgarrie and other sites.

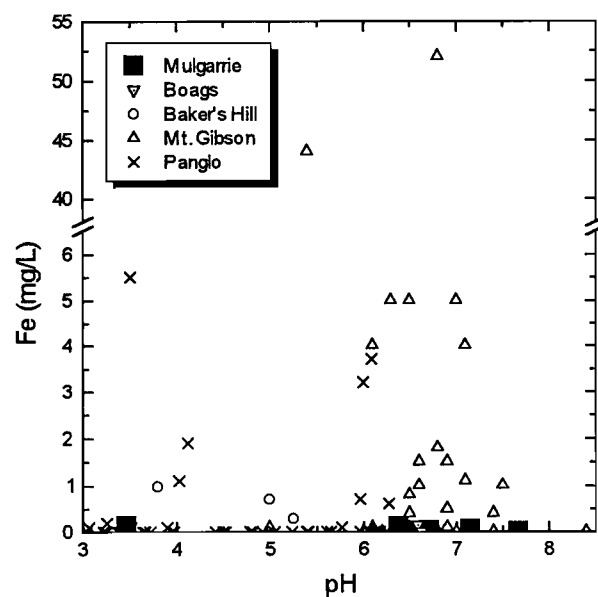


Figure 13: Fe vs. pH for groundwaters from Mulgarrie and other sites.

### 3.3.3 Major ion chemistry

In Table 4, the results for the species Na, Mg, Ca, K, Cl,  $\text{SO}_4^{2-}$  and Br are given as the ratios of the ion over TDS, hereafter described as TDS ratios. The rationale for using these ratios is demonstrated in Figure 14, which shows Na concentration plotted vs TDS, with sea water data used to derive the line of possible values if sea water were diluted with freshwater or concentrated by evaporation, hereafter denoted as the sea water line, and shown in Figures 14 - 17 as the dotted line. As observed, Na content and TDS are closely correlated, and the points tend to fall on the sea water line. Most of the major ions are correlated with TDS, so that derivations from the sea water line may have significance.

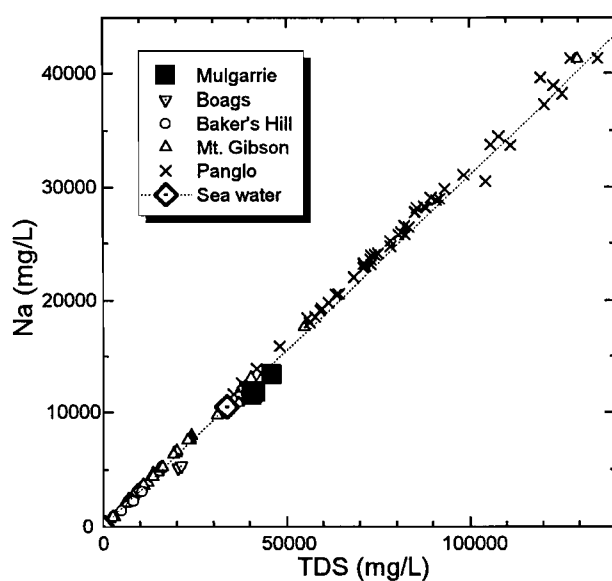


Figure 14: Na vs. TDS for Groundwaters from Mulgarrie and other sites.

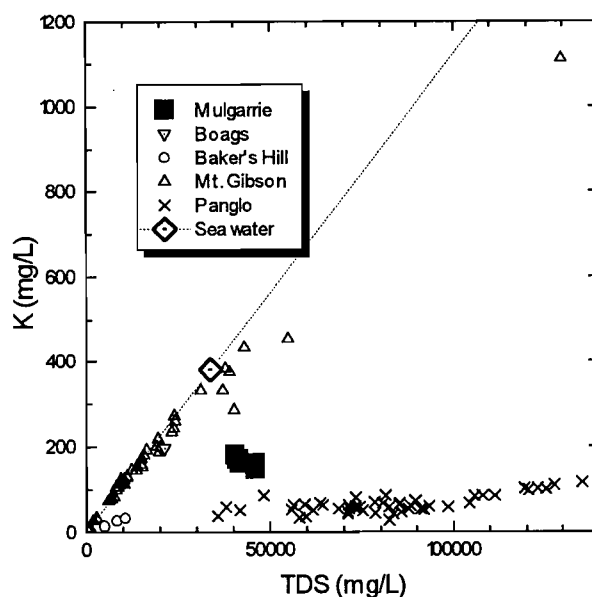


Figure 15: K vs. TDS for Groundwaters from Mulgarrie and other sites.

Waters from Mulgarrie site are markedly depleted in K relative to sea water (Figure 15), though to a lesser extent than Panglo. This K depletion may be related to processes such as illitization (*i.e.*, absorption of  $K^+$  by smectite to form mica) which may be important at Mulgarrie, or alunite formation (Gray, 1990), which is important in acid systems. In addition, the Mulgarrie waters are strongly enriched in Mg and  $SO_4^{2-}$ , relative to sea water (Figures 16 and 17), which may be due to the regional presence of carbonate and sulphide rich lithologies. The general similarity in major ion chemistry between Mul 2 - 7 and Mul 1, 2 km away, suggests that this effect to be regional rather than local. Thus, the major ion chemistry may not commonly give useful local exploration data, although having use in delineating regional lithological changes.

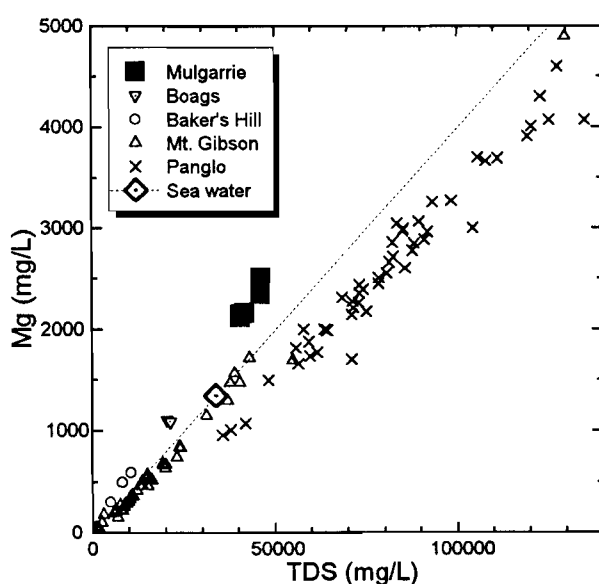


Figure 16: Mg vs. TDS for Groundwaters from Mulgarrie and other sites.

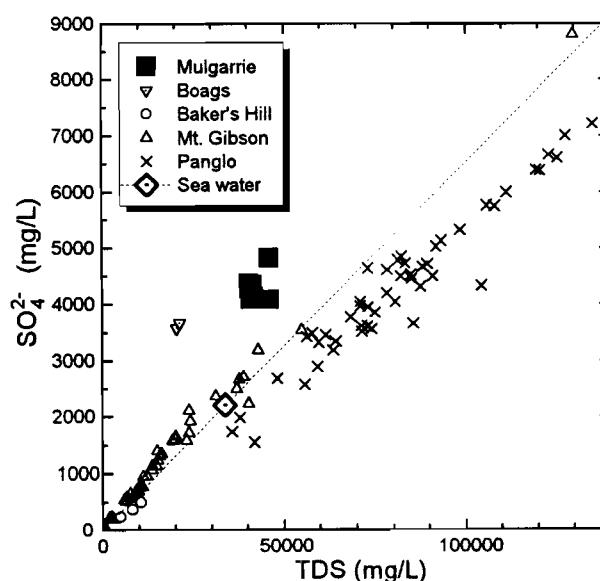


Figure 17:  $SO_4^{2-}$  vs. TDS for Groundwaters from Mulgarrie and other sites.

Speciation analysis has been carried using the program PHREEQE (Parkhurst *et al.*, 1980). This program, and the data derived from it, are described in detail in Gray (1990) and Gray (1991). For the purposes of this discussion, only the solubility index (SI) parameter, which is calculated for a number of mineral phases for each water sample, is considered. If the SI parameter equals zero (empirically from -0.5 to 0.5) the water is in equilibrium with the solid phase, under the conditions specified. Where the SI is less than zero (say  $< -0.5$ ), the solution is under-saturated with respect to the phase, so that, if present, the phase may dissolve. If the SI is greater than zero (say  $> 0.5$ ) the solution is over-saturated with respect to this phase and the phase can precipitate. Note that this analysis only specifies possible reactions, as kinetic constraints may rule out reactions that are thermodynamically allowed. Thus, for example, waters are commonly in equilibrium with calcite, but may become over-saturated with respect to dolomite (as observed here; Table 5), due to the slow speed of solution equilibration with this mineral (Drever, 1982).

The SI values of the water samples for a number of relevant solid phases are given in Table 5, with samples Mul 2 to Mul 7 given in order of position in the transect shown in Figure 5. The Mulgarrie groundwaters are undersaturated with respect to halite (NaCl), but are generally in equilibrium with

calcite ( $\text{CaCO}_3$ ), gypsum ( $\text{CaSO}_4 \cdot 2\text{H}_2\text{O}$ ), celestine ( $\text{SrSO}_4$ ) and barite ( $\text{BaSO}_4$ ), in similarity with groundwaters at other sites (Gray, 1990, 1991, 1992). Close to Palm (Mul 3), and at the eastern edge of the Trial Pit (Mul 2) waters are over-saturated with respect to dolomite [ $\text{CaMg}(\text{CO}_3)_2$ ] and magnesite ( $\text{MgCO}_3$ ), supporting earlier observations of the Mg enrichment of these waters (Figure 16).

Table 5: SI Values for the Mulgarrie groundwaters.

Mineral	Solution Parameter / Mineral Formula	Mul 1	Mul 3	Mul 6	Mul 4	Mul 5	Mul 7	Mul 2
	pH	3.47	7.15	6.66	6.38	6.43	6.71	7.67
	Eh (mV)	325	137	163	179	177	162	286
	TDS (mg/L)	46200	40500	40500	41000	41500	41800	46100
Halite	$\text{NaCl}$	-2.4	-2.5	-2.5	-2.5	-2.5	-2.5	-2.4
Calcite	$\text{CaCO}_3$	-	0.4	-0.2	-0.5	-0.5	-0.1	0.8
Gypsum	$\text{CaSO}_4 \cdot 2\text{H}_2\text{O}$	-0.9	-0.5	-0.5	-0.5	-0.5	-0.5	-0.5
Dolomite	$\text{CaMg}(\text{CO}_3)_2$	-	1.7	0.7	0.0	0.0	0.7	2.7
Magnesite	$\text{MgCO}_3$	-	0.8	0.3	-0.1	-0.1	0.3	1.3
Celestine	$\text{SrSO}_4$	-0.5	-0.5	-0.5	-0.5	-0.5	-0.5	-0.4
Barite	$\text{BaSO}_4$	0.4	0.9	-0.2	0.0	-0.2	0.5	-0.4
Quartz	$\text{SiO}_2$	1.2	0.3	0.6	0.7	0.6	0.6	0.8
Amorphous silica	$\text{SiO}_2$	-0.1	-0.9	-0.6	-0.6	-0.7	-0.6	-0.5
Gibbsite	$\text{Al}(\text{OH})_3$	-1.9	-	-	-	-	-	-
Kaolinite	$\text{Al}_2\text{Si}_2\text{O}_5(\text{OH})_4$	-0.7	-	-	-	-	-	-
Siderite	$\text{FeCO}_3$	-	-1.7	-	-2.2	-2.9	-2.5	-
Ferrihydrite	$\text{Fe}(\text{OH})_3$	-7.4	0.1	-	-1.2	-1.7	-1.1	-
Rhodocrosite	$\text{MnCO}_3$	-	1.3	-1.3	-1.3	-0.7	-0.5	-0.1
Tenorite	$\text{Cu}(\text{OH})_2 \cdot \text{H}_2\text{O}$	-8.2	-5.4	-5.8	-6.6	-6.9	-5.5	-1.7
Smithsonite	$\text{ZnCO}_3$	-	-2.6	-3.0	-3.9	-3.6	-3.2	-2.3
Otavite	$\text{CdCO}_3$	-	-2.0	-2.2	-2.5	-2.8	-2.0	-1.1
Cerrusite	$\text{PbCO}_3$	-	-1.8	-2.2	-2.0	-2.5	-2.2	-1.4
$\text{Ni}(\text{OH})_2$	$\text{Ni}(\text{OH})_2$	-10.0	-2.5	-4.0	-4.5	-4.4	-3.8	-2.7
Iodyrite	$\text{AgI}$	-2.5	-1.8	-2.7	-	-	-	-
$\text{CoCO}_3$	$\text{CoCO}_3$	-	-1.7	-3.7	-3.6	-	-3.5	-
$\text{Cr}_2\text{O}_3$	$\text{Cr}_2\text{O}_3$	-10.1	-	6.1	5.4	5.6	-	9.6
Au (metal)	Au	4.8	7.4	8.3	6.8	7.6	7.0	4.7

- not applicable (at least one of the elements in the mineral below detection in the groundwater).

### 3.3.4 Minor ion chemistry

Acidity can significantly control the solution concentration of many metals. For example, Al concentration is virtually zero under neutral conditions, but will have a very high concentration under acidic conditions (Figure 18). Other metals may be controlled in a similar manner, and for this reason the groundwater chemistry of a particular metal (with the exception of the major ions and Au) is commonly best perceived by plotting the solution concentration vs. pH.

Silicon concentration is controlled by lithology, pH and salinity and the Mulgarrie waters have comparable Si contents to the other sites (Table 4). The waters are generally oversaturated with

respect to quartz (the least soluble Si phase) and undersaturated with respect to amorphous silica (Table 5), indicating complex controls, possibly involving reactions with quartz, opaline silica and/or Si minerals with intermediate solubility (*e.g.*, chalcedony).

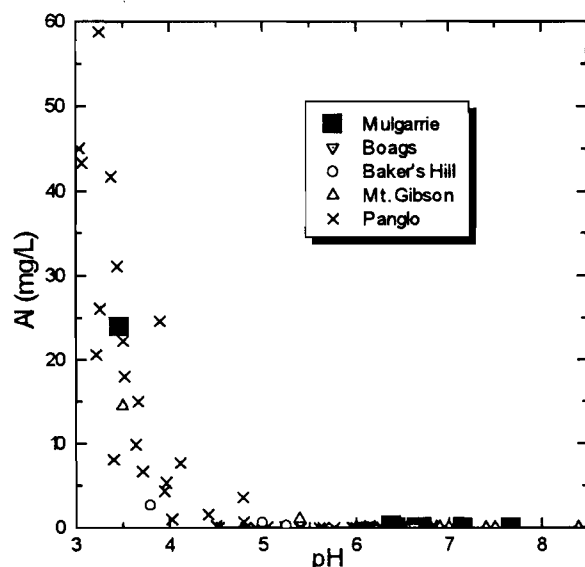


Figure 18: Al vs. pH for Groundwaters from Mulgarrie and other sites.

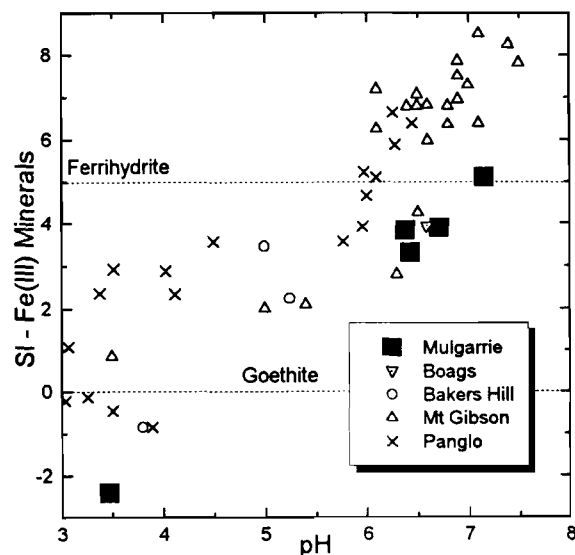


Figure 19: Fe(III) mineral solubility indexes for Groundwaters from Mulgarrie and other sites.

All other elements are undersaturated with respect to the relevant least soluble mineral phase, with the exception of Cr, which is oversaturated with respect to  $\text{Cr}_2\text{O}_3$ , indicating slow equilibration with this phase. The undersaturation of most of the trace elements may reflect control by other reactions such as adsorption on mineral surfaces, or simply that the elements are not been dissolved during weathering at a fast enough rate to reach saturation.

As discussed previously (Section 3.3.2; Figure 13), Fe concentrations are low in these waters, suggesting a low rate of pyrite oxidation. However, the concentrations approach equilibrium with ferrihydrite, a highly soluble Fe(III) phase (Table 5; Figure 19), while many of the Panglo and Mt. Gibson waters are strongly oversaturated with respect to ferrihydrite. This indicates that at Mulgarrie, Fe is in solution equilibrium, in comparison with these other sites where Fe is being quickly released into solution via other reactions such as pyrite oxidation (Eqn. 1). Manganese concentrations are generally comparable with those at other sites (Figure 20), with the exception of Mul 3, which has anomalously high Mn (discussed in Section 3.3.6). As expected, Co distribution (Figure 21) is similar to that of Mn, though the Mul 3 water is less anomalous for Co than for Mn.

Concentrations of Ni and Cr, which are expected to be dissolved during weathering of ultramafic rocks (Gray, 1990), are relatively high in the Mulgarrie groundwaters (Figures 22 and 23) and are similar to groundwaters at Panglo that are in contact with ultramafic lithologies (Gray, 1990). The high Cr concentrations in neutral groundwaters at both sites indicate that appreciable Cr is present in easily weatherable minerals such as chlorite, because resistant phases such as chromite would be expected to release Cr into solution extremely slowly.

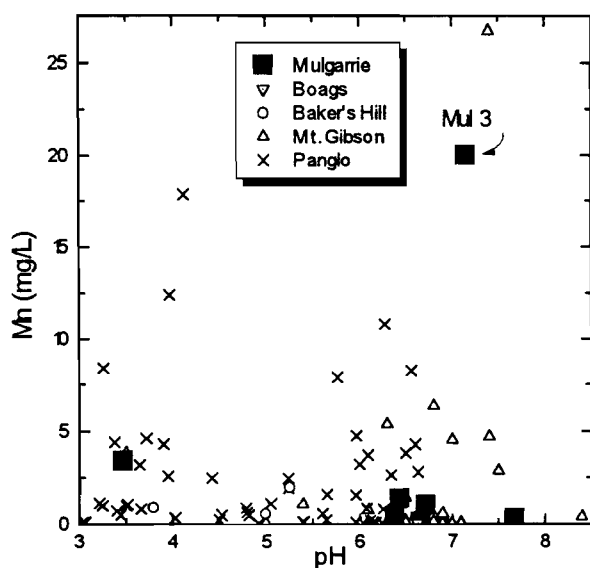


Figure 20: Mn vs. pH for Groundwaters from Mulgarrie and other sites.

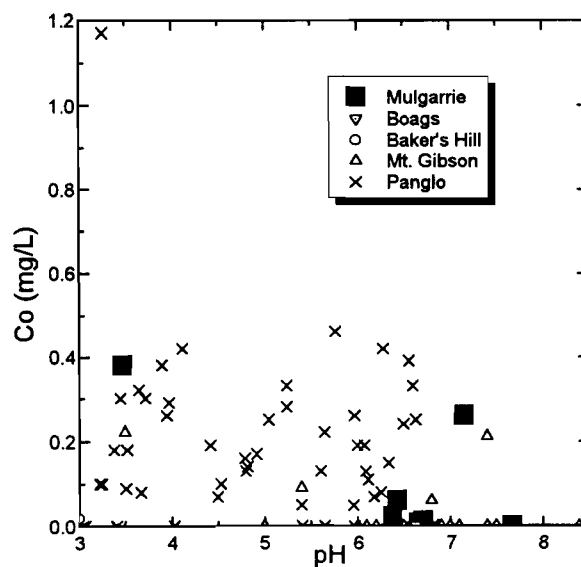


Figure 21: Co vs. pH for Groundwaters from Mulgarrie and other sites.

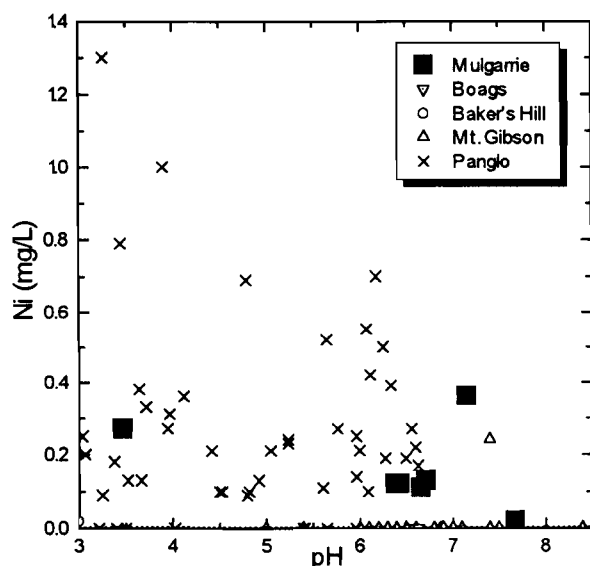


Figure 22: Ni vs. pH for groundwaters from Mulgarrie and other sites.

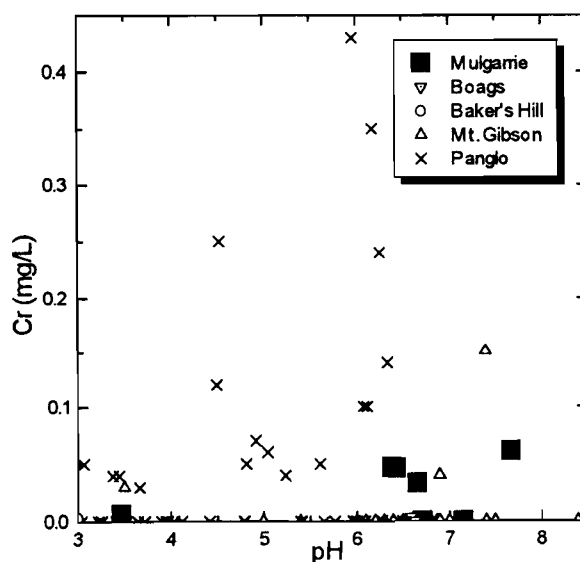


Figure 23: Cr vs. pH for groundwaters from Mulgarrie and other sites.

With the exception of Mul 1, which is a highly acid water and will readily dissolve base metals, concentrations of Cu, Zn, Ag, Cd and Pb in the Mulgarrie groundwater samples are low (Table 4), implying that these metals are not present in any soluble mineral phase. The low concentrations of V, As and Sb may also reflect a low concentration in the solid material, and may be due to the high affinity of these elements for iron oxides (Section 3.1.6).

Iodide concentrations at Mulgarrie are much higher than sea water (Figure 24), similarly to the other mineralized sites Boags, Mount Gibson and Panglo (Gray, 1990, 1991, 1992), and I<sup>-</sup> concentrations are highest adjacent to the Palm Pit (Section 3.3.6). This is consistent with work suggesting that I is a

chalcophile element (Fuge and Johnson, 1984, 1986) and extensively enriched in sulphide environments (Chitayeva *et al.*, 1971).

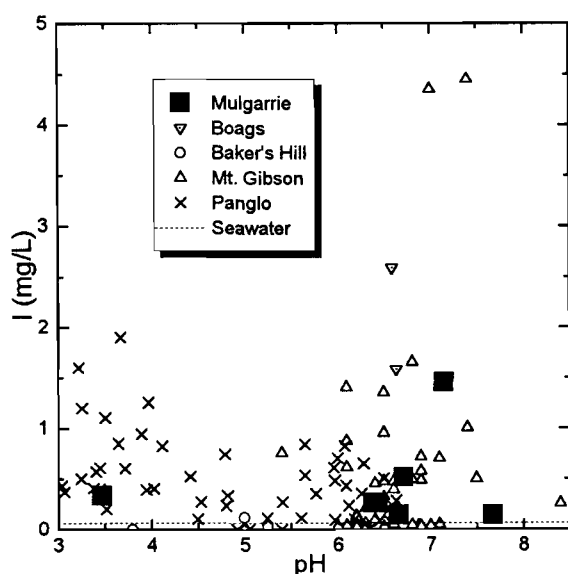


Figure 24: Iodide vs. pH for Groundwaters from Mulgarrie and other sites.

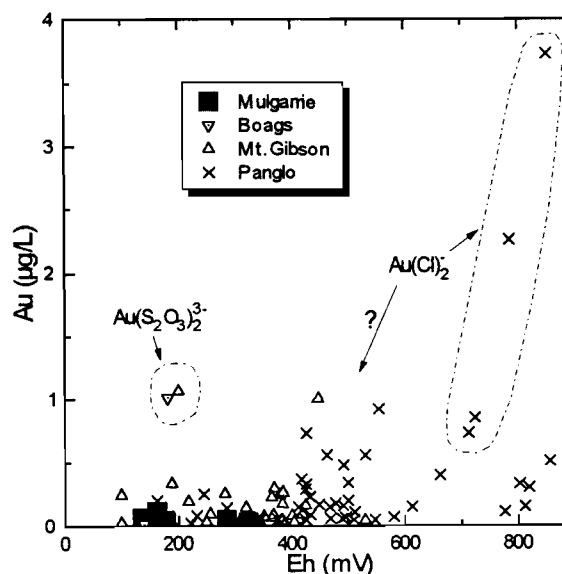


Figure 25: Au vs. Eh for Groundwaters from Mulgarrie and other sites.

### 3.3.5 Gold chemistry

Gold concentrations in the Mulgarrie groundwaters are low, relative to other mineralized sites (Figure 25). Gold is probably present as either the chloride ( $\text{AuCl}_2^-$ ) or the thiosulphate complex  $[\text{Au}(\text{S}_2\text{O}_3)_2]^{3-}$  (Gray, 1988 and references given therein). At Panglo, in particular, there is a general correlation between Au content and Eh (Figure 25), with the very oxidized waters ( $\text{Eh} \gg 800 \text{ mV}$ ) having the highest Au concentration, consistent with Au being mobilized as the chloride complex (Gray, 1990). Specific oxidized waters at Mount Gibson may also contain Au as the chloride complex (Gray, 1991). In comparison, some Au-rich waters at Boags (Gray, 1992) and parts of Mount Gibson are neutral with a low Eh. The waters are from areas with neutral sulphide weathering, and, in some cases, observable thiosulphate in solution, suggesting that Au is present as  $\text{Au}(\text{S}_2\text{O}_3)_2^{3-}$ . However, present-day sulphide oxidation appears to be occurring at a negligible rate in the Mulgarrie study area (Section 3.3.2), and therefore thiosulphate is probably not being produced in significant quantities. Thus, neither of the conditions required for Au dissolution - either acid and oxidizing, or generating thiosulphate - appear to be occurring at this site, and dissolved Au is therefore low, despite the high concentrations of Au within the solid material.

Thus, unlike other sites, Au in groundwater does not appear to be a useful exploration tool at Mulgarrie, although other elements such as Mn or I may have some value (Sections 3.3.4 and 3.3.6). This points to the need in hydrogeochemistry, as in any other exploration method, to perform an orientation study of a site to assess the potential of the method.

### 3.3.6 Hydrogeochemical changes between Palm and Trial Pit

Specific changes in groundwater chemistry were observed for a number of elements across the transect shown in Figure 5, and these changes may be significant in terms of the exploration potential of groundwater at this site. Thus, the groundwater concentration of Mn declines sharply, from about 20 mg/L at Mul 3, to less than 2 mg/L only 60m away (Figure 26). The Mul 3 groundwater is significantly oversaturated with respect to rhodocrosite (Table 5), indicating that the Mn is being released from a weathering mineral of high solubility. However, processes such as dilution, precipitation or adsorption appear to reduce the Mn concentration to equilibrium levels down-gradient of the Palm Pit. The Mn-rich Mul 3 sample was collected from hole MC500, which intersected the Mn oxide zone (Figure A1.2). The water table is several metres below the Mn oxide zone (Figure A1.2) and the waters are oversaturated with respect to Mn oxides, so it is probable that Mn oxides are precipitating rather than dissolving.

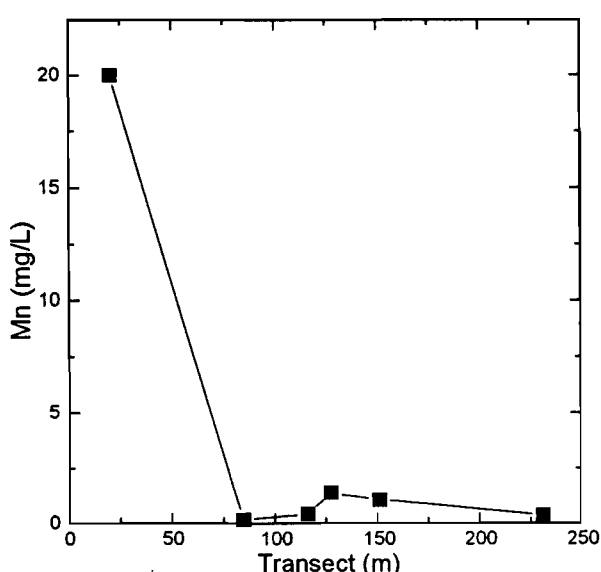


Figure 26: Groundwater Mn concentration across the Mulgarrie transect shown in Figure 5.

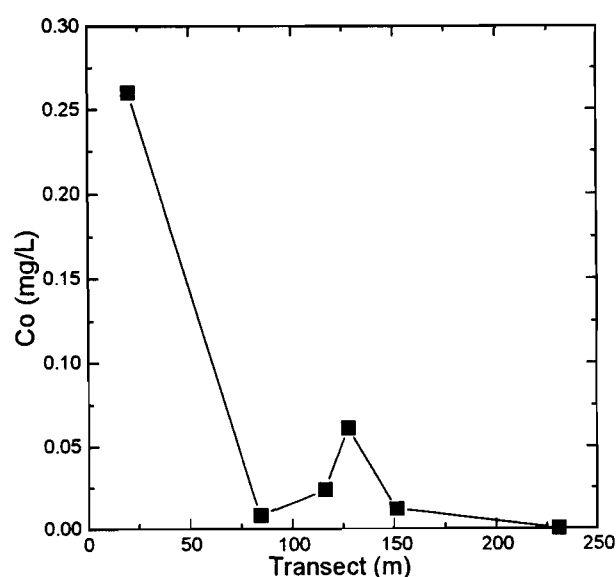


Figure 27: Groundwater Co concentration across the Mulgarrie transect shown in Figure 5.

Similar groundwater trends are observed for Co (Figure 27), though at about 2 orders of magnitude lower than the equivalent Mn concentrations, Ba (Figure 28), which is oversaturated with respect to barite (Table 5) in Mul 3, and iodide (Figure 29). Nickel is also anomalously high close to Palm (Figure 30), but with a higher background, presumably due to moderate levels of Ni released during weathering of the barren alluvium. Conversely, Cr (Figure 31), Fe, Zn, Cu, Pb, Cd and Au (Appendix 5) are not enriched close to Palm Pit.

The higher concentrations of Mn, Co, Ba, I and Ni in Mul 3 are presumably due to weathering of residual material close to Palm, since groundwater contacting the barren alluvium in the channel lacks this signature. The signature compares closely with that for the mineralized Midway area at Mt. Gibson (Gray, 1991), for which the groundwater was anomalously high in Mn, Co, Ba, I, Ni, Au, Cd and Fe. The final three elements, anomalously high at Mount Gibson but not at Mulgarrie, are possibly related to greater sulphide weathering at Mount Gibson.

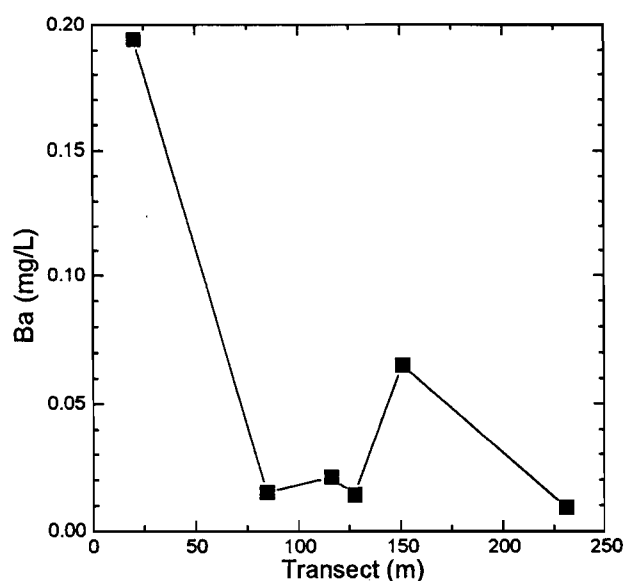


Figure 28: Groundwater Ba concentration across the Mulgarrie transect shown in Figure 5.

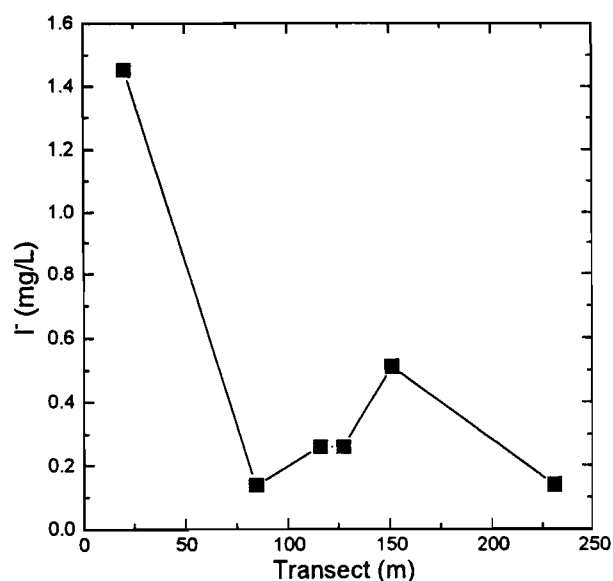


Figure 29: Groundwater I⁻ concentration across the Mulgarrie transect shown in Figure 5.

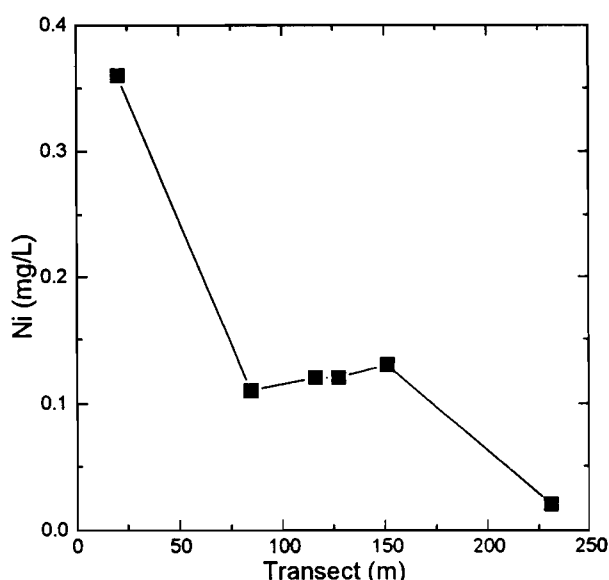


Figure 30: Groundwater Ni concentration across the Mulgarrie transect shown in Figure 5.

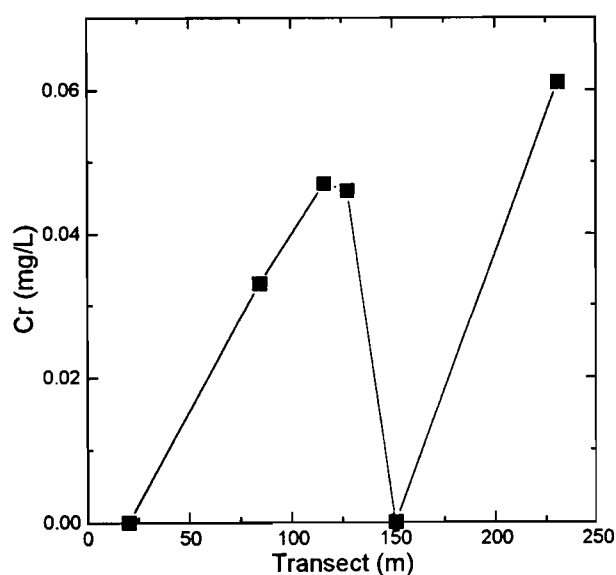


Figure 31: Groundwater Cr concentration across the Mulgarrie transect shown in Figure 5.

The presence of a mineralized signature in the Mul 3 groundwater, but not in the water samples within the drainage channel, suggests that the groundwater does not indicate mineralization concealed beneath barren alluvium. This is in contrast with other sites such as the southern part of the Panglo study area (Gray, 1990) and the Midway area at Mt. Gibson (Gray, 1991), where significant Au, base metal and iodide concentrations were observed in groundwater in areas of transported cover. The lack of mineralized signatures in the Mulgarrie drainage is possibly due the neutral pH of the groundwater and the absence of sulphur compounds able to solubilize Au, leading to lowered ion solubilities.

## 4 GENERAL DISCUSSION

### 4.1 Processes at Mulgarrie and comparisons with other sites

Various processes have affected the geomorphology, mineralogy, and geochemistry of the Mulgarrie study area. The primary geomorphological process has been the infilling of the palaeodrainage channel with alluvial sediments. Across the south margin of the palaeodrainage, as represented by MC500, MC505 and MC529, the sediments are derived from barren ultramafic rock (Section 3.1.1), presumably from up-drainage of the study area. The unconformity is marked by decreased Mg, Zn, Ni and Au in the alluvium overlying the residual saprolite.

The high Mg abundances at surface, particularly in MC529 (Figure A1.3), in which magnesite ( $\text{MgCO}_3$ ) was observed within 2 m of the surface (Appendix 2), probably represent an additional contribution of Mg eroded from the ultramafic outcrop upslope (Section 3.1.8).

Elements associated with the surface carbonates are Th (Section 3.1.8) and Au (Section 3.1.9). The enhancement of Au concentrations in the soil carbonate layer has been observed throughout the southern Yilgarn. The mobilities of both elements increase in organic-rich horizons (Section 3.1.8; Gray *et al.*, 1990) and they presumably occur in dynamic equilibrium in these soils, with continual cycling between soil, plant and dissolved forms. Iodide extractions and other soil experiments (Gray *et al.*, 1990; Section 3.2) have shown that Au associated with the carbonate is highly soluble, reflecting this high mobility in soils. However, the reason for the enrichment is unclear. One possibility is that the metals have been taken up by deeply rooting plants and then deposited on the soil surface. The abundance of Au in the soil decreases from MC500 to MC529 (Figure 8). This may be due to a lateral (chemical or physical) transport from the Palm Pit, with dilution with distance, or by an upward movement from the buried mineralization, with the magnitude of the soil Au anomaly decreasing with increasing depth of burial (Section 3.1.9; Figure 9).

Identification of both the basement and the alluvium as ultramafic was facilitated by examining the Ti/Zr ratios and the Cr contents of the various samples (Section 3.1.1). At the surface, samples appeared to be depleted in Ti, relative to Zr (Figure 6). This is possibly due to organic acids close to the surface dissolving Ti (Bonneau and Souchier, 1982), and has been observed for some other profiles in the Yilgarn (Robertson, 1991).

The relative timing of iron and Mn oxide enrichment of the alluvium is not known. The iron oxides control the distribution of several elements, particularly V, Cr, As and, to a lesser extent, Sb (Section 3.1.4). The Mn oxides have a critical role in the accumulation of Co, Ba and REEs (but see Section 3.1.5), and possibly Cu, Mg, Ca, Zn, Ni and S (Section 3.1.5).

The Mn oxides may also have a critical role in the mobilization of Au. Gold in Mn oxide zones is generally extremely soluble in iodide reagent, but only when the material is finely crushed (Section 3.2). Therefore, it is inferred that Au in Mn oxide zones is highly mobile, with only that Au which has been totally occluded by other phases being retained. Gold so mobilized could be the source for secondary deposits. Such a mechanism could have important exploration consequences.

Present-day groundwater conditions at this site are very unreactive, with neutral, non-oxidizing conditions, low Fe concentrations, and low rates of sulphide oxidation in the study area (Section 3.3.2). Under these conditions, base metals and other trace elements are expected to have low groundwater concentrations. Some elements are enhanced, either due to significant lithological enrichment (*e.g.*, Ni and Cr from ultramafics; Section 3.3.4) or possibly related to mineralization (*e.g.*, Mn, Ba, I; Section 3.3.6). Down gradient of the main study area, the groundwater is acidic and most of the base metals have high dissolved concentrations (Section 3.3.4), similarly to other sites with acid groundwater conditions (Gray, 1990, 1991).

The groundwater closest to Palm (Mul 3) has highly anomalous concentrations of Mn, Co, Ba, I and Ni, similar to those in the mineralized Midway area at Mt. Gibson (Gray, 1991). The mineralized groundwater at Mt. Gibson is also enriched in Au, Cd and Fe, possibly due to greater sulphide weathering. Gold concentrations at Mulgarrie are low, relative to other sites, probably because neither acid/oxidizing conditions or neutral sulphide weathering are present.

#### 4.2 Exploration implications

At Mulgarrie the mineralized ultramafic basement is concealed by barren alluvium of similar ultramafic origin. Both are deeply weathered and, in some areas, the alluvium has been enriched in Mn oxides close to the unconformity. However, the boundaries still appear to correlate with geochemical differences (Section 3.1.2), suggesting that such multi-element discrimination may be useful at other sites.

The use of Cr contents and Zr/Ti ratios is commonly successful in determining broad lithological types (Hallberg, 1984) including the origin of the alluvium, but give equivocal results in near-surface horizons (Section 3.1.2).

Bromine is an ineffective indicator of water-rich or evaporitic zones, due to high *in situ* concentrations of Br in various rocks (Section 3.1.7). Either Na (assuming the absence of Na-containing minerals such as feldspars), or, even better, Cl would be recommended for determining what material has accumulated groundwater salts.

The association of Au with carbonates provides a very useful exploration target but the origin of the surface Au anomaly is not clear from the data available at this site. Iodide extraction may distinguish Au associated with carbonate (high solubility) from that associated with iron oxides (low solubility; Gray *et al.*, 1990) or from primary Au (very low solubility; Section 3.2). Such distinctions may well be significant in understanding and utilizing exploration data.

Groundwaters at various sites have been shown to have specific depletions or enrichments of some of the major ions, such as Mg or  $\text{SO}_4^{2-}$  (Section 3.3.3). Data suggest that in most cases these major element effects are regional (*i.e.*, observed over distances of km rather than m). These effects may be useful in distinguishing different lithological regions, and further work on these phenomena are progressing. The underlying lithology of an area may also be reflected by the groundwater abundances of specific elements. Thus, at Mulgarrie and elsewhere (Gray, 1990), Cr and Ni enhancements are very clearly observed in waters contacting ultramafic lithologies, even where these waters are neutral and would be expected to have low base metal concentrations.

Close to Palm, groundwater has highly enhanced levels of Mn, I, Ba, Co and Ni (Section 3.3.6), similarly to waters contacting mineralized zones at Mt. Gibson (Gray, 1991). However, groundwater contacting the barren alluvium in the channel lacks this signature. This suggests that the groundwater does not indicate mineralization concealed beneath barren alluvium. This is in contrast with other sites such as the southern part of the Panglo study area (Gray, 1990) and the Midway area at Mt. Gibson (Gray, 1991), where significant Au, base metal and iodide concentrations were observed in groundwater in areas of transported cover.

Mulgarrie is different from other Au deposits investigated in the Yilgarn, in that the groundwater has very low concentrations of Au (Section 3.3.5; Figure 25). This is thought to be a consequence of the lack of a groundwater mobilization mechanism, which is an interesting negative result, compared with the clear ability of groundwaters at other sites to mobilize Au (Gray, 1990, 1991, 1992); with a possible mechanism being indicated for each of these sites. Note that the Au contents of Mulgarrie groundwater would be classified as background at these other sites. The groundwater results point to the need to check hydrogeochemistry, like any exploration method, for its usefulness for a particular site.

In summary, the Mulgarrie site demonstrated particular problems that can arise in the exploration for Au in mineralized areas occurring under cover. However, "Areas under Transported Overburden" include a wide variety of environments, depending on the original mineralized lithology, type of cover, and groundwater conditions. How all these conditions may affect the form and extent of secondary anomalies and the groundwater chemistry needs to be fully understood before an extensive system for exploration in such environments is devised.

## **Acknowledgments**

I would like to thank the staff of Newcrest, particularly Steve Devlin and James Tyers, for their assistance during the sample collection.

I would also like to thank CSIRO staff for their support in the preparation of this report. M.J. Lintern and C. Dornan assisted in sample collection and in giving advice on site characteristics. Staff who assisted in the analysis of waters included G.D. Longman, M.J. Willing, D.C. Wright and A.K. Howe at Floreat Park and J. Eames at North Ryde. Solid samples were prepared by J. Crabb and G.D. Longman and analysed at CSIRO by XRF by M.K.W. Hart and using INAA by Becquerel Laboratories. Standard X-ray diffraction analysis was performed by M.K.W. Hart and G.D. Longman and sedimented aggregate X-Ray diffraction analysis was conducted with the assistance and advice of M.K.W. Hart. Artwork was done by C.R. Steel and A. Vartesi, and C.R.M. Butt and M.J. Lintern gave extensive advice in report preparation.

## References

- Bonneau, M. and Souchier, B., 1982. "Constituents and Properties of Soils." (Translator V.C. Farmer. Academic Press: London.)
- Borggaard, O.K., Lindgreen, H.B. and Mørup, S., 1982. Oxidation and reduction of structural iron in chlorite at 480°C. *Clays and Clay Minerals*, 29:67-68.
- Brindley, G.W., 1981. Note: long-spacing organics for calibrating long spacings of interstratified clay minerals. *Clays and Clay Minerals*, 30:353-364.
- Brindley, G.W. and Ali, S.Z., 1950. X-ray study of thermal transformations in some magnesian chlorite minerals. *Acta Crystallographica*, 3:25-30.
- Brindley, G.W. and Brown, G. (Eds.), 1980. *Crystal Structures of Clay Minerals and their X-Ray Identification*. 495 p. (Mineralogical Society: London.)
- Butt, C.R.M., 1991. Geochemical dispersion in the regolith, Mystery Zone, Mt. Percy mine, Kalgoorlie, Western Australia. CSIRO Division of Exploration Geoscience Restricted Report 156R. Vols I and II. 226pp.
- Chitayeva, N.A., Miller, A.D., Grosse, Yu.I. and Christyakova, N.I., 1971. Iodine distribution in the supergene zone of the Gay chalcopyrite deposit. *Geochemistry International*, 8(3):426-36.
- Dionex, 1985. Technical Note 16. (PO Box 3603 Sunnyvale, California, USA).
- Drever, J.I., 1982. "The Geochemistry of Natural Waters." (Prentice-Hall, Inc., Englewood Cliffs, N.J. U.S.A.). 388 p.
- Fuge, R. and Johnson, C.C., 1984. Evidence for the chalcophile nature of iodine. *Chemical Geology*, 43:347-52.
- Fuge, R. and Johnson, C.C., 1986. The geochemistry of iodine - a review. *Environmental geochemistry and Health*, 8:31-54.
- Goldhaber, M.B., 1983. Experimental study of metastable sulfur oxyanion formation during pyrite oxidation at pH 6-9 and 30°C. *American Journal of Science*, 283: 193-217.
- Granger, H.C. and Warren, C.G., 1969. Unstable sulfur compounds and the origin of roll-type uranium deposits. *Economic Geology*, 64: 160-171.
- Gray, D.J., 1986. The geochemistry of uranium and thorium during weathering of chloritic schists at the Alligator Rivers Uranium Province, N.T., Australia. (PhD Dissertation: University of Sydney, Sydney, NSW, Australia.)
- Gray, D.J., 1988. The Aqueous Chemistry of Gold in the Weathering Environment. (AMIRA P240/P241). CSIRO Division of Exploration Geoscience Restricted Report EG 4R. 64pp.
- Gray, D.J., 1990. Hydrogeochemistry of the Panglo Gold Deposit. (AMIRA P241: Weathering Processes). CSIRO Division of Exploration Geoscience Restricted Report 125R. 74pp.
- Gray, D.J., 1991. Hydrogeochemistry in the Mount Gibson Gold District. (AMIRA P240: Laterite Geochemistry). CSIRO Division of Exploration Geoscience Restricted Report 120R. 80pp.
- Gray, D.J., 1992. Hydrogeochemistry of Sulphide Weathering at Boags Pit, Bottle Creek, Western Australia. (AMIRA P241A: Weathering Processes). CSIRO Division of Exploration Geoscience Restricted Report 237R. 13pp.
- Gray, D.J., Lintern, M.J. and Longman, G.D., 1990. Chemistry of Gold in some Western Australian Soils. (AMIRA P241: Weathering Processes). CSIRO Division of Exploration Geoscience Restricted Report 126R. 62pp.
- Greene-Kelly, R., 1953. Irreversible dehydration in montmorillonite, part II. *Clay Minerals Bulletin*, 2:52-56.

- Hallberg, J.A. (1984). A geochemical aid to igneous rock type identification in deeply weathered terrain. *Journal of Geochemical Exploration*, 20: 1-8.
- Hansen, R.O. and Huntington, G.L., 1969. Thorium movement in morainal soils of the High Sierra, California. *Soil Science*, 108:257-265.
- Hansen, R.O. and Stout, P.R., 1968. Isotopic distributions of uranium and thorium in soils. *Soil Science*, 105:44-50.
- Langmuir, D. and Herman, J.S., 1980. The mobility of thorium in natural waters at low temperatures. *Geochimica et Cosmochimica Acta*, 44:1753-1766.
- Lintern, M.J., 1989. Study of the distribution of gold in soils at Mt. Hope, Western Australia. (AMIRA P241: Weathering Processes). CSIRO Division of Exploration Geoscience Restricted Report 24R. 36pp.
- Lintern, M.J. and Butt, C.R.M., 1991. Distribution of gold and other elements in soils from the Mulline area, Western Australia. (AMIRA P241: Weathering Processes). CSIRO Division of Exploration Geoscience Restricted Report 159R. 56pp.
- Lintern, M.J. and Butt, C.R.M., 1992. The distribution of gold and other elements in soils and vegetation at Zulieka, Western Australia. (AMIRA P241A: Weathering Processes). CSIRO Division of Exploration Geoscience Restricted Report 328R. 90pp.
- Lintern, M.J. and Scott, K.M., 1990. The distribution of gold and other elements in soils and vegetation at Panglo, Western Australia. (AMIRA P241: Weathering Processes). CSIRO Division of Exploration Geoscience Restricted Report 129R. 96pp.
- Lintern, M.J., Churchward, H.M. and Butt, C.R.M., 1989. Multi-element soil survey of the Mount Hope area, Western Australia. (AMIRA P241: Weathering Processes). CSIRO Division of Exploration Geoscience Restricted Report 109R. 76pp.
- McIntyre, D.S., 1974. Appendix 4. Definitions of particle size by settling velocity and standard sieves. In "Methods for Analysis of Irrigated Soils." (Ed J. Loveday) pp 188-192. (Technical Communication No. 54 of the Commonwealth Bureau of Soils, Wilkie and Co. Ltd.: Clayton, Victoria.)
- Miekeley, N., Dotto, R.M., Kuchler, I.L. and Linsalata, P. (1985). The importance of organic compounds on the mobilization and bioassimilation of Th in the Morro de Ferro Environment. *Materials Research Society Symposia Proceedings*, 44:591-597. (Summary obtained from Chemical Abstracts.)
- Parkhurst, D.L., Thorstenson, D.C. and Plummer, L.N., 1980. PHREEQE, a computer program for geochemical calculations. *U.S. Geol. Surv. Water Resources Investigations* 80-96, 210p.
- Robertson, I.D.M., 1991. Multi-element dispersion in the saprolite at Beasley Creek gold mine, Laverton, Western Australia. (AMIRA P241: Weathering Processes). CSIRO Division of Exploration Geoscience Restricted Report 152R. Volumes I and II. 122pp.
- Ross, G.J. and Kodama, H., 1974. Experimental transformation of a chlorite into a vermiculite. *Clays and Clay Minerals*, 22:205-211.
- Rubtsov, D.M., 1972. Thorium and uranium content in the clay fraction of podzolic mountain soils of thin forests. *Radioekologicheskie Issledovaniya v Prirodnykh Biogeotsenozakh*, pp 53-66. (Summary obtained from Chemical Abstracts.)
- Scott, K.M., 1989. Mineralogy and geochemistry of weathered mafic/ultramafic volcanics from section 4200N at Panglo, Eastern Goldfields, W.A. (AMIRA P241: Weathering Processes). CSIRO Division of Exploration Geoscience Restricted Report 42R. 22pp.
- Weast, R.C., Astle, M.J. and Beyer, W.H., 1984. "CRC Handbook of Chemistry and Physics." F-154 Elements in Sea Water. (64th Edition; CRC Press Inc., Florida, USA).

Webster, J.G., 1984. Thiosulphate complexing of gold and silver during the oxidation of a sulphide-bearing carbonate lode system, Upper Ridges Mine, P.N.G. A.I.M.M. Perth and Kalgoorlie Branches, Regional Conf. on "Gold Mining, Metallurgy and Geology", Oct 1984.

## **Appendices**

## Appendix 1: Geochemical Data

Majors in %, minors in mg/kg (ppm), with methods as listed in Section 2.2.1.

### Appendix 1A: Tabulated Data for Drill Hole MC500

Sample	Depth	SiO <sub>2</sub>	Al <sub>2</sub> O <sub>3</sub>	Fe <sub>2</sub> O <sub>3</sub>	MnO	MgO	CaO	Na <sub>2</sub> O	K <sub>2</sub> O	TiO <sub>2</sub>	P <sub>2</sub> O <sub>5</sub>	S	Au	As	Ba	Br	Ce	Cl	Co
04-4001	0.5	24.40	5.69	24.51	0.050	1.54	20.43	0.08	0.26	0.34	0.026	0.034	0.219	22	11	6	15	110	30
04-4002	1.5	30.64	9.67	20.80	0.031	5.62	11.92	0.31	0.14	0.63	0.021	0.067	0.423	23	34	15	16	1510	45
04-4003	2.5	22.02	10.25	31.72	0.014	6.35	8.82	0.20	0.12	0.73	0.015	0.034	0.135	21	92	11	17	790	38
04-4004	3.5	31.58	18.30	24.69	0.012	3.37	3.49	0.39	0.12	0.83	0.012	0.228	0.135	20	48	12	13	1130	72
04-4005	4.5	33.05	21.20	29.18	0.014	1.07	0.27	0.44	0.23	0.97	0.017	0.091	0.095	22	76	12	17	1160	85
04-4017	7.5	30.80	17.69	38.91	0.015	0.57	0.02	0.41	0.32	0.96	0.019	0.049	0.486	24	102	13	19	20	77
04-4018	12.5	58.75	14.20	17.11	0.017	0.39	0.01	0.25	1.03	0.67	0.012	0.108	0.117	13	71	16	3	550	56
04-4019	17.5	57.97	13.37	18.61	0.038	0.53	0.01	0.28	0.77	0.71	0.010	0.093	0.055	10	75	9	5	1530	76
04-4020	19.5	62.88	12.86	14.04	0.031	0.56	0.02	0.40	1.64	0.84	0.009	0.190	0.288	10	128	12	3	2340	41
04-4021	21.5	66.55	11.05	13.73	0.093	0.50	0.02	0.38	0.93	0.64	0.003	0.227	3.260	9	165	8	15	1420	57
04-4022	22.5	66.84	9.63	13.71	0.938	0.46	0.02	0.30	0.61	0.52	0.006	0.133	0.308	8	708	7	28	1740	643
04-4023	24.5	46.68	10.66	12.27	3.60	3.98	5.09	0.39	0.56	0.61	0.008	0.478	0.125	6	1576	10	132	2240	3020
04-4024	26.5	66.18	7.81	13.65	1.217	1.49	0.07	0.45	0.81	0.66	0.028	0.403	0.386	13	258	15	35	2630	1120
04-4025	27.5	64.78	9.38	13.77	0.455	1.62	0.58	0.29	0.71	0.62	0.016	0.23	1.010	10	162	11	25	790	442
04-4026	28.5	68.59	6.86	10.93	0.980	1.95	1.00	0.26	0.59	0.48	0.014	0.248	0.458	7	354	8	50	1360	694
04-4027	31.5	53.87	11.12	19.58	0.319	2.73	0.23	0.51	1.11	0.79	0.027	0.303	4.640	11	148	14	27	3720	208
04-4028	36.5	58.61	9.58	15.41	0.342	5.18	0.06	0.65	1.07	0.82	0.031	0.353	0.204	7	131	13	10	2110	141
04-4029	38.5	67.17	7.15	13.52	0.178	4.36	0.05	0.49	0.87	0.68	0.028	0.238	0.299	8	122	12	4	3080	118
04-4030	40.5	63.23	7.80	13.02	0.232	6.68	0.08	0.84	0.49	0.72	0.034	0.153	0.029	3	62	12	7	2740	133
04-4031	42.5	41.21	6.04	10.27	0.169	15.96	5.22	0.43	0.28	0.5	0.029	0.179	0.121	4	44	3	7	880	104
04-4032	43.5	40.18	5.70	9.79	0.160	15.28	5.27	0.65	0.62	0.49	0.025	0.442	0.178	4	65	19	4	5730	96
04-4033	45.5	41.81	5.19	9.04	0.151	15.36	5.35	0.19	0.48	0.45	0.027	0.254	0.073	7	52	3	4	590	100

Sample	Depth	Cr	Cs	Cu	Eu	Ga	Ge	Hf	La	Lu	Nb	Ni	Pb	Rb	Sb	Sc	Sm	Sr	Th	V	W	Y	Yb	Zn	Zr
04-4001	0.5	2520	1	85	1	18	<1	2	10	0.2	3	225	8	9	1	19	2	185	2	455	19	13	1	19	39
04-4002	1.5	2740	<1	93	<1	14	<1	2	5	<0.2	3	396	9	5	1	25	2	267	2	324	9	13	1	23	46
04-4003	2.5	4250	2	82	<1	18	1	2	2	<0.2	<1	356	6	4	1	37	1	320	1	512	24	11	1	10	47
04-4004	3.5	4330	<1	144	<1	21	<1	2	2	0.2	<1	607	5	4	2	54	1	169	2	390	17	11	1	10	64
04-4005	4.5	4680	3	187	<1	27	1	3	2	0.3	<1	769	7	7	2	68	1	63	2	503	21	14	1	17	71
04-4017	7.5	5660	1	169	1	24	1	2	3	<0.2	1	689	13	10	2	91	1	27	1	616	12	13	1	16	66
04-4018	12.5	2750	2	109	<1	14	2	<1	1	<0.2	2	483	3	28	2	65	1	10	<1	263	18	11	1	16	41
04-4019	17.5	2660	1	160	<1	14	1	<1	1	<0.2	3	673	4	17	2	86	1	9	<1	282	7	12	1	32	39
04-4020	19.5	2790	2	140	1	16	1	<1	2	<0.2	4	678	8	40	2	71	1	13	<1	304	14	14	1	36	46
04-4021	21.5	2160	2	149	1	13	1	1	3	<0.2	<1	613	35	22	1	50	2	11	<1	255	9	16	1	20	36
04-4022	22.5	2140	<1	244	2	9	2	1	10	<0.2	3	920	22	15	1	49	4	20	<1	219	12	18	1	39	30
04-4023	24.5	2010	1	568	4	11	2	<1	36	0.4	1	2297	1	12	1	47	13	52	<1	308	3	37	2	135	35
04-4024	26.5	2540	1	277	2	11	1	1	17	0.2	3	2849	3	18	1	34	8	18	<1	230	6	22	1	230	36
04-4025	27.5	2780	<1	218	1	12	1	<1	8	<0.2	1	1666	34	17	2	41	4	18	<1	232	13	14	1	118	38
04-4026	28.5	1770	<1	242	1	8	<1	<1	11	<0.2	<1	1954	22	13	2	26	5	20	<1	184	7	17	1	150	28
04-4027	31.5	3410	2	163	2	16	<1	2	13	0.3	3	2867	11	24	2	46	6	18	1	398	8	28	1	178	56
04-4028	36.5	2610	1	148	<1	13	<1	1	7	<0.2	1	1937	3	24	1	41	3	26	<1	321	7	19	1	113	46
04-4029	38.5	2460	<1	86	<1	10	1	<1	4	<0.2	<1	1790	4	18	1	34	2	17	<1	244	5	16	1	118	36
04-4030	40.5	2510	<1	111	<1	12	2	1	5	<0.2	2	1433	1	11	2	34	2	18	<1	231	3	14	1	91	35
04-4031	42.5	1990	<1	70	<1	9	1	<1	3	<0.2	2	1159	4	6	1	26	2	37	<1	165	3	10	<1	71	27
04-4032	43.5	1860	<1	61	<1	8	1	<1	3	<0.2	<1	986	6	15	1	25	2	45	<1	148	4	9	1	65	27
04-4033	45.5	1870	<1	86	<1	9	<1	<1	2	<0.2	3	965	7	10	1	23	1	39	<1	144	7	9	<1	69	22

# Appendix 1B: Tabulated Data for Drill Hole MC505

Sample	Depth	SiO <sub>2</sub>	Al <sub>2</sub> O <sub>3</sub>	Fe <sub>2</sub> O <sub>3</sub>	MnO	MgO	CaO	Na <sub>2</sub> O	K <sub>2</sub> O	TiO <sub>2</sub>	P <sub>2</sub> O <sub>5</sub>	S	Au	As	Ba	Br	Ce	Cl	Co
04-4075	0.5	38.99	7.19	12.44	0.171	5.44	15.36	0.41	0.28	0.52	0.023	0.059	0.074	13	138	16	18	1370	192
04-4076	1.5	18.57	4.37	10.33	0.055	12.19	20.85	0.21	0.23	0.18	0.011	0.197	0.166	12	274	10	18	230	37
04-4077	2.5	27.97	11.45	35.99	0.050	4.73	4.35	0.41	0.10	0.51	0.011	0.286	0.096	50	387	14	12	930	121
04-4078	3.5	39.72	13.94	32.27	0.043	2.60	0.17	0.44	0.10	0.59	0.014	0.241	0.038	41	125	15	19	1100	124
04-4079	4.5	37.16	15.40	32.58	0.042	1.79	0.05	0.44	0.08	0.53	0.017	0.203	0.045	40	40	16	16	740	132
04-4168	6.5	39.20	15.87	32.82	0.026	1.00	0.03	0.34	0.09	0.78	0.019	0.195	0.023	18	31	15	15	1110	101
04-4169	8.5	35.82	18.77	32.60	0.015	0.54	0.00	0.27	0.09	0.60	0.020	0.189	0.013	25	41	20	8	1030	55
04-4170	10.5	43.17	14.84	31.73	0.012	0.36	0.00	0.23	0.08	0.81	0.025	0.165	0.009	32	14	17	11	910	26
04-4171	12.5	41.41	14.39	34.26	0.010	0.27	0.00	0.20	0.09	0.81	0.021	0.164	0.010	38	16	17	10	1120	25
04-4172	14.5	41.72	15.07	33.58	0.010	0.26	0.00	0.16	0.15	0.90	0.020	0.135	0.012	34	24	13	11	310	22
04-4173	16.5	40.03	17.91	30.48	0.011	0.32	0.01	0.29	0.23	1.17	0.014	0.101	0.022	27	32	10	7	1270	33
04-4174	18.5	34.91	23.44	27.37	0.008	0.26	0.01	0.31	0.23	0.91	0.006	0.121	0.019	12	19	8	10	950	35
04-4175	20.5	39.41	19.36	29.05	0.009	0.30	0.01	0.31	0.32	1.30	0.007	0.077	0.036	22	38	9	10	1030	28
04-4176	22.5	38.76	21.66	26.66	0.009	0.30	0.02	0.34	0.66	1.17	0.006	0.071	0.057	27	69	9	8	1500	24
04-4177	24.5	44.63	14.34	30.29	0.013	0.29	0.02	0.25	0.32	1.15	0.010	0.067	0.061	34	49	7	8	1080	28
04-4178	26.5	47.11	14.28	28.08	0.014	0.25	0.03	0.29	0.12	1.29	0.008	0.069	1.290	35	33	8	10	1560	25
04-4179	28.5	34.70	22.04	29.63	0.022	0.28	0.05	0.47	0.11	0.83	0.006	0.231	0.467	26	20	13	27	3010	34
04-4180	30.5	39.79	16.94	26.73	0.034	1.42	1.64	0.41	0.31	0.98	0.010	0.317	4.480	33	39	13	17	3410	63
04-4181	32.5	53.92	12.59	20.46	0.048	0.86	0.61	0.48	0.22	0.86	0.008	0.463	0.023	25	31	18	20	4760	113
04-4182	34.5	57.05	11.49	20.22	0.056	0.47	0.06	0.52	0.31	0.84	0.012	0.262	0.036	26	27	19	25	5450	192
04-4183	36.5	61.39	9.31	16.48	0.055	3.33	0.08	0.54	0.15	0.71	0.016	0.297	0.051	12	22	17	16	4600	196
04-4184	38.5	62.66	9.34	15.59	0.084	3.17	0.05	0.53	0.66	0.71	0.025	0.356	0.018	15	62	15	13	3100	231
04-4185	40.5	57.43	11.03	17.08	0.138	4.18	0.05	0.71	0.44	0.90	0.038	0.266	0.007	14	65	16	7	4840	258
04-4186	42.5	56.84	11.41	16.18	0.278	4.17	0.06	0.75	0.67	0.92	0.029	0.384	0.010	23	128	18	9	5470	356
04-4187	44.5	58.55	11.02	15.97	0.182	3.52	0.05	0.62	0.85	0.89	0.035	0.328	0.005	16	101	10	9	3100	124
04-4188	46.5	59.11	9.73	13.99	0.030	7.41	0.04	0.60	0.49	0.79	0.049	0.228	<0.005	18	38	12	8	3140	110

Sample	Depth	Cr	Cs	Cu	Eu	Ga	Ge	Hf	La	Lu	Nb	Ni	Pb	Rb	Sb	Sc	Sm	Sr	Th	V	W	Y	Yb	Zn	Zr
04-4075	0.5	1890	<1	90	0.8	9	<1	1	8	<0.2	2	1642	2	10	0.8	24	3	224	2.4	201	3	14	1.4	111	55
04-4076	1.5	1600	<1	33	<0.5	6	<1	<1	9	<0.2	2	324	5	10	0.8	15	2	672	2.8	176	<2	8	0.7	23	39
04-4077	2.5	6080	<1	151	<0.5	17	3	2	4	<0.2	<1	1173	3	1	2.4	56	1	194	2.1	555	<2	7	1.1	35	48
04-4078	3.5	4870	<1	130	<0.5	19	<1	1	4	<0.2	2	1056	6	2	1.7	57	1	38	1.1	524	<2	10	1.1	33	45
04-4079	4.5	5110	<1	139	<0.5	22	<1	1	4	<0.2	1	984	2	4	1.5	60	1	28	1.5	524	<2	7	1.0	25	46
04-4168	6.5	4350	<1	117	<0.5	21	1	<1	2	<0.2	4	800	1	2	1.8	48	1	9	1.2	481	7	10	<0.5	20	59
04-4169	8.5	5680	<1	102	<0.5	21	1	2	1	<0.2	1	590	5	3	1.6	48	<1	4	0.9	473	3	6	0.6	11	42
04-4170	10.5	5290	<1	69	<0.5	20	<1	1	<1	<0.2	4	400	<1	3	1.9	38	1	3	0.6	482	6	10	<0.5	10	49
04-4171	12.5	5320	<1	68	<0.5	24	3	2	1	<0.2	5	371	<1	5	1.9	33	1	3	0.9	542	7	8	0.8	11	45
04-4172	14.5	4600	<1	64	<0.5	21	2	2	<1	<0.2	5	327	<1	4	2.0	31	1	2	0.7	506	9	12	0.8	10	53
04-4173	16.5	4300	<1	96	<0.5	22	2	2	1	<0.2	5	491	2	9	2.3	40	1	3	0.6	493	11	13	0.8	16	65
04-4174	18.5	3870	<1	174	<0.5	22	2	2	1	<0.2	2	665	<1	7	1.9	87	1	8	0.9	414	8	11	<0.5	15	65
04-4175	20.5	3220	1	142	<0.5	22	1	3	1	<0.2	6	535	2	10	2.7	74	1	9	<0.5	466	13	16	0.9	19	74
04-4176	22.5	3620	1	149	<0.5	25	<1	3	1	<0.2	3	502	2	17	2.3	87	1	9	0.8	447	11	16	0.9	17	73
04-4177	24.5	3240	<1	94	<0.5	20	3	2	1	<0.2	6	421	5	9	2.4	62	1	9	0.8	512	11	13	0.9	19	68
04-4178	26.5	2530	<1	86	0.8	18	2	3	4	0.3	5	430	6	2	2.6	53	2	7	1.2	480	14	28	0.9	19	88
04-4179	28.5	3960	<1	96	1.0	30	2	2	11	0.3	1	561	3	3	1.9	68	4	16	1.2	504	15	28	1.1	20	68
04-4180	30.5	4410	<1	121	0.8	22	3	2	6	0.3	4	746	7	6	1.8	77	3	18	0.8	468	15	25	0.7	38	64
04-4181	32.5	3690	<1	198	1.4	15	3	2	5	0.3	4	996	9	5	1.4	50	5	17	<0.5	308	10	20	1.3	85	56
04-4182	34.5	3690	<1	194	1.3	14	4	2	6	0.3	3	1283	2	6	1.4	41	5	17	<0.5	317	13	21	1.4	142	48
04-4183	36.5	4100	<1	126	1.2	11	2	1	5	0.3	<1	2602	<1	4	1.3	33	5	12	<0.5	246	3	17	1.1	241	37
04-4184	38.5	3580	<1	97	0.9	12	2	2	5	<0.2	4	1891	2	12	1.2	32	4	17	<0.5	243	4	18	0.7	184	37
04-4185	40.5	2880	<1	153	1.0	14	2	2	6	0.2	0	1872	<1	8	1.4	38	3	18	<0.5	263	12	20	0.9	200	45
04-4186	42.5	2770	<1	130	0.7	14	2	1	6	0.2	3	1817	<1	12	1.4	37	3	28	<0.5	266	11	21	1.2	172	49
04-4187	44.5	1650	<1	121	0.6	14	2	1	3	<0.2	4	1597	1	16	0.9	22	2	23	<0.5	273	10	18	0.5	148	46
04-4188	46.5	3010	<1	132	<0.5	13	1	2	3	<0.2	1	1707	0	9	1.3	32	2	13	<0.5	242	4	15	0.7	154	39

# Appendix 1C: Tabulated Data for Drill Hole MC529

Sample	Depth	SiO <sub>2</sub>	Al <sub>2</sub> O <sub>3</sub>	Fe <sub>2</sub> O <sub>3</sub>	MnO	MgO	CaO	Na <sub>2</sub> O	K <sub>2</sub> O	TiO <sub>2</sub>	P <sub>2</sub> O <sub>5</sub>	S	Au	As	Ba	Br	Ce	Cl	Co
04-4133	0.5	45.70	9.61	13.21	0.318	6.78	6.69	1.14	0.22	0.72	0.041	0.146	0.042	9	117	18	20	1000	122
04-4134	1.5	30.60	6.40	8.31	0.098	11.64	15.06	0.45	0.33	0.40	0.013	0.621	0.055	8	248	14	25	1130	43
04-4135	2.5	22.81	4.90	6.05	0.071	15.44	18.76	0.40	0.22	0.31	0.014	0.666	0.019	7	126	12	14	370	38
04-4136	3.5	19.62	4.36	6.34	0.095	31.13	1.64	0.39	0.16	0.27	0.007	0.206	0.011	9	45	11	17	1330	56
04-4137	4.5	32.87	8.17	15.41	0.185	18.63	0.50	0.52	0.26	0.44	0.009	0.137	0.008	26	76	14	47	1770	154
04-4138	5.5	26.29	10.67	33.98	0.263	10.96	0.43	0.49	0.10	0.50	0.009	0.119	0.010	54	256	10	59	1360	368
04-4139	6.5	30.01	13.49	43.53	0.042	2.95	0.06	0.40	0.07	0.57	0.014	0.092	0.012	74	105	9	25	480	159
04-4140	8.5	35.47	13.97	33.05	0.023	4.51	0.02	0.45	0.06	0.54	0.008	0.239	0.005	27	25	20	13	990	178
04-4141	10.5	35.77	17.82	30.96	0.013	1.50	0.01	0.30	0.05	0.75	0.014	0.254	0.006	33	3	29	15	1480	87
04-4142	12.5	33.84	16.65	35.74	0.020	0.72	0.01	0.30	0.04	0.68	0.019	0.197	0.007	30	19	22	15	1220	89
04-4143	14.5	43.64	19.68	23.90	0.008	0.46	0.01	0.32	0.05	0.94	0.011	0.262	0.012	27	3	42	6	2330	38
04-4144	16.5	43.17	19.64	25.55	0.008	0.27	0.01	0.25	0.04	0.89	0.013	0.189	0.010	33	64	19	2	1560	25
04-4145	18.5	34.95	21.63	29.77	0.014	0.24	0.02	0.30	0.03	1.17	0.012	0.207	0.019	31	13	14	5	510	24
04-4146	20.5	32.38	21.75	31.29	0.011	0.17	0.01	0.28	0.04	0.97	0.011	0.206	0.018	32	1	8	10	830	31
04-4147	22.5	26.72	16.51	44.14	0.016	0.19	0.02	0.30	0.03	1.09	0.014	0.156	0.008	48	15	9	21	1420	58
04-4148	24.5	36.44	20.95	28.99	0.024	0.23	0.02	0.32	0.15	1.32	0.010	0.082	0.024	34	37	8	10	1900	34
04-4149	26.5	47.76	30.02	5.64	0.014	0.24	0.03	0.48	0.09	1.49	0.004	0.131	0.016	11	20	12	32	2840	24
04-4150	28.5	40.96	29.72	15.57	0.025	0.36	0.02	0.48	1.73	0.91	0.015	0.122	<0.005	7	505	10	18	3140	17
04-4151	30.5	48.30	13.99	25.33	0.036	0.26	0.03	0.32	0.04	2.51	0.020	0.199	0.046	103	39	11	14	3030	45
04-4152	32.5	24.69	22.97	35.40	0.026	0.45	0.27	0.53	0.03	0.68	0.024	0.469	<0.005	28	13	16	16	4590	39
04-4153	34.5	52.17	14.35	22.00	0.012	0.31	0.05	0.55	0.05	1.07	0.054	0.328	0.642	5	14	18	12	5990	56
04-4154	36.5	55.71	13.78	20.12	0.022	0.29	0.05	0.54	0.02	1.11	0.077	0.199	0.008	3	20	18	19	4700	64
04-4155	38.5	54.56	14.07	19.87	0.034	0.31	0.05	0.51	0.04	1.08	0.056	0.234	<0.005	6	25	18	11	5320	80
04-4156	40.5	65.60	19.72	2.28	0.005	0.39	0.05	0.54	0.11	1.47	0.005	0.037	6.540	3	43	15	5	2910	20
04-4157	42.5	57.14	12.86	15.61	0.020	2.49	0.07	0.62	0.04	1.06	0.055	0.127	2.130	13	24	17	9	4590	109
04-4158	44.5	56.47	10.89	18.11	0.053	3.74	0.06	0.60	0.03	0.91	0.066	0.270	0.072	22	15	17	9	5820	113

Sample	Depth	Cr	Cs	Cu	Eu	Ga	Ge	Hf	La	Lu	Nb	Ni	Pb	Rb	Sb	Sc	Sm	Sr	Th	V	W	Y	Yb	Zn	Zr
04-4133	0.5	1680	1	107	0.9	13	<1	2	9	<0.2	2	811	6	10	1.3	31	3	188	2.6	248	<2	21	1.8	122	61
04-4134	1.5	956	1	46	0.6	8	<1	2	12	<0.2	2	301	3	16	0.6	16	3	564	4.0	149	<2	12	1.3	40	56
04-4135	2.5	768	<1	47	0.5	6	1	1	8	<0.2	4	287	5	9	0.5	13	2	606	2.8	103	<2	10	1.0	34	46
04-4136	3.5	1020	<1	68	0.5	7	<1	<1	6	<0.2	1	427	4	7	0.5	15	2	82	1.9	116	<2	11	1.0	40	36
04-4137	4.5	2430	<1	98	0.9	11	<1	2	14	<0.2	0	874	10	10	1.0	32	3	43	3.6	283	<2	14	1.4	41	58
04-4138	5.5	7080	<1	123	1.1	15	<1	1	29	<0.2	3	1403	7	1	2.4	53	5	35	1.8	553	<2	20	1.0	30	42
04-4139	6.5	7430	<1	115	0.6	22	1	2	6	<0.2	2	1395	8	4	3.3	59	1	10	1.5	682	2	9	<0.5	23	39
04-4140	8.5	6350	<1	84	<0.5	18	2	<1	1	<0.2	<1	1622	5	2	1.8	61	1	9	0.9	535	<2	7	0.6	21	34
04-4141	10.5	6960	<1	92	0.5	17	2	2	1	<0.2	3	721	2	1	2.0	58	<1	4	0.9	451	<2	8	0.6	10	53
04-4142	12.5	6900	<1	98	<0.5	20	2	2	1	<0.2	<1	655	2	3	1.7	60	1	4	0.9	517	<2	8	0.7	15	44
04-4143	14.5	5830	<1	61	<0.5	24	2	2	1	<0.2	2	429	<1	5	1.9	49	1	6	0.8	338	4	12	0.9	9	58
04-4144	16.5	6330	<1	60	<0.5	20	<1	2	1	<0.2	2	368	<1	1	1.8	46	0	2	0.8	367	5	10	0.7	5	59
04-4145	18.5	6930	<1	44	<0.5	24	3	2	1	<0.2	5	326	3	1	1.9	41	1	8	1.1	446	3	14	1.0	8	76
04-4146	20.5	4670	<1	65	<0.5	23	2	2	1	<0.2	4	364	<1	3	1.7	47	1	6	1.4	434	4	12	0.9	9	72
04-4147	22.5	6850	<1	40	<0.5	26	2	3	9	<0.2	5	403	1	1	2.6	45	1	8	1.5	685	4	14	0.9	22	67
04-4148	24.5	6150	1	73	0.6	22	1	3	3	<0.2	6	489	3	9	2.2	71	1	11	1.4	483	6	18	1.3	49	95
04-4149	26.5	4330	<1	35	<0.5	32	3	3	3	<0.3	6	457	1	3	1.8	49	1	11	1.5	215	5	19	1.2	26	134
04-4150	28.5	597	2	64	<0.5	36	1	3	15	<0.2	6	149	2	44	0.8	28	2	56	5.5	218	2	10	<0.5	33	148
04-4151	30.5	4770	<1	35	1.1	16	2	5	9	<0.6	7	456	1	2	2.8	34	4	15	1.2	455	7	37	2.0	33	181
04-4152	32.5	6770	<1	109	0.7	22	4	<1	7	<0.2	0	762	1	1	1.0	87	3	15	<0.5	493	<2	18	0.9	49	36
04-4153	34.5	4760	<1	179	1.0	20	2	1	5	<0.3	1	858	<1	2	2.7	50	3	14	0.6	438	<2	23	1.4	66	59
04-4154	36.5	2890	<1	182	0.9	19	1	<1	5	<0.3	1	1012	<1	0	2.3	45	4	13	<0.5	394	<2	26	1.4	78	59
04-4155	38.5	2490	<1	221	0.9	19	2	1	7	<0.3	4	1149	<1	2	2.7	46	5	13	<0.5	415	<2	28	1.5	103	64
04-4156	40.5	4190	<1	31	<0.5	22	1	2	6	<0.2	5	434	2	4	3.3	33	2	18	0.8	89	<2	26	1.0	42	94
04-4157	42.5	5400	<1	151	1.1	16	1	2	7	<0.3	3	2821	<1	2	2.8	46	4	15	<0.5	302	2	26	1.3	262	62
04-4158	44.5	3610	<1	143	1.2	13	<1	1	6	<0.2	3	3160	<1	2	2.4	41	4	11	<0.5	294	3	22	1.1	273	47

# Appendix 1D: Tabulated Data for Additional Samples

Sample	Description	Fraction	SiO <sub>2</sub>	Al <sub>2</sub> O <sub>3</sub>	Fe <sub>2</sub> O <sub>3</sub>	MnO	MgO	CaO	Na <sub>2</sub> O	K <sub>2</sub> O	TiO <sub>2</sub>	P <sub>2</sub> O <sub>5</sub>	S	Au	As	Ba	Br	Ce	Cl	Co
04-4159	Ultramafic	(Rock)	42.96	9.33	12.93	0.157	21.34	5.51	0.65	0.03	0.42	0.012	0.003	<0.005	2	24	<2	<1	40	108
04-4160	Basalt	(Rock)	47.33	13.54	11.62	0.177	7.68	12.04	1.58	0.28	0.76	0.042	0.006	0.019	4	115	<2	<1	100	59
04-4161	Ultramafic / Basalt	(Rock)	62.18	14.05	5.65	0.018	7.10	0.86	4.81	0.03	0.51	0.174	0.001	0.005	7	33	<2	90	20	10
04-4162	Basalt	(Rock)	48.39	14.88	12.65	0.202	7.93	10.96	1.50	0.15	0.89	0.059	0.001	<0.005	<2	39	<2	9	0	57
04-4163	Mn	Sub. A	12.51	10.37	27.66	8.39	6.55	9.16	1.00	0.35	0.40	0.037	0.093	0.117	11	2077	39	212	9950	1290
	Horizon	Sub. B	12.48	10.38	27.64	8.33	6.49	9.08	0.95	0.34	0.40	0.035	0.092	0.109	11	2086	38	215	10600	1270
04-4164	Mn Sand	Sub. A	84.56	2.16	0.91	5.22	0.41	0.07	1.23	0.38	0.49	0.010	0.097	<0.005	<2	194	46	15	12370	583
		Sub. B	85.08	2.09	0.98	5.22	0.42	0.06	1.21	0.38	0.47	0.009	0.094	<0.005	<2	206	48	8	10240	601
04-4165	Conglomerate (34.5 m)	> 2000µm	46.92	31.89	3.06	0.050	1.90	0.11	0.81	0.09	0.71	0.145	0.045	<0.005	<2	38	<2	36	3750	1
		180-2000µm	96.36	2.05	0.63	0.037	0.07	0.01	0.02	0.02	0.11	0.004	0.002	<0.005	<2	31	<2	25	<30	10
		20 - 180 µm	63.98	19.90	2.61	0.136	2.49	0.07	0.12	0.06	0.89	0.030	0.002	0.021	3	72	<2	74	10	61
		< 20 µm	99.61	0.14	0.61	0.006	<0.02	<0.01	0.02	0.00	0.00	0.000	0.000	0.018	5	7	20	16	10	29
04-4166	Ultramafic Clay (36 m)	Sample A	49.95	13.03	8.20	0.025	16.23	0.04	1.10	0.03	0.54	0.027	0.070	6.260	28	21	41	<5	11650	74
		Sample B	50.13	13.18	8.26	0.025	16.11	0.04	1.14	0.03	0.55	0.028	0.072	6.240	27	21	39	<8	10490	69
04-4167	Conglomerate (29 m)	> 2000µm	99.43	0.34	0.76	0.061	0.00	0.00	0.00	0.01	0.03	0.000	0.002	<0.005	<2	32	<2	6	<20	5
		180-2000µm	99.15	0.49	0.63	0.057	0.08	0.01	0.10	0.03	0.11	0.002	0.003	<0.005	<2	20	<2	11	260	8
		20 - 180 µm	nd	nd	nd	nd	nd	nd	nd	nd	nd	nd	nd	0.030	<2	nd	<2	nd	nd	212
		< 20 µm	45.97	32.35	1.65	0.395	0.64	0.10	1.90	1.02	1.14	0.712	0.115	0.007	<2	325	50	14	12020	55
04-4191	Calcite rich		nd	nd	nd	nd	nd	nd	nd	nd	nd	nd	nd	0.052	<2	nd	5	nd	nd	9
04-4192	Mn rich		nd	nd	nd	nd	nd	nd	nd	nd	nd	nd	nd	<0.013	18	nd	11	nd	nd	3290
04-4193	Mn/Calcite		nd	nd	nd	nd	nd	nd	nd	nd	nd	nd	nd	0.013	18	nd	14	nd	nd	1530
04-4194	Mn Sand		nd	nd	nd	nd	nd	nd	nd	nd	nd	nd	nd	0.008	<2	nd	15	nd	nd	319
04-4195	Clay		nd	nd	nd	nd	nd	nd	nd	nd	nd	nd	nd	3.250	6	nd	18	nd	nd	159

Sample	Fraction	Cr	Cs	Cu	Eu	Ga	Ge	Hf	La	Lu	Nb	Ni	Pb	Rb	Sb	Se	Sm	Sr	Th	V	W	Y	Yb	Zn	Zr
04-4159	(Rock)	3620	<1	37	<2	7	<1	<1	1	<0.5	2	884	6	3	0.6	30	1.0	21	<0.5	175	<2	10	1.2	102	2
04-4160	(Rock)	198	2	107	<2	13	<1	1	3	<0.5	1	141	<1	7	<0.2	47	1.6	145	<0.5	271	<2	13	1.7	73	4
04-4161	(Rock)	177	<1	20	<2	20	<1	5	46	<0.5	3	171	5	2	1.1	12	6.6	98	11.4	94	<2	11	<0.5	143	12
04-4162	(Rock)	340	<1	65	<2	18	<1	2	5	<0.5	<1	189	3	7	<0.2	43	2.8	88	<0.5	246	<2	28	3.1	92	4
04-4163	Sample A	494	<1	39	<2	13	<1	<1	53	<0.5	5	615	14	6	0.6	14	5.2	438	2.9	344	<2	56	3.0	589	5
	Sample B	481	<1	40	<2	11	<1	2	50	<0.5	5	619	7	8	0.7	14	5.1	434	3.0	340	<2	52	2.7	585	5
04-4164	Sample A	227	<1	14	<2	4	<1	8	9	<0.5	0	82	<1	2	0.4	4	1.8	165	0.7	118	<2	6	<0.5	16	28
	Sample B	214	<1	34	<2	2	<1	6	9	<0.5	<1	82	<2	3	0.4	4	1.9	163	0.8	120	<2	7	<0.5	23	26
04-4165	> 2000µm	43	<1	22	<2	17	<1	<1	<1	<0.5	1	381	<1	2	0.5	0	<0.2	19	<0.5	72	<2	9	<0.5	33	5
	180-2000µm	232	<1	17	<2	1	<1	<1	1	<0.5	2	42	6	2	<0.2	3	0.2	3	<0.5	12	<2	1	<0.5	9	2
	20 - 180 µm	1880	<1	17	<2	10	<1	20	4	<0.5	3	348	10	4	0.4	27	1.2	19	1.8	55	<2	16	2.2	46	72
	< 20 µm	2800	<1	<1	<2	<1	<1	2	6	<0.5	0	26	<1	3	0.4	38	1.0	2	1.5	2	<2	<3	<0.5	<1	1
04-4166	Sample A	5610	<1	69	<2	12	<1	<1	2	<0.5	1	1652	2	3	1.1	33	0.8	8	<0.5	156	<2	7	<0.5	113	2
	Sample B	5390	<1	65	<2	12	<1	<1	1	<0.5	1	1664	<1	<1	1.1	32	0.8	6	<0.5	152	<2	10	<0.5	118	3
04-4167	> 2000µm	12	<1	<1	<2	<1	<1	<1	1	<0.5	<1	37	<1	4	0.3	<1	<0.2	7	<0.5	7	<2	<1	<0.5	<1	1
	180-2000µm	32	<1	54	<2	<1	<1	<1	1	<0.5	<1	84	<1	2	0.4	1	0.3	6	<0.5	8	<2	0	<0.5	2	1
	20 - 180 µm	220	<1	nd	<2	nd	nd	9	7	<0.5	nd	nd	nd	nd	1.0	7	2.2	nd	3.2	nd	3	nd	1.4	nd	nd
	< 20 µm	290	2	6	<2	37	<1	4	21	<0.5	6	278	<1	28	0.5	17	2.4	69	2.9	72	2	11	<0.5	76	12
04-4191		549	<1	nd	1	nd	nd	<1	14	0.2	nd	nd	nd	nd	0.2	9	3.0	nd	1.8	nd	<2	nd	1.3	nd	nd
04-4192		412	3	nd	12	nd	nd	3	233	1.1	nd	nd	nd	nd	0.6	20	32.4	nd	4.2	nd	<2	nd	7.2	nd	nd
04-4193		321	<1	nd	2	nd	nd	2	65	<0.2	nd	nd	nd	nd	0.7	15	8.2	nd	4.8	nd	<2	nd	1.5	nd	nd
04-4194		672	<1	nd	1	nd	nd	7	8	<0.2	nd	nd	nd	nd	0.4	5	2.0	nd	1.3	nd	2	nd	0.8	nd	nd
04-4195		1180	3	nd	1	nd	nd	3	11	<0.2	nd	nd	nd	nd	0.7	15	2.2	nd	5.2	nd	<2	nd	1.0	nd	nd

nd: not determined

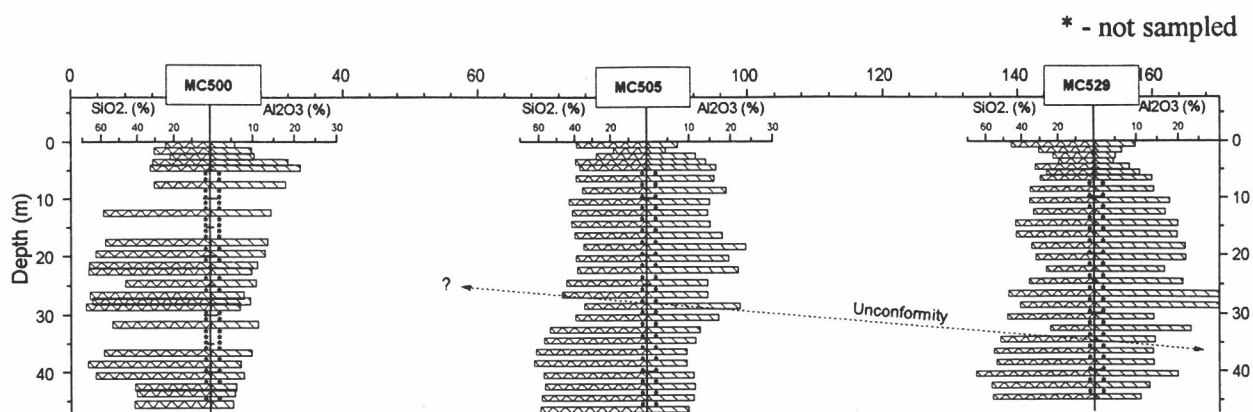


Figure A1.1:  $\text{SiO}_2$  and  $\text{Al}_2\text{O}_3$  for section from Palm to Trial pits.

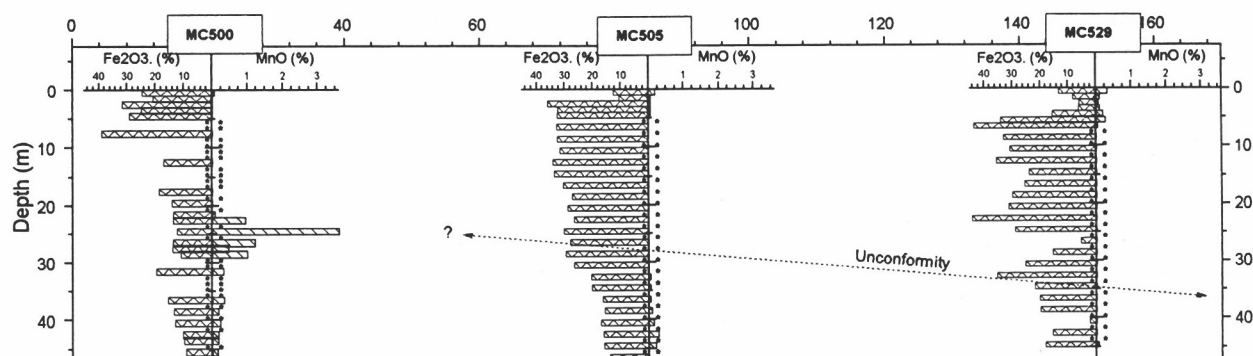


Figure A1.2:  $\text{Fe}_2\text{O}_3$  and  $\text{MnO}$  for section from Palm to Trial pits.

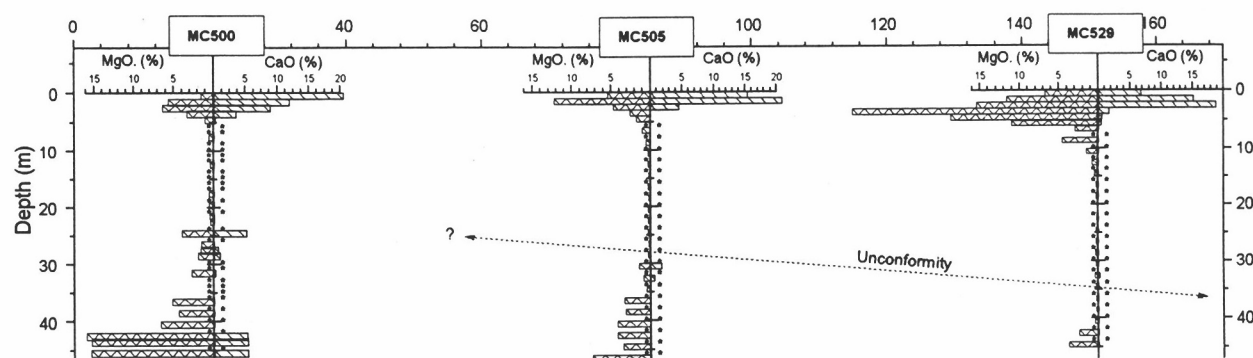


Figure A1.3:  $\text{MgO}$  and  $\text{CaO}$  for section from Palm to Trial pits.

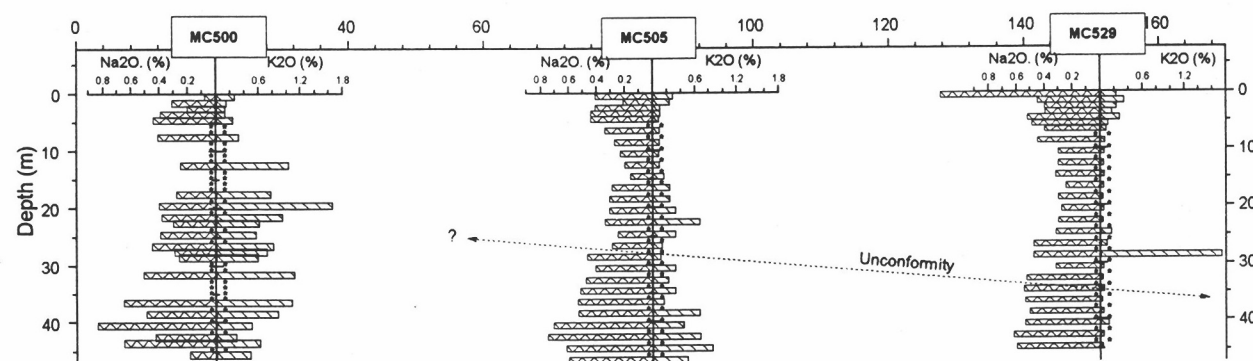


Figure A1.4:  $\text{Na}_2\text{O}$  and  $\text{K}_2\text{O}$  for section from Palm to Trial pits.

\* - not sampled

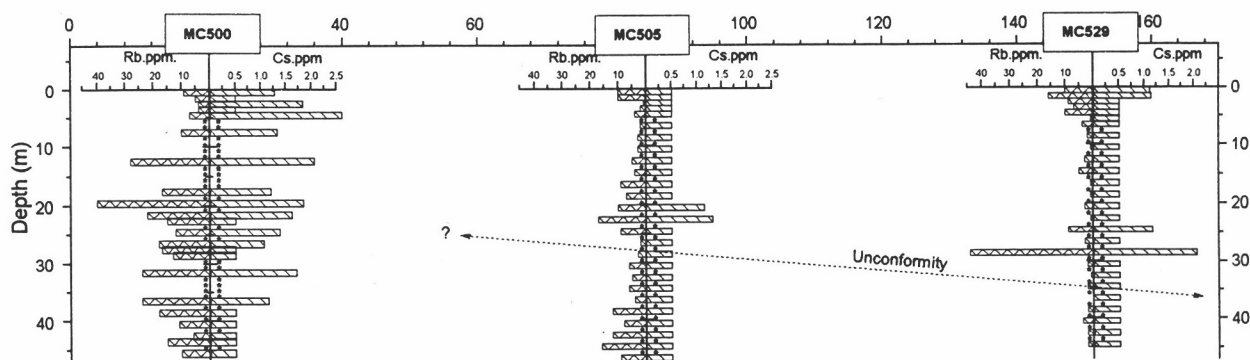


Figure A1.5: Rubidium and Cs for section from Palm to Trial pits.

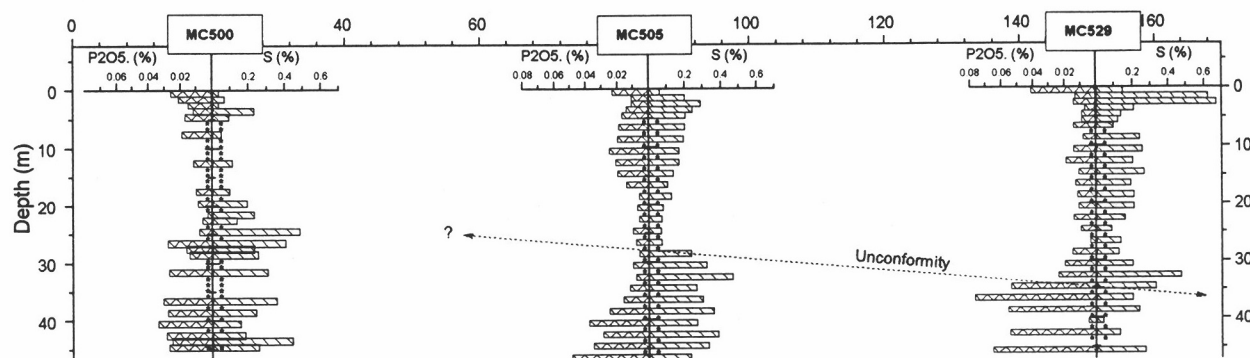


Figure A1.6:  $P_2O_5$  and S for section from Palm to Trial pits.

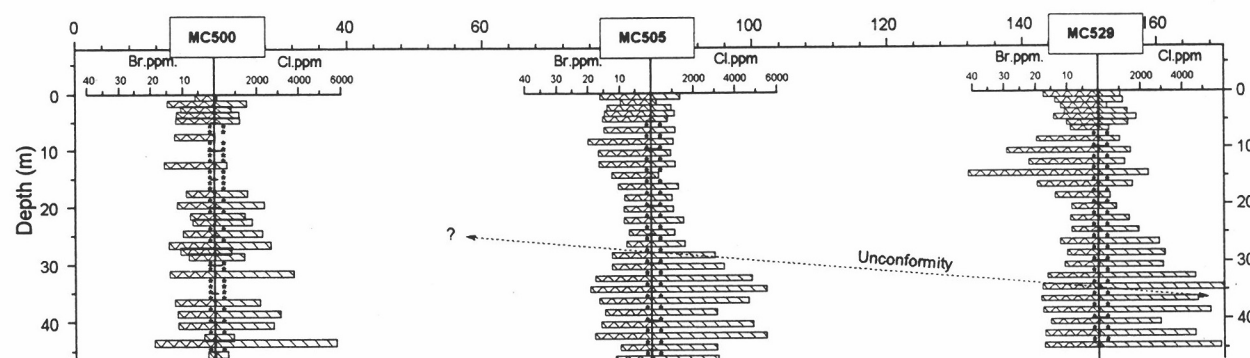


Figure A1.7: Bromine and Cl for section from Palm to Trial pits.

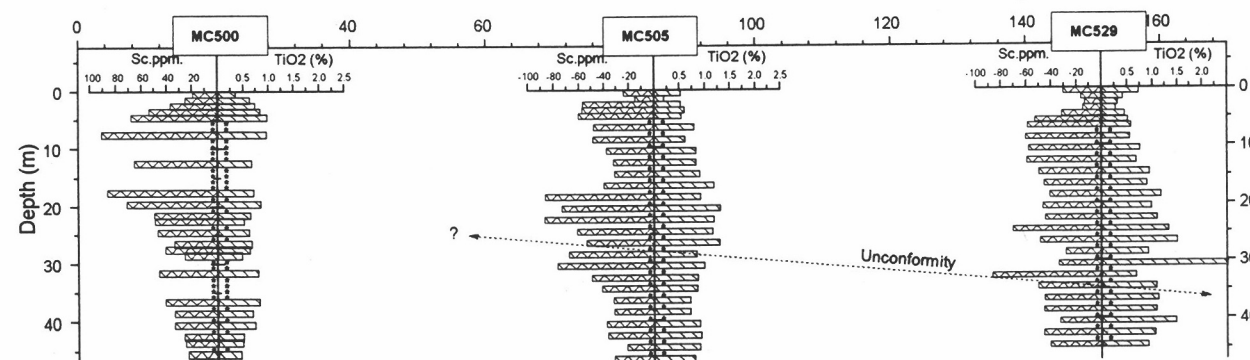


Figure A1.8: Scandium and  $TiO_2$  for section from Palm to Trial pits.

\* - not sampled

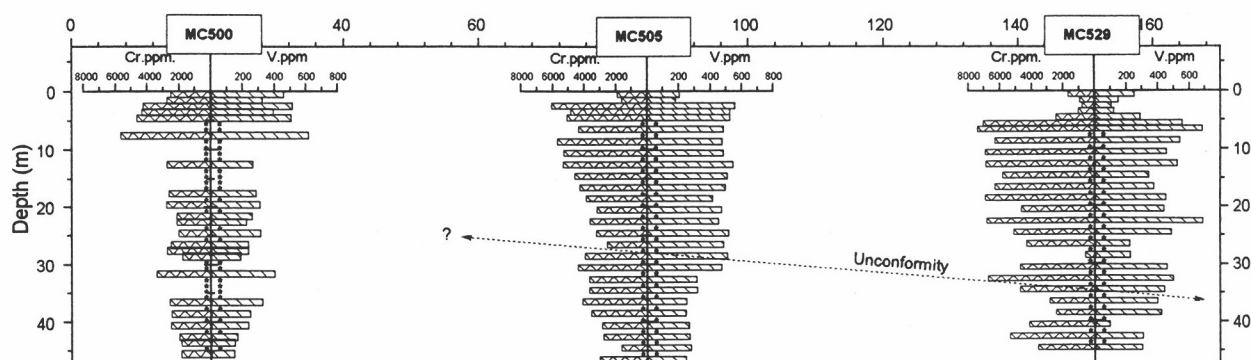


Figure A1.9: Chromium and V for section from Palm to Trial pits.

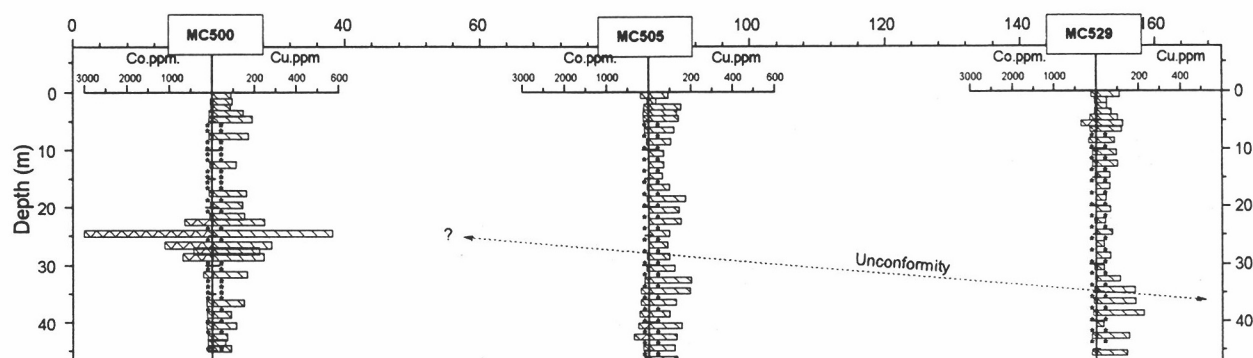


Figure A1.10: Cobalt and Cu for section from Palm to Trial pits.

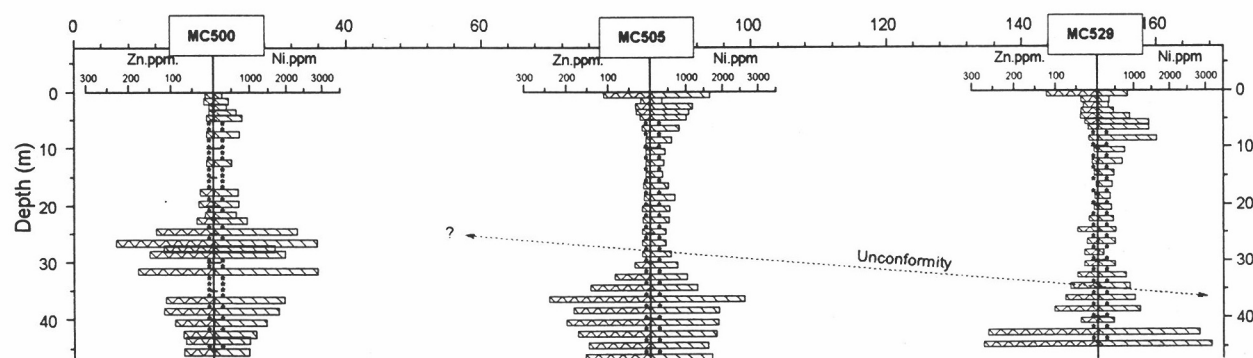


Figure A1.11: Zinc and Ni for section from Palm to Trial pits.

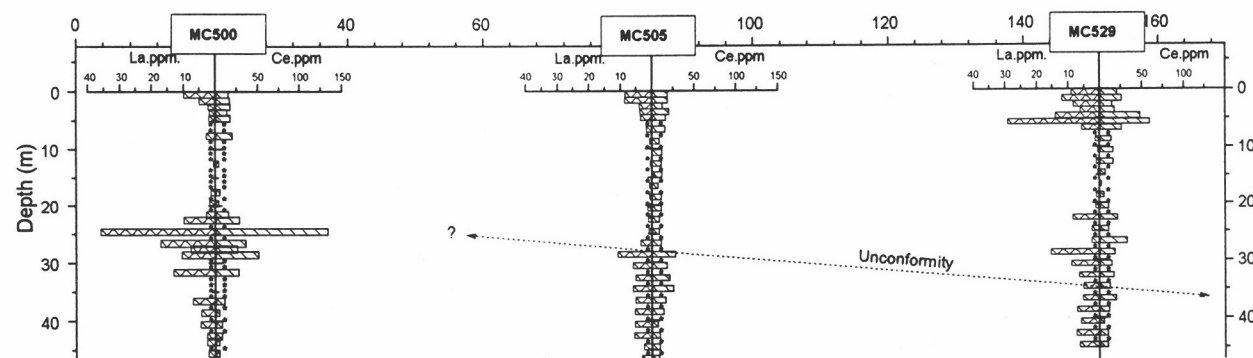


Figure A1.12: Lanthanum and Ce for section from Palm to Trial pits.

\* - not sampled

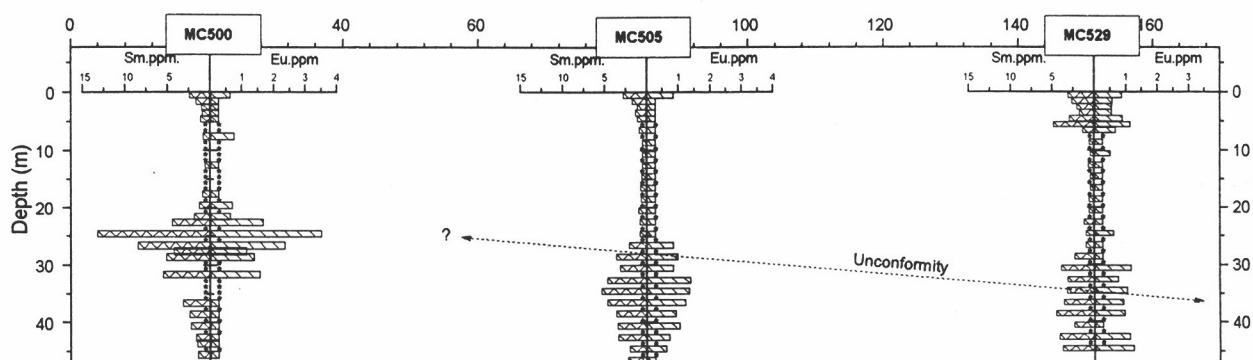


Figure A1.13: Samarium and Eu for section from Palm to Trial pits.

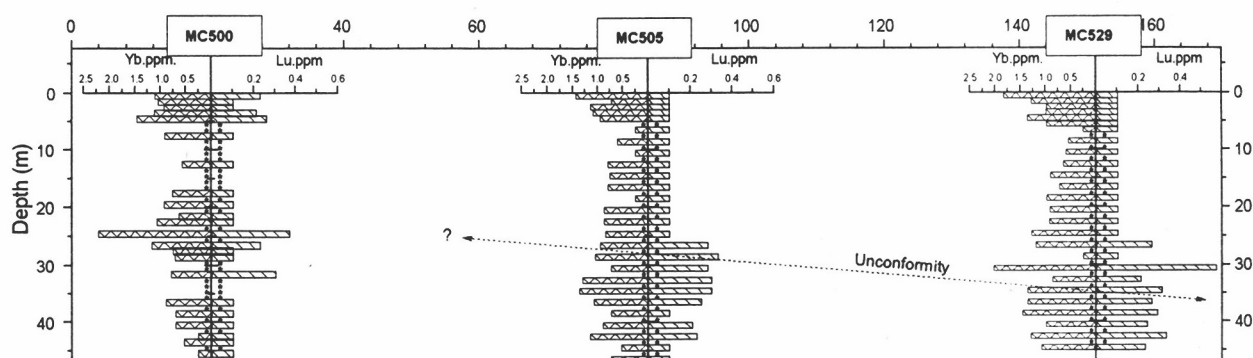


Figure A1.14: Ytterbium and Lu for section from Palm to Trial pits.

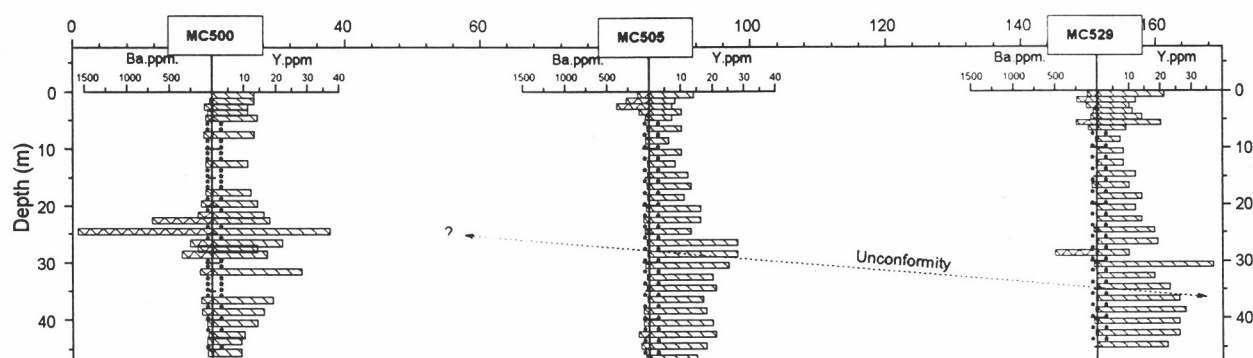


Figure A1.15: Barium and Y for section from Palm to Trial pits.

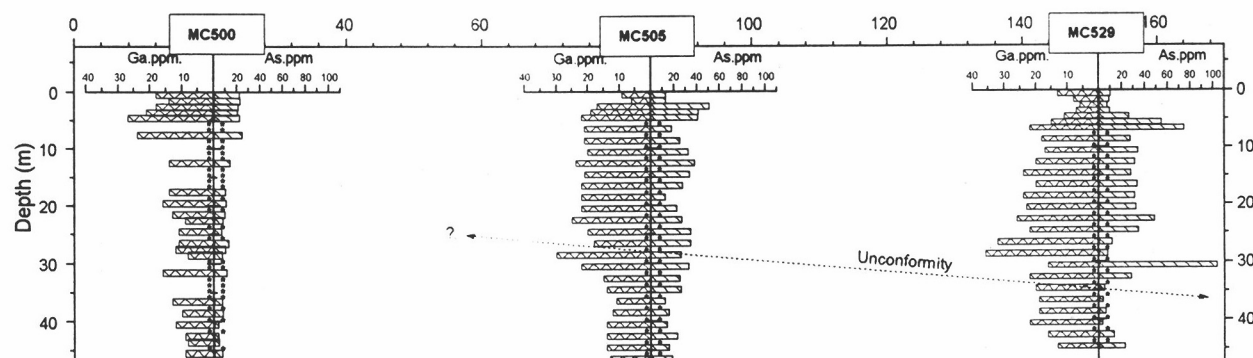


Figure A1.16: Gallium and As for section from Palm to Trial pits.

\* - not sampled

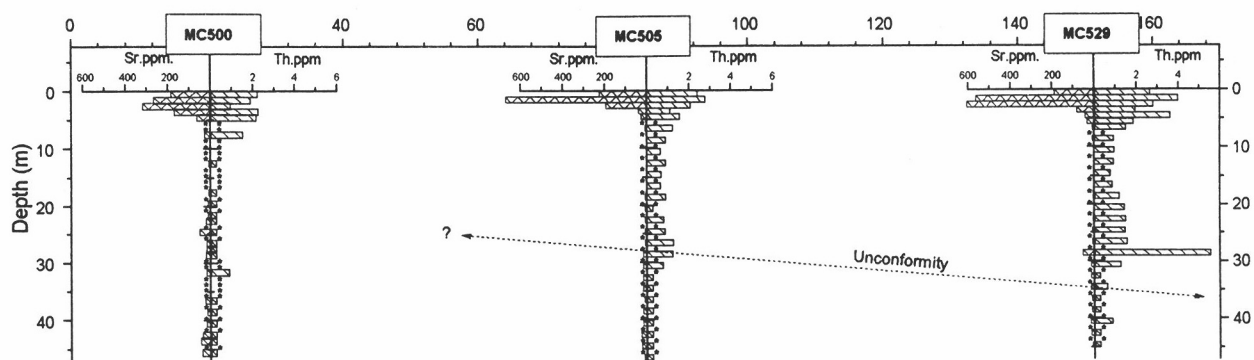


Figure A1.17: Strontium and Th for section from Palm to Trial pits.

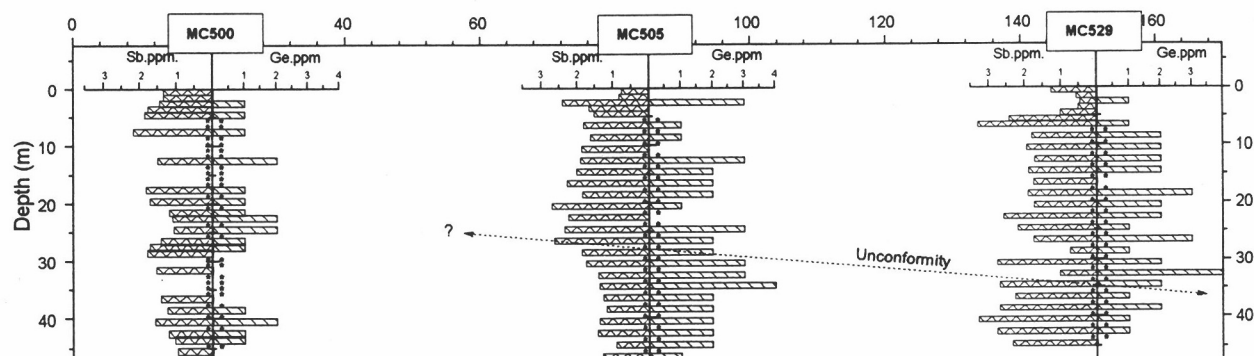


Figure A1.18: Antimony and Ge for section from Palm to Trial pits.

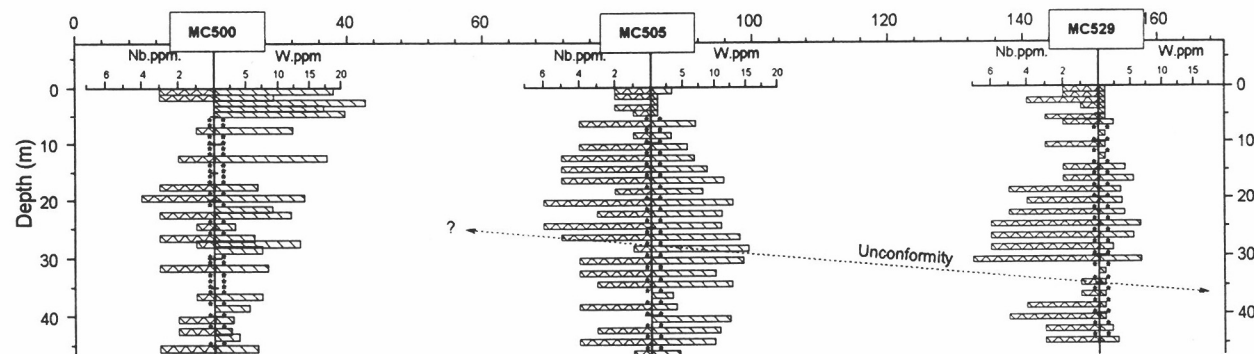


Figure A1.19: Niobium and W for section from Palm to Trial pits.

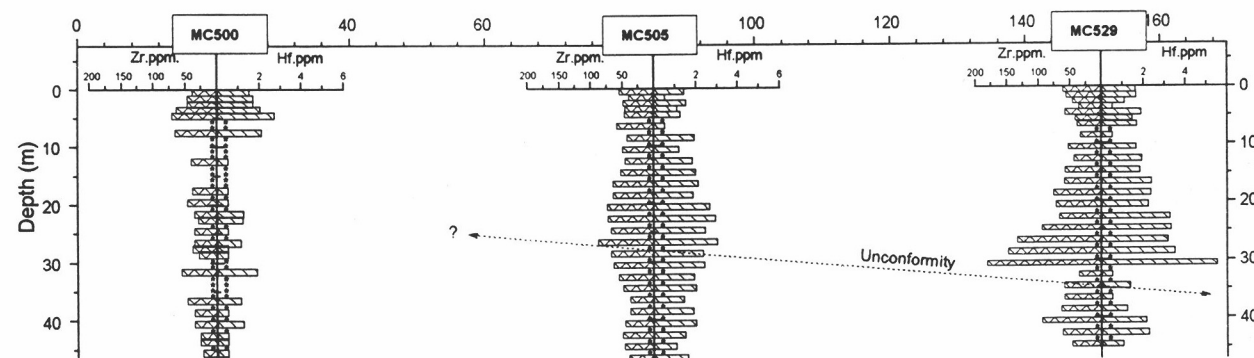


Figure A1.20: Zirconium and Hf for section from Palm to Trial pits.

\* - not sampled

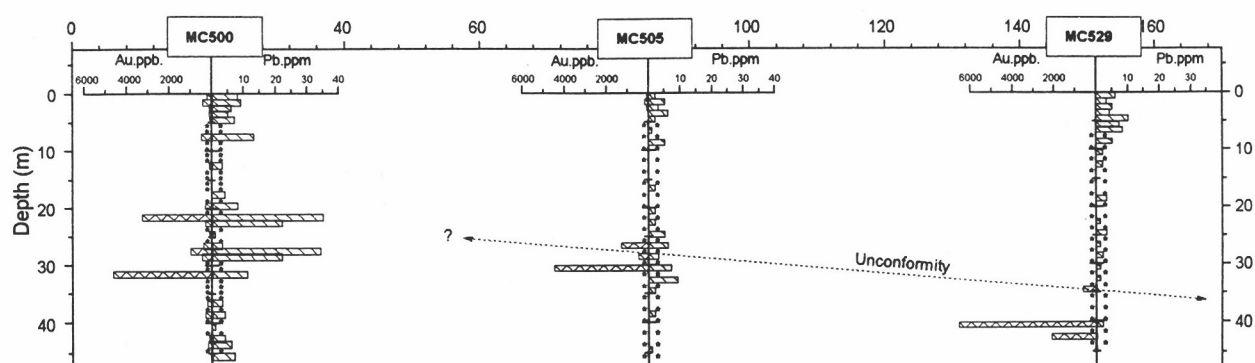


Figure A1.21: Gold and Pb for section from Palm to Trial pits.

## Appendix 2: X-ray Diffraction Data

Sample	Profile/ Description	Depth	Horn- blende	Feld- spar	Chlorite/ Smectite	Talc	Mica	Quartz	Ana- tase	Rut- ile	Kaolin	Goe- thite	Hema- tite	Crypto- melane	Lithio- phorite	Palygor- skite	Cal- cite	Dolo- mite	Magne- site	Gyp- sum	Hal- ite
04-4001	MC500	0.5 m		?	?			X	X	X	XX	XX	XXX			XX	XXX				
04-4003	"	2.5 m			X		X	XX		X	XXX	XX	XXX				X	XXX			
04-4005	"	4.5 m			?			XX		X	XXX	XXX						X			
04-4019	"	17.5 m					XXX	XX	?	X	XXX	XX						X			
04-4021	"	21.5 m					XXX	XXX		X	XXX	XXX						X			
04-4023	"	24.5 m				XX	XXX	XXX		X	XXX	XX	?					XXX		?	
04-4025	"	27.5 m			XX		XXX	XXX		X	XXX	XX						X			
04-4027	"	31.5 m			XXX		XXX	XXX		X	XXX	XXX									
04-4028	"	36.5 m			XXX		XXX	XXX		X		X	?								
04-4029	"	38.5 m			XXX		XXX	XXX		X		X	X								
04-4030	"	40.5 m			XXX		XX	XXX		X		X	X					X			
04-4033	"	45.5 m			XXX		XXX	XX										XXX	XXX		
04-4075	MC505	0.5 m			XX	X		XXX			XX	X	X				XXX	XX			
04-4076	"	1.5 m			X	X		X			XX	X	X				X	XX			
04-4077	"	2.5 m			X	XX		X			XXX	XX	XXX					X			
04-4078	"	3.5 m			X	XX		X			XXX	XXX	X								
04-4079	"	4.5 m			X	XX		X			XXX	XXX	XX								
04-4172	"	14.5 m						XX	X	X	XXX	XXX	XXX								
04-4176	"	22.5 m					XX	XX		X	XXX	XXX	XXX				X				
04-4180	"	30.5 m					XX	XX	X	X	XXX	XXX	XX				X	X		?	
04-4184	"	38.5 m			XXX		XXX	XXX	XX	X	?	XX	XX				X	X		?	
04-4188	"	46.5 m			XXX		XX	XXX		X	?	XX						X			
04-4133	MC529	0.5 m		X	XXX	X		XX	X	X	XXX	XX					XX	XXX			
04-4134	"	1.5 m			XX	XX		XX			XX	X						XXX			
04-4135	"	2.5 m			XX	XX		XX			XX	X						XXX			
04-4136	"	3.5 m			XX	XX		XX	X		XXX	X	X			X		XX	X		
04-4137	"	4.5 m			XX	XX		XX	X		XXX	X	XX			XX		XXX	XXX	?	
04-4140	"	8.5 m				XXX		X			XXX	XXX	XX					XXX	X		
04-4143	"	14.5 m						XX		X	XXX	XXX	XXX								
04-4146	"	20.5 m						XX		X	XXX	XXX	XX								
04-4149	"	26.5 m						X	X	X	XXXX	XX									
04-4150	"	28.5 m					XXX	X			XXXX	XXX									
04-4151	"	30.5 m						XX	X	XX	XXX	XXX									
04-4153	"	34.5 m						XXX	X	X	XXX	XXX						X			
04-4156	"	40.5 m						XXX	XX	XX	XXXX	X						X			
04-4159	Ultramafic		XXX		XXX	XX		?													
04-4160	Basalt			XXXX	X			X													
04-4161	Ultramafic / Basalt			XXX	XXX			XX													
04-4162	Basalt		XXX	XX	XXX			XX													
04-4163	Mn Horizon							X			XXX	XXX	?		X		X	XX			
04-4164	Mn Sand					?		XXX	XX		XXX			XX							XX
04-4165	Conglom. > 2000µm 180 - 2000µm 20 - 180µm <20µm				XX			XXX	XX		XX										
					XXX	XX		XXX	XX		XXX	X									
					XX	XX		X			XXX	XX									
04-4166	Ultramafic Clay					XXX					XXX	XX									X
04-4191	Calcite rich										XXX						X	XXX			
04-4192	Mn rich										XXX	XXX			XXX						
04-4193	Mn/Calcite										XXX	XXX			XXX		X	XX			
04-4194	Mn Sand							XXX	XX		XXX			XXX							X
04-4195	Clay							X			XXX	XX									

### Key

? Presence uncertain (due to interference from other reflections)  
 X Trace  
 XX Minor  
 XXX Major  
 XXXX Dominant

### Appendix 3: X-ray Diffraction of Sedimented Aggregates

Samples were prepared by shaking in deionized water with sufficient Calgon (sodium metaphosphate) for proper dispersion and then a  $< 2 \mu\text{m}$  fraction, as defined by Stokes' Law (McIntyre, 1974), was collected by siphoning off a small sample at 10 cm depth, 8 h after agitation, at 20°C. This suspension was then filtered through a ceramic tile and the clay material on the tile surface then saturated with a particular cation and washed with deionized water, forming a sedimented aggregate for XRD analysis.

Magnesium-saturated sedimented aggregates were examined saturated with water, air-dry and after equilibration with glycerol [abbreviated Mg(wet), Mg(ad) and Mg(gly)]. Potassium-saturated sedimented aggregates were examined saturated with water, air-dry and after stepwise heat treatment from 110° up to 550°C [K(wet), K(ad), K(110), K(300), K(550)]. Li-saturated sedimented aggregates were used to distinguish beidellite from montmorillonite (Greene-Kelly, 1953) and were examined saturated with water, air-dry, heated to 300°C, and treated with glycerol subsequent to heating to 300°C [Li(wet), Li(ad), Li(300) and Li(300-gly)].

The diffractometer was calibrated in the  $2 - 14^\circ 2\theta$  region using the poly-alcohol tetradecanol (Brindley, 1981). The combined results are given overleaf, with brief explanations of the interpretations given below. Readers are directed to standard texts (e.g., Brindley and Brown, 1980) for further details. Where other specific results from other sources are utilized, these will be referenced in the text.

#### 04-4003

The major reflection observed below  $14^\circ 2\theta$  is at  $7.22 \text{ \AA}$ , due to kaolinite. This reflection is unaffected by cation or heat treatment up to 300°C. At 550°C the reflection disappears, reflecting a decomposition of the kaolinite at this temperature. Small concentrations of mica are present, as indicated by the reflection at  $10 \text{ \AA}$  in the Mg-saturated sample. A small reflection at about  $9.5 \text{ \AA}$  may be due to trace concentrations of talc.

Smectite, a swelling mineral, is also present. This is evidenced by the reflection at about  $16 \text{ \AA}$  in the Mg(dry) XRD pattern, which swells to  $20 \text{ \AA}$  when wet and to  $18 \text{ \AA}$  when glycerated, and collapses to  $10 \text{ \AA}$  when heated, consistent with known properties of smectite. When heated with Li and then glycerated, the reflection re-swells to  $20 \text{ \AA}$ , indicating the smectite to be beidellitic, as would be expected if the smectite had originated from the degradation of chlorite.

Small concentrations of chlorite (a primary mineral) are observed. The chlorite reflection is at  $14.3 \text{ \AA}$ , causing interference from smectite. However, the chlorite reflection can be most clearly observed in the K(550) pattern, due to the removal of the smectite interference, and the increase in the intensity of the chlorite reflection (Brindley and Ali, 1950).

Thus, the clay minerals observed in 04-4003 are kaolinite (major), smectite (major), chlorite (minor), mica (minor) and talc (possible trace).

#### 04-4075

The major mineral observed is chlorite, with a 001 reflection (*i.e.*, equal to the spacing of the unit cell) at  $14.5 \text{ \AA}$  and a 002 reflection at  $7.16 \text{ \AA}$  (*i.e.*, at half the d-spacing of the 001 reflection). In unweathered chlorites the  $14.5 \text{ \AA}$  reflection has a considerably lower intensity than the  $7.16 \text{ \AA}$  reflection: however, in this sample the two reflections have similar intensities. This alteration is commonly observed in partially weathered horizons (Gray, 1986), and has been simulated in the laboratory by artificial oxidation of Fe(II)

in chlorites (Ross and Kodama, 1974; Borggaard *et al.*, 1982). At 550°C the intensity of the 14.5 Å reflection is enhanced and that of the 7.16 Å reflection severely reduced, similarly to previous observations (Brindley and Ali, 1950; Gray, 1986).

The 7.16 Å reflection of chlorite will interfere with analysis for kaolinite using the 7.2 Å reflection. The presence of kaolinite is indicated by the diagnostic 1.490 Å reflection in the standard XRD pattern (not shown). There is a minor 10 Å reflection due to mica.

Thus, the clay minerals identified in 04-4075 are chlorite (partially oxidized but structurally intact), kaolinite (major) and mica (minor).

#### 04-4133

The major clay mineral observed in 04-4133 is a complex weathered chlorite. When Mg saturated, the 14.5 Å and 7.23 Å reflections observed are those expected for chlorite, though the relative intensities are strongly altered, suggesting significant oxidation of the interstitial Fe (discussed for 04-4075), and/or degradation of the chlorite. In addition, there are higher order reflections not commonly observed for a simple chlorite. Thus, for example, in the Mg(dry) pattern there are additional 30 Å (2 times 14.5 Å) and 9.6 Å (30 Å divided by 3) reflections. This infers that the crystal is composed of two different phases, both with a spacing of about 14.5 Å when Mg saturated.

When K-saturated and heated [the K(550) pattern provides the best example] the phase is observed to have a spacing of about 24 Å, giving 12.3 Å (24/2) and a 8.1 Å (24/3) reflections. When Li-saturated, heated to 300°C and then glycerated the reflection returned to its unheated spacing, indicating a beidellitic/vermiculitic phase. Thus the mineral is a interstratified (*i.e.*, mixture of) chlorite/vermiculite and presumably represents the first stage in the weathering of chlorite. Similar minerals have been observed during initial weathering of chlorite in the Northern Territory and at other sites through-out the world (Gray, 1986 Section 3.3.3 and references given therein)

The presence of kaolinite is confirmed by the 7.2 Å reflection in the K saturated patterns. As expected, this reflection is lost when heated to 550°C.

Thus, the clay minerals observed in 04-4133 are interstratified chlorite/vermiculite (essentially partially degraded chlorite) and kaolinite.

#### 04-4137

Chlorite (partially oxidized but structurally intact) is indicated by the 14.5 Å and 7.2 Å reflections, altered in intensity with heating to 550°C. The sharp, stable reflection at 9.5 Å represents talc, with the reflection at 10.7 Å thought to be due to palygorskite. The presence of smectite is indicated by reflections at 18 Å in the Mg(gly) and at 20 Å in the Mg(wet) patterns. This smectite is indicated to be beidellitic by the re-swelling of the reflection to 19 Å when the sample was Li-saturated, heated to 300°C and then glycerated. Kaolinite was indicated by the 1.490 Å reflection.

Thus, the clay minerals observed in 04-4137 are chlorite, beidellitic smectite, talc, palygorskite and kaolinite

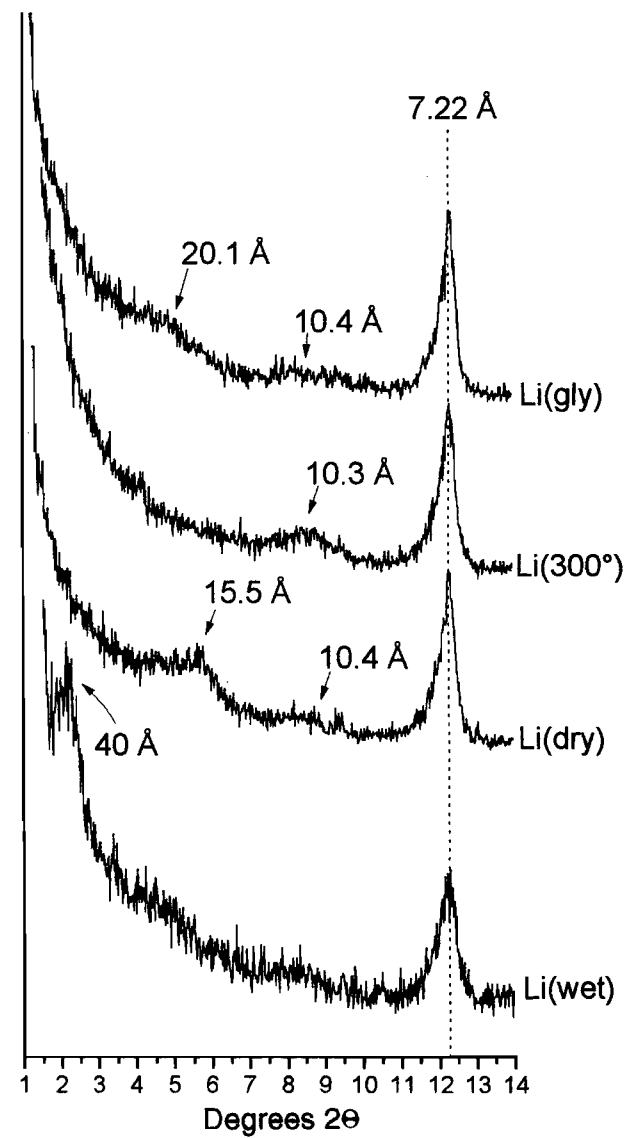
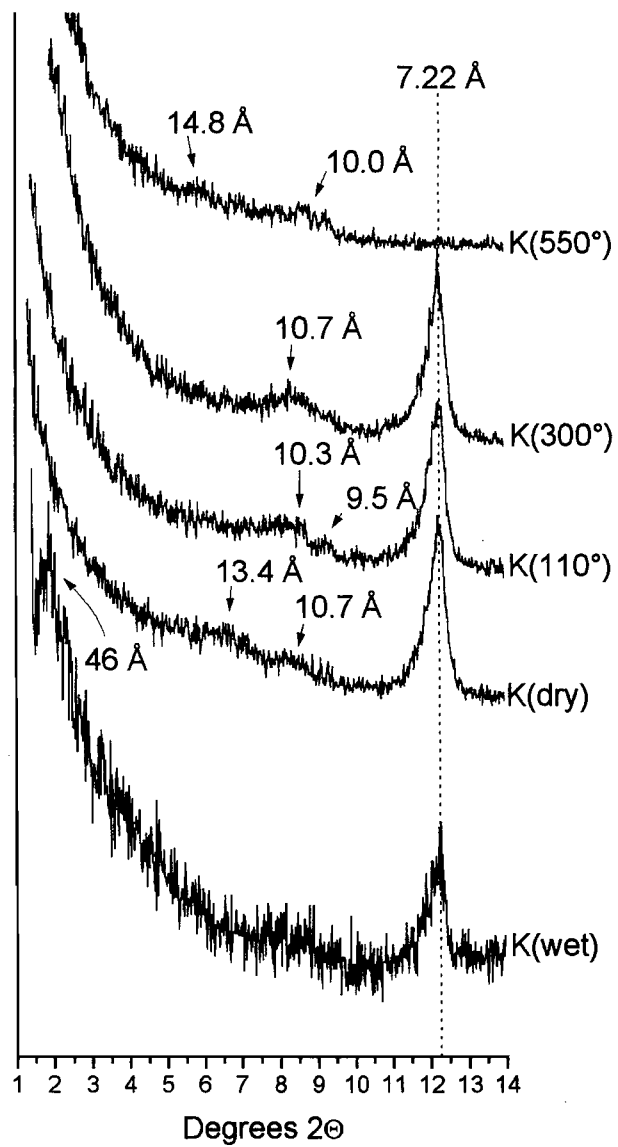
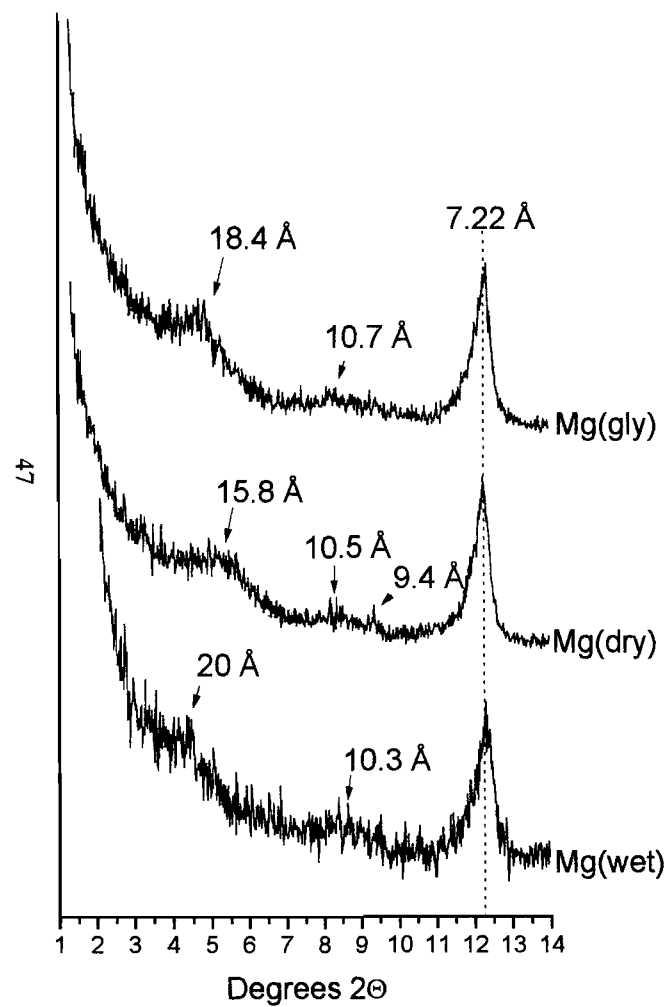
#### 04-4166

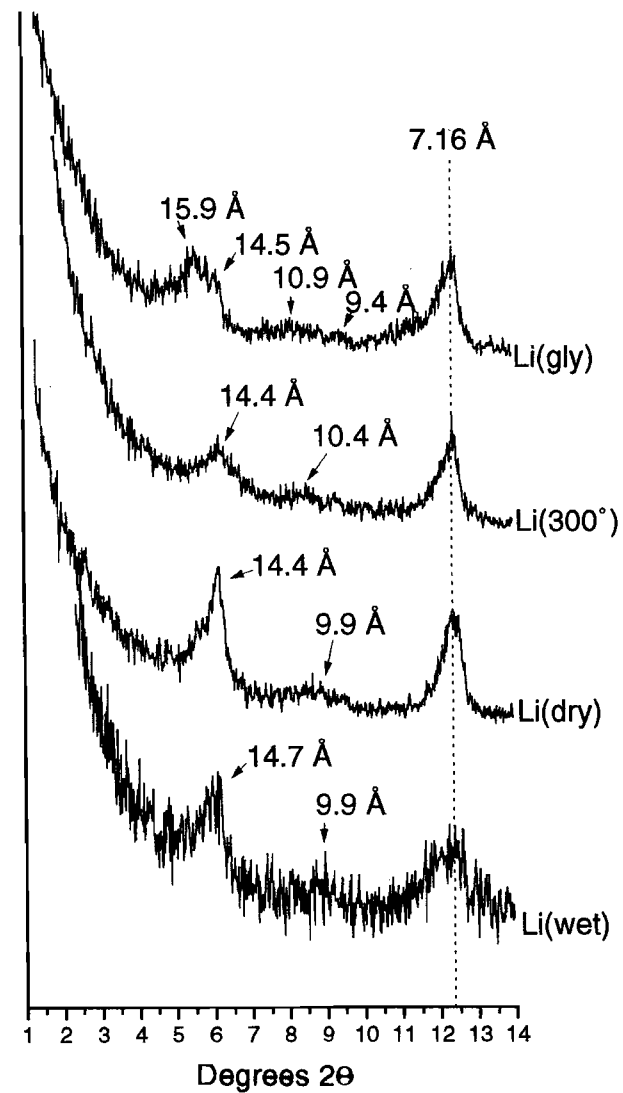
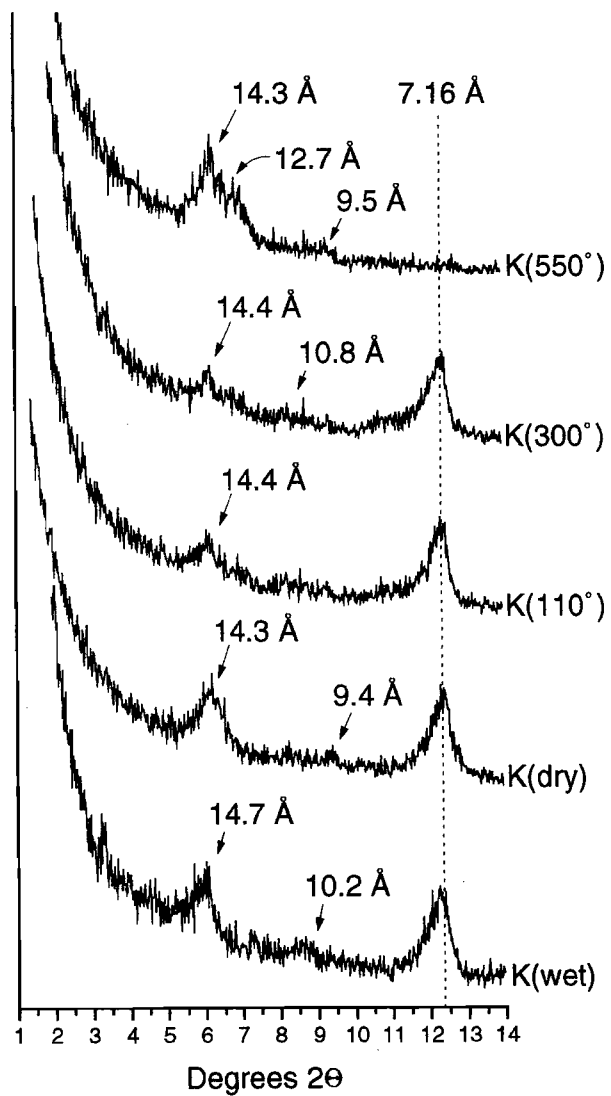
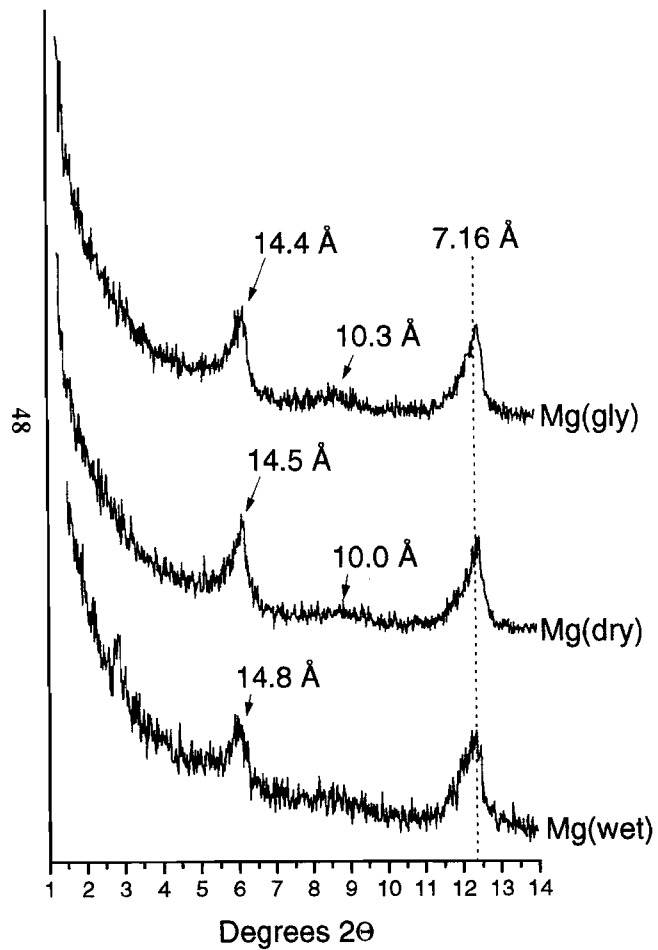
The two reflections observed below 14°2 $\theta$  are at 7.22 Å, due to kaolinite, and at 9.4 Å, due to talc.

**04-4184**

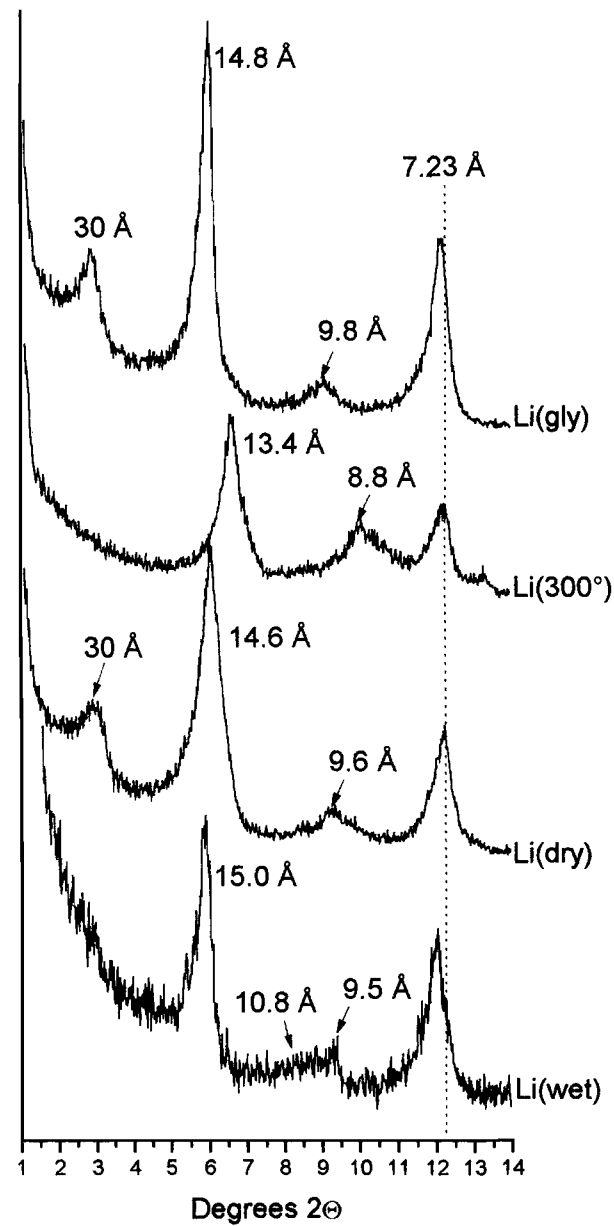
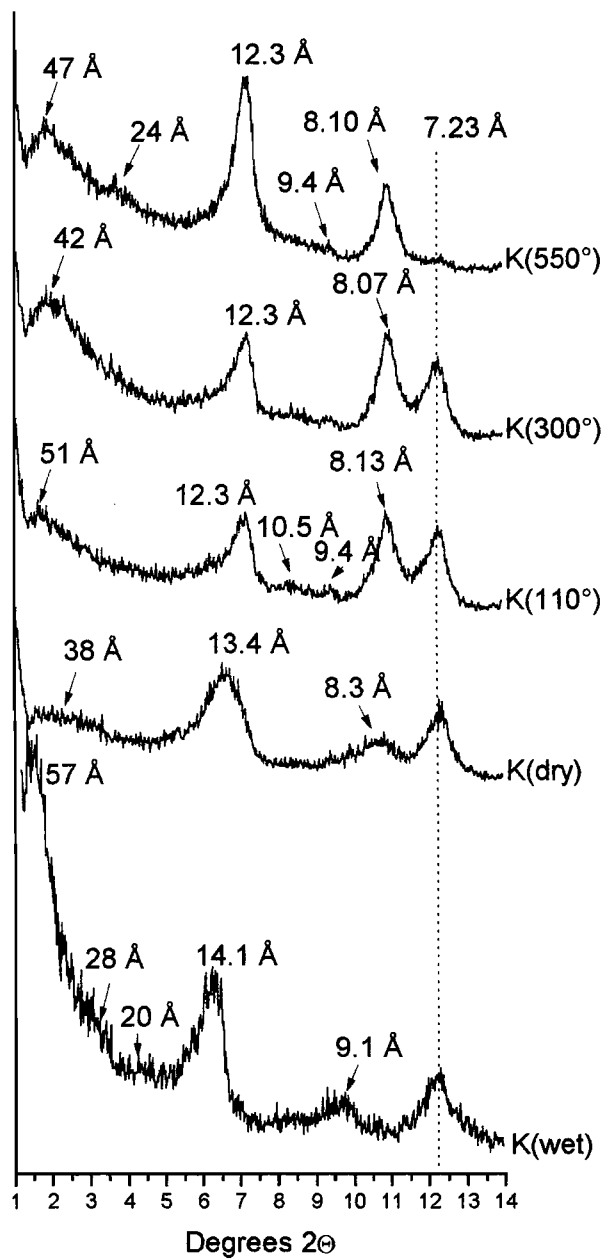
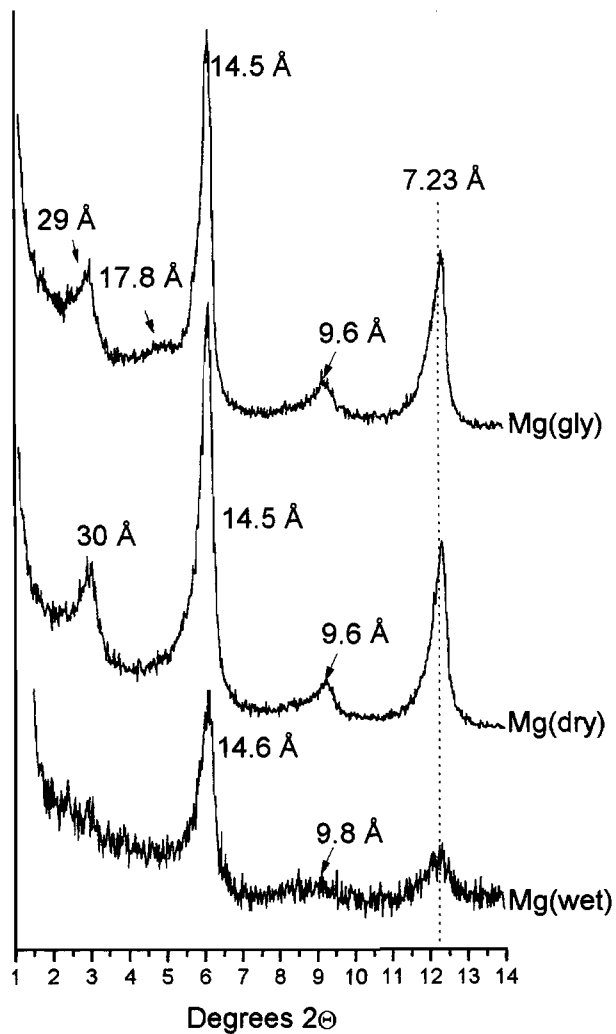
Two chloritic phases are observed. The first mineral has reflections at 14.4 Å and 7.2 Å, and is only affected when heated to 550°C. These properties are very similar to the partially oxidized chlorite observed in 04-4075. The second mineral does not swell when Mg-saturated and wetted or glycerated, but collapses to a spacing of 12.5 Å when K-saturated and heated, and re-swells when the sample was Li-saturated, heated to 300°C and then glycerated. These properties are very similar to the interstratified chlorite/vermiculite observed in 04-4133. There is a separate mica phase. The 1.490 Å kaolinite reflection was not distinguished.

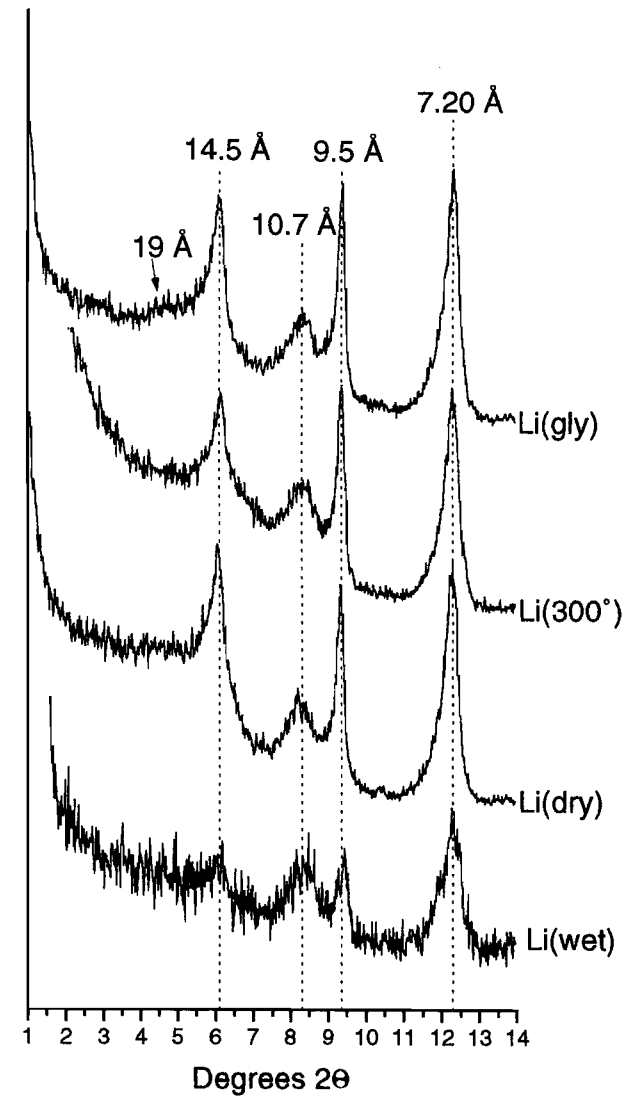
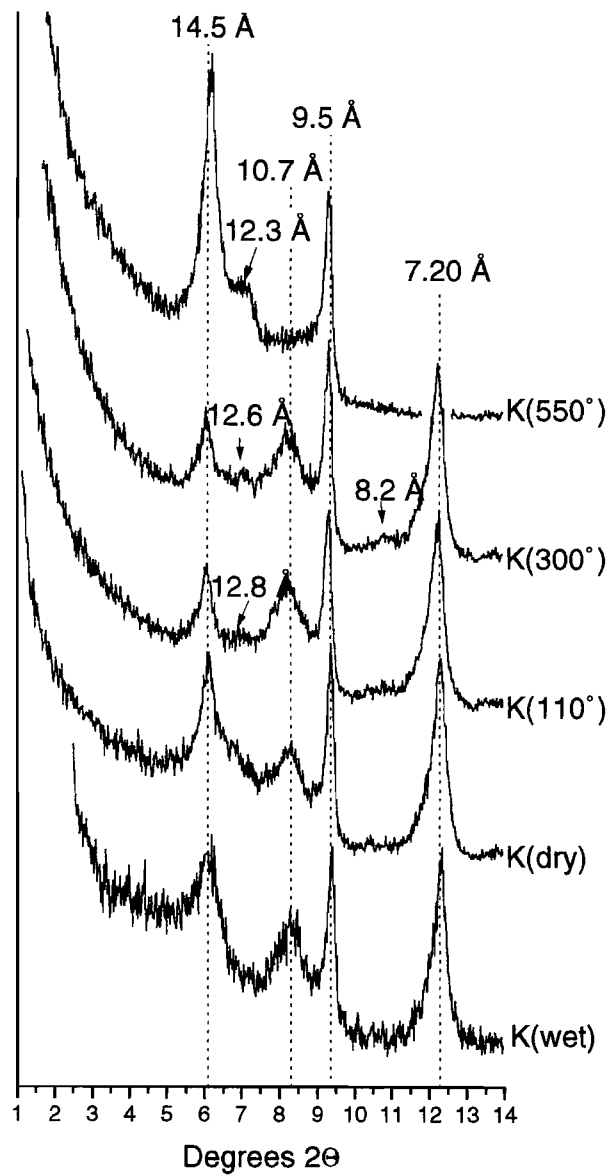
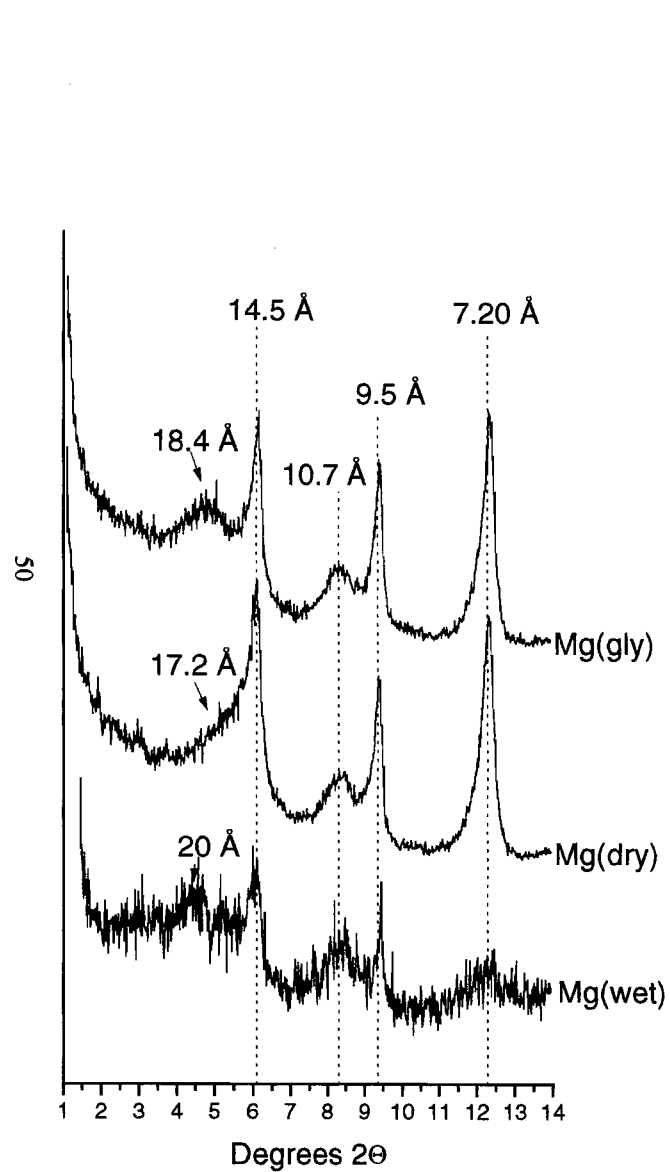
Thus, the clay minerals observed in 04-4133 are chlorite (partially oxidized but structurally intact), interstratified chlorite/vermiculite (essentially partially degraded chlorite) and mica.

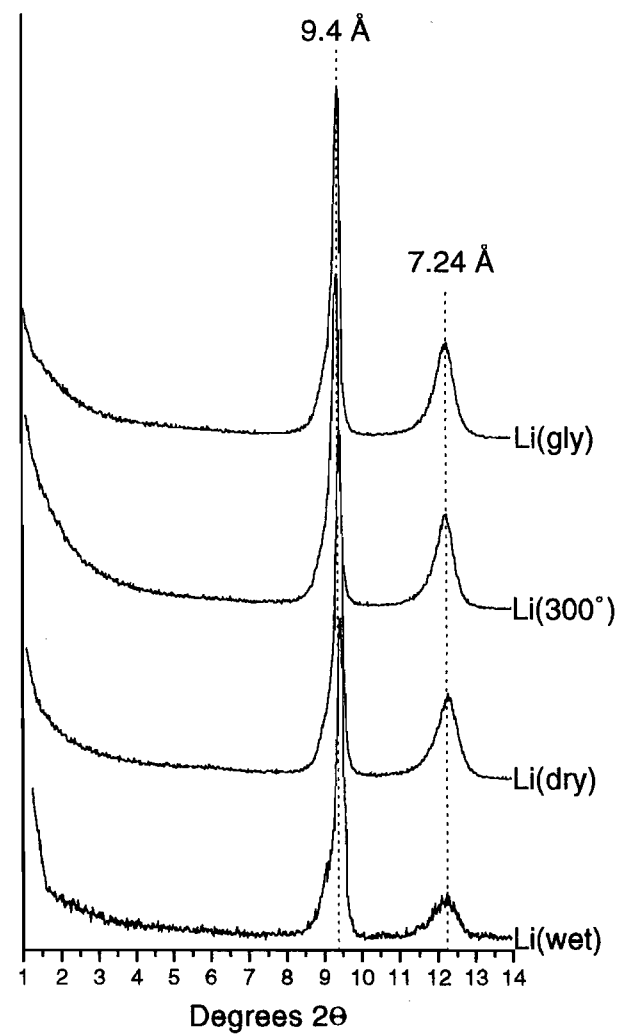
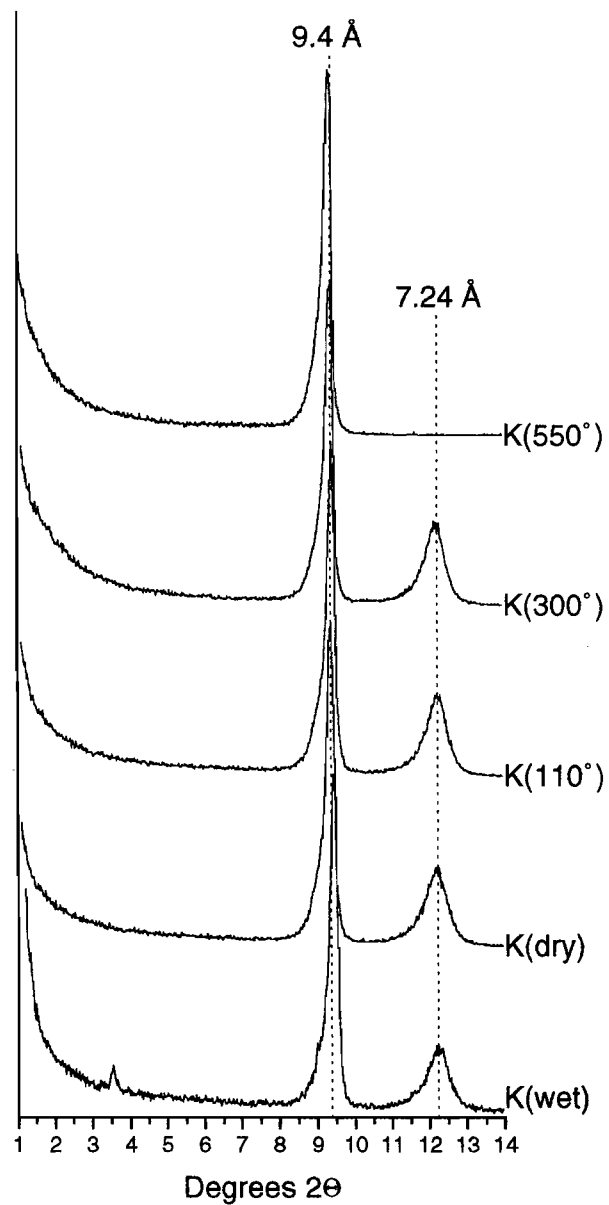
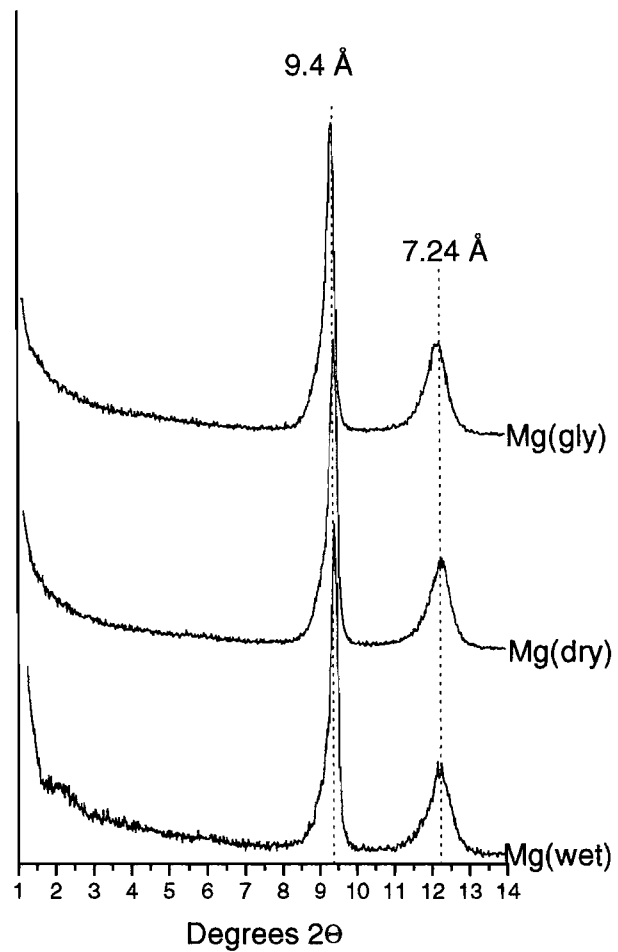


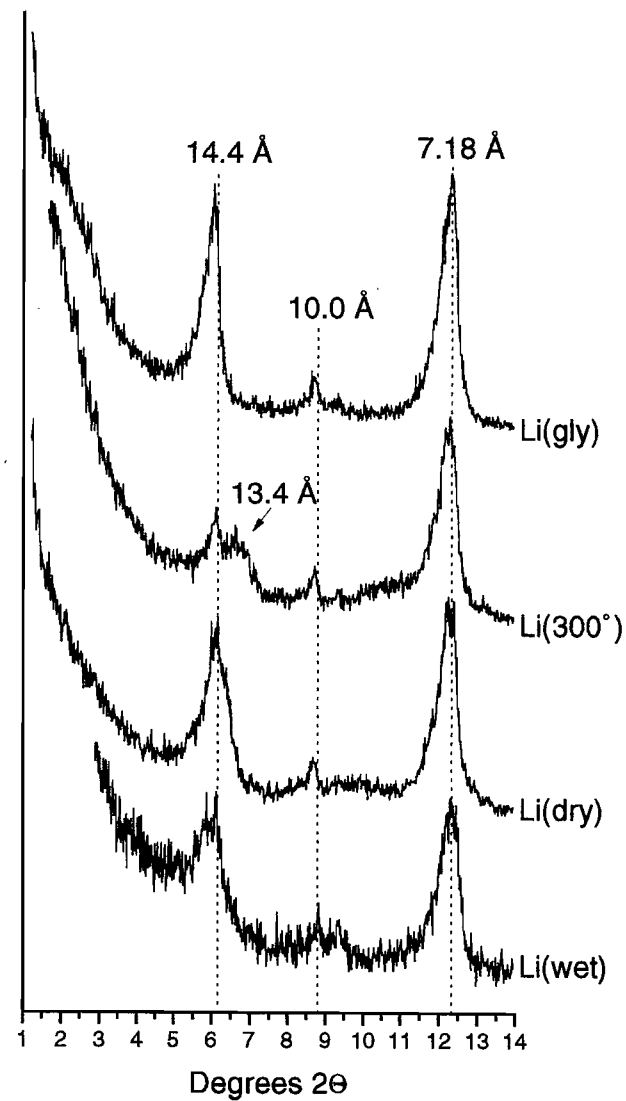
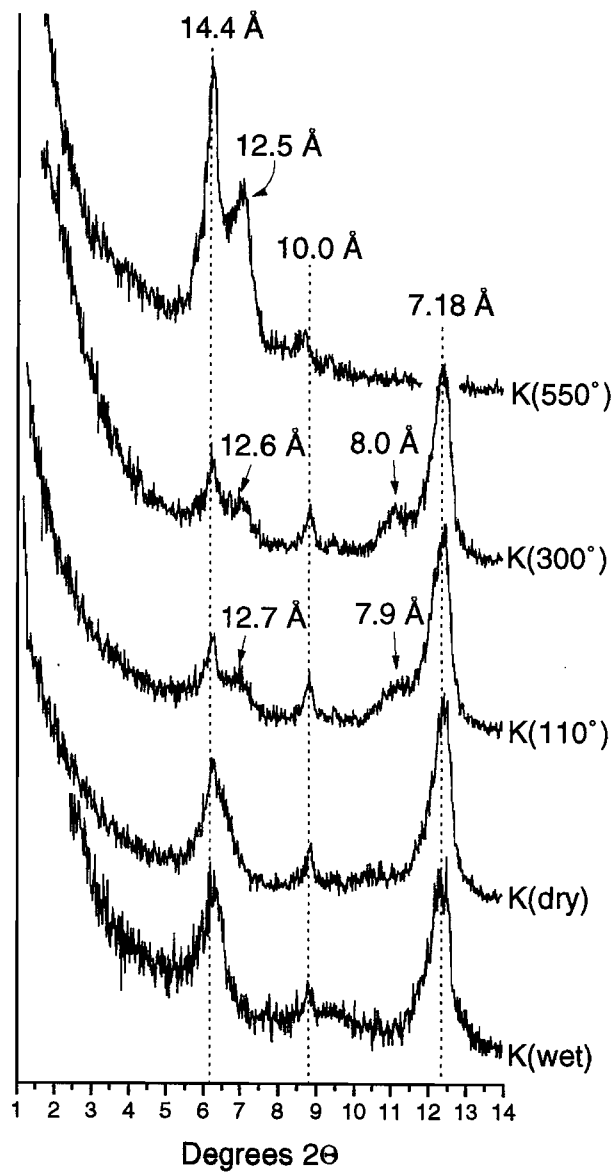
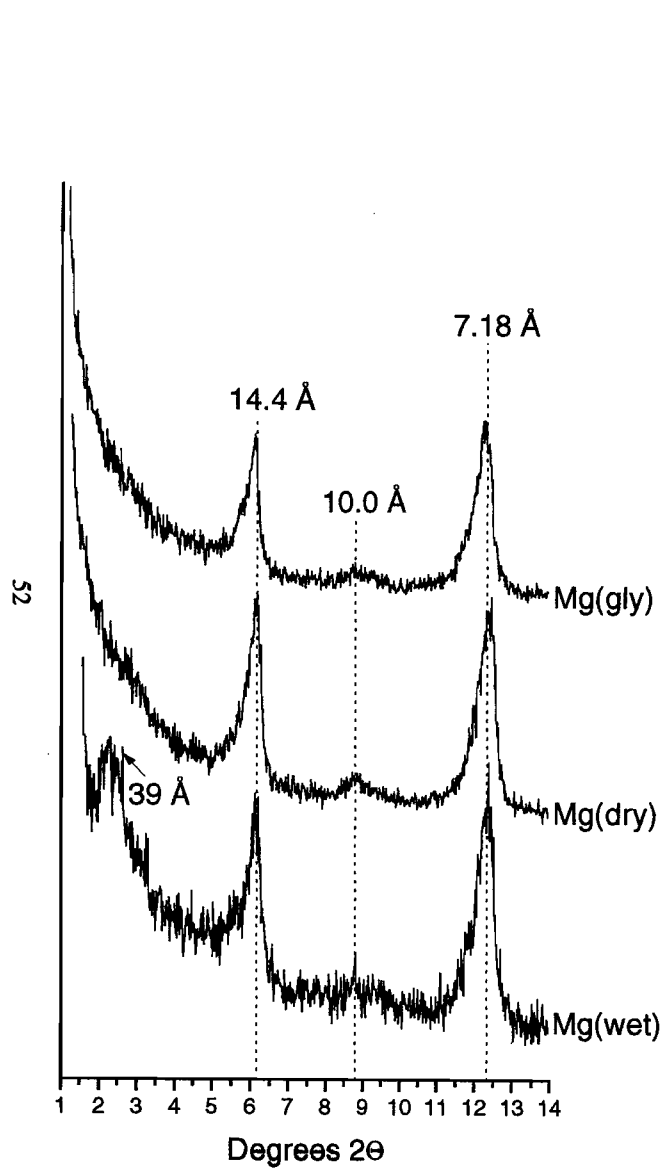


Sedimented Aggregate XRD Analysis of 04-4075









## Appendix 4: Correlation Coefficient Tables for Mulgarrie solids.

Four different data sets are shown here:

- (i) Drill holes MC500, MC505 and MC529;
- (ii) Samples from the top 5m of the three drill holes;
- (iii) Samples from below 5m depth for the three drill holes;
- (iv) high Mn samples from MC500.

The first page lists the important statistical data for each variable (minimum, maximum, median, mean and standard deviation. Also listed are the number of samples and the correlation coefficients required for the correlation to be significant to the 95%, 99% and 99.9% significance level.

The coefficients are then listed in the following pages. Correlations significant to 99.9% are listed in a large bold font, those significant to 99% in a large italics font and those significant to 95% in a large font. Correlations with significance less than 95% are listed in a small font.

**Appendix 4A: Correlation Coefficients for Data Set 1: all MC500, MC505 and MC529 Samples.**

Number of samples=74                      0.193   0.27   0.375  
 Degrees of Freedom=72                    95%   99%   99.9%

	Minimum	Maximum	Median	Mean	Std Dev
Depth	0.5	46.5	22	22	14
SiO <sub>2</sub>	19	69	42	44	14
Al <sub>2</sub> O <sub>3</sub>	4	30	13	14	6
Fe <sub>2</sub> O <sub>3</sub>	2	44	20	22	10
MnO	0.0	3.6	0.0	0.2	0.5
MgO	0	31	1	4	5
CaO	0	21	0	2	5
Na <sub>2</sub> O	0.08	1.14	0.41	0.42	0.17
K <sub>2</sub> O	0.0	1.7	0.2	0.3	0.4
TiO <sub>2</sub>	0.2	2.5	0.8	0.8	0.3
P <sub>2</sub> O <sub>5</sub>	0.003	0.077	0.015	0.020	0.015
S	0.03	0.67	0.20	0.21	0.13
As	3	103	21	22	17
Au	0.003	6.540	0.04	0.40	1.12
Ba	1	1576	47	111	209
Br	2	42	13	14	6
Ce	2	132	14	17	17
Cl	20	5990	1490	2134	1600
Co	17	3020	76	164	378
Cr	597	7430	3615	3769	1728
Cs	0.5	2.6	0.5	0.7	0.5
Cu	31	568	109	122	75
Eu	0.3	3.5	0.4	0.6	0.6
Ga	6	36	17	17	6
Ge	0.0	4.0	1.0	1.3	1.1
Hf	0.5	5.5	1.6	1.6	0.9
La	0	36	5	6	6
Lu	0.10	0.57	0.10	0.16	0.09
Nb	0.0	7.0	2.5	2.6	1.9
Ni	149	3160	754	1003	721
Pb	0	35	3	5	7
Rb	0	44	7	9	8
Sb	0.5	3.3	1.7	1.7	0.6
Sc	13	91	46	46	19
Sm	0.5	13.3	1.9	2.4	2.1
Sr	2	672	17	62	131
Th	0.3	5.5	0.8	1.0	1.0
V	89	685	353	363	144
W	1	24	5	7	6
Y	6	37	14	16	7
Yb	0.3	2.2	0.9	0.9	0.4
Zn	5	273	34	65	68
Zr	22	181	48	55	26

Oxides and S in %, all other elements in mg/kg

Name	Depth	SiO2	Al2O3	Fe2O3	MnO	MgO	CaO	Na2O	K2O	TiO2	P2O5	S	As	Au	Ba	Br	Ce	Cl	Co	Cr	Cs	Cu
Depth	1	<b>0.67</b>	0.0	<b>-0.37</b>	0.1	-0.1	<b>-0.42</b>	<b>0.40</b>	<b>0.28</b>	<b>0.34</b>	<b>0.45</b>	<b>0.24</b>	<b>-0.28</b>	<b>0.22</b>	0.0	-0.1	-0.1	<b>0.73</b>	0.1	<b>-0.20</b>	-0.2	0.2
SiO2	<b>0.67</b>	1	-0.2	<b>-0.48</b>	0.22	<b>-0.32</b>	<b>-0.45</b>	<b>0.35</b>	<b>0.49</b>	0.21	<b>0.31</b>	0.1	<b>-0.37</b>	<b>0.27</b>	0.1	0.0	0.0	<b>0.48</b>	<b>0.21</b>	<b>-0.31</b>	0.0	<b>0.36</b>
Al2O3	0.0	-0.2	1	<b>0.46</b>	-0.24	<b>-0.61</b>	<b>-0.48</b>	-0.1	-0.1	<b>0.56</b>	<b>-0.25</b>	<b>-0.30</b>	<b>0.24</b>	0.0	-0.2	0.2	-0.1	0.0	<b>-0.22</b>	<b>0.51</b>	0.1	-0.1
Fe2O3	<b>-0.37</b>	<b>-0.48</b>	<b>0.46</b>	1	-0.27	<b>-0.45</b>	<b>-0.30</b>	<b>-0.36</b>	<b>-0.44</b>	0.2	-0.2	<b>-0.31</b>	<b>0.70</b>	-0.21	<b>-0.24</b>	0.1	-0.1	<b>-0.29</b>	<b>-0.21</b>	<b>0.79</b>	-0.1	-0.1
MnO	0.1	0.22	-0.24	-0.27	1	0.0	0.1	0.0	0.22	-0.2	-0.1	<b>0.30</b>	-0.21	0.0	<b>0.89</b>	-0.1	<b>0.84</b>	0.0	<b>0.99</b>	-0.26	0.1	<b>0.80</b>
MgO	-0.1	<b>-0.32</b>	<b>-0.61</b>	<b>-0.45</b>	0.0	1	<b>0.41</b>	0.2	0.0	<b>-0.53</b>	0.0	0.25	-0.23	-0.1	0.0	-0.2	0.1	-0.1	0.0	<b>-0.43</b>	-0.1	-0.2
CaO	<b>-0.42</b>	<b>-0.45</b>	<b>-0.48</b>	-0.30	0.1	<b>0.41</b>	1	-0.2	-0.1	<b>-0.46</b>	0.0	0.2	-0.2	-0.1	0.1	-0.2	0.1	<b>-0.30</b>	0.0	<b>-0.41</b>	0.1	-0.2
Na2O	<b>0.40</b>	<b>0.35</b>	-0.1	<b>-0.36</b>	0.0	0.2	-0.2	1	0.1	0.0	<b>0.47</b>	<b>0.29</b>	<b>-0.27</b>	0.1	0.0	0.21	0.0	<b>0.58</b>	0.0	<b>-0.21</b>	-0.1	0.1
K2O	<b>0.28</b>	<b>0.49</b>	-0.1	<b>-0.44</b>	0.22	0.0	-0.1	0.1	1	-0.1	-0.1	0.1	<b>-0.41</b>	0.1	<b>0.32</b>	<b>-0.25</b>	0.0	0.1	0.2	<b>-0.55</b>	<b>0.56</b>	<b>0.23</b>
TiO2	<b>0.34</b>	<b>0.21</b>	<b>0.56</b>	0.2	-0.2	<b>-0.53</b>	<b>-0.46</b>	0.0	-0.1	1	0.1	<b>-0.27</b>	<b>0.39</b>	0.2	<b>-0.24</b>	0.0	<b>-0.20</b>	<b>0.27</b>	-0.2	<b>0.27</b>	0.0	-0.1
P2O5	<b>0.45</b>	<b>0.31</b>	-0.25	-0.2	-0.1	0.0	0.0	<b>0.47</b>	-0.1	0.1	1	0.1	<b>-0.24</b>	-0.1	-0.2	0.2	-0.2	<b>0.53</b>	-0.1	-0.1	-0.1	0.1
S	<b>0.24</b>	<b>0.1</b>	<b>-0.30</b>	<b>-0.31</b>	<b>0.30</b>	0.25	0.2	<b>0.29</b>	0.1	<b>-0.27</b>	0.1	1	<b>-0.20</b>	-0.1	<b>0.24</b>	<b>0.24</b>	<b>0.22</b>	<b>0.37</b>	<b>0.30</b>	<b>-0.21</b>	-0.2	<b>0.22</b>
As	<b>-0.28</b>	<b>-0.37</b>	<b>0.24</b>	<b>0.70</b>	-0.21	-0.23	-0.2	<b>-0.27</b>	<b>-0.41</b>	<b>0.39</b>	<b>-0.24</b>	-0.20	1	-0.2	-0.2	0.0	0.0	<b>-0.21</b>	-0.2	<b>0.64</b>	-0.20	<b>-0.25</b>
Au	<b>0.22</b>	<b>0.27</b>	0.0	-0.21	0.0	-0.1	-0.1	0.1	0.1	0.2	-0.1	-0.1	-0.2	1	0.0	0.0	0.0	0.1	0.0	0.0	0.1	0.0
Ba	0.0	0.1	-0.2	-0.24	<b>0.89</b>	0.0	0.1	0.0	<b>0.32</b>	<b>-0.24</b>	-0.2	<b>0.24</b>	-0.2	0.0	1	-0.21	<b>0.79</b>	-0.1	<b>0.87</b>	<b>-0.29</b>	<b>0.25</b>	<b>0.70</b>
Br	-0.1	0.0	0.2	0.1	-0.1	-0.2	-0.2	<b>0.21</b>	<b>-0.25</b>	0.0	0.2	<b>0.24</b>	0.0	0.0	-0.21	1	-0.1	<b>0.33</b>	-0.1	<b>0.36</b>	-0.2	-0.1
Ce	-0.1	0.0	-0.1	-0.1	<b>0.84</b>	0.1	0.1	0.0	0.0	-0.20	-0.2	<b>0.22</b>	0.0	0.0	<b>0.79</b>	-0.1	1	0.0	<b>0.85</b>	-0.1	0.1	<b>0.68</b>
Cl	<b>0.73</b>	<b>0.48</b>	0.0	<b>-0.29</b>	0.0	-0.1	<b>-0.30</b>	<b>0.58</b>	0.1	<b>0.27</b>	<b>0.53</b>	<b>0.37</b>	-0.21	0.1	-0.1	<b>0.33</b>	0.0	1	0.1	-0.1	-0.2	<b>0.20</b>
Co	0.1	<b>0.21</b>	<b>-0.22</b>	<b>-0.21</b>	<b>0.99</b>	0.0	0.0	0.0	0.2	-0.2	-0.1	<b>0.30</b>	-0.2	0.0	<b>0.87</b>	-0.1	<b>0.85</b>	0.1	1	-0.2	0.1	<b>0.83</b>
Cr	<b>-0.20</b>	<b>-0.31</b>	<b>0.51</b>	<b>0.79</b>	-0.26	<b>-0.43</b>	<b>-0.41</b>	-0.21	<b>-0.55</b>	<b>0.27</b>	-0.1	-0.21	<b>0.64</b>	0.0	<b>-0.29</b>	<b>0.36</b>	-0.1	-0.1	-0.2	1	<b>-0.22</b>	-0.2
Cs	-0.2	0.0	0.1	-0.1	0.1	-0.1	0.1	-0.1	<b>0.56</b>	0.0	-0.1	-0.2	-0.20	0.1	<b>0.25</b>	-0.2	0.1	-0.2	0.1	-0.22	1	<b>0.21</b>
Cu	0.2	<b>0.36</b>	-0.1	-0.1	<b>0.80</b>	-0.2	-0.2	0.1	<b>0.23</b>	-0.1	0.1	<b>0.22</b>	-0.25	0.0	<b>0.70</b>	-0.1	<b>0.68</b>	<b>0.20</b>	<b>0.83</b>	-0.2	<b>0.21</b>	1
Eu	<b>0.24</b>	<b>0.35</b>	<b>-0.27</b>	<b>-0.25</b>	<b>0.77</b>	-0.1	0.0	0.2	0.1	0.0	0.1	<b>0.36</b>	-0.1	0.1	<b>0.64</b>	0.0	<b>0.74</b>	<b>0.37</b>	<b>0.79</b>	-0.20	0.1	<b>0.77</b>
Ga	-0.1	<b>-0.26</b>	<b>0.92</b>	<b>0.60</b>	<b>-0.31</b>	<b>-0.60</b>	<b>-0.41</b>	-0.2	-0.2	<b>0.51</b>	-0.2	<b>-0.40</b>	<b>0.33</b>	0.0	-0.23	0.1	-0.1	-0.1	<b>-0.28</b>	<b>0.54</b>	0.2	-0.19
Ge	<b>0.30</b>	0.1	<b>0.35</b>	<b>0.25</b>	0.0	<b>-0.39</b>	<b>-0.35</b>	0.0	-0.1	<b>0.34</b>	-0.1	0.2	0.2	0.0	0.0	0.2	0.0	<b>0.31</b>	0.0	<b>0.31</b>	-0.21	0.1
Hf	0.0	-0.2	<b>0.55</b>	<b>0.32</b>	-0.26	<b>-0.36</b>	-0.19	-0.1	-0.2	<b>0.75</b>	<b>-0.22</b>	<b>-0.31</b>	<b>0.56</b>	0.1	-0.2	-0.1	-0.1	0.0	-0.25	<b>0.30</b>	0.1	<b>-0.29</b>
La	0.0	0.0	<b>-0.27</b>	<b>-0.25</b>	<b>0.71</b>	<b>0.21</b>	<b>0.20</b>	<b>0.20</b>	0.2	<b>-0.20</b>	0.0	<b>0.27</b>	0.0	0.1	<b>0.72</b>	-0.2	<b>0.84</b>	0.1	<b>0.71</b>	-0.24	0.1	<b>0.52</b>
Lu	<b>0.37</b>	<b>0.22</b>	0.1	-0.1	<b>0.21</b>	-0.24	-0.1	0.2	-0.2	<b>0.53</b>	<b>0.23</b>	0.2	0.2	<b>0.28</b>	0.1	0.1	<b>0.26</b>	<b>0.57</b>	<b>0.25</b>	0.0	0.0	<b>0.31</b>
Nb	0.1	0.0	<b>0.33</b>	0.1	-0.2	<b>-0.29</b>	-0.1	<b>-0.23</b>	0.0	<b>0.58</b>	-0.1	-0.21	<b>0.28</b>	0.1	-0.1	-0.19	-0.2	0.0	-0.2	0.0	0.0	<b>-0.28</b>
Ni	<b>0.48</b>	<b>0.53</b>	<b>-0.39</b>	<b>-0.27</b>	<b>0.40</b>	0.0	-0.20	<b>0.47</b>	<b>0.22</b>	-0.2	<b>0.46</b>	<b>0.30</b>	-0.21	0.1	<b>0.23</b>	0.1	<b>0.28</b>	<b>0.48</b>	<b>0.45</b>	-0.1	-0.1	<b>0.51</b>
Pb	-0.1	<b>0.21</b>	-0.26	-0.2	0.1	0.0	0.1	-0.2	<b>0.30</b>	<b>-0.28</b>	<b>-0.27</b>	-0.1	-0.1	<b>0.29</b>	0.2	<b>-0.29</b>	0.2	-0.25	0.1	-0.22	0.2	<b>0.22</b>
Rb	0.1	<b>0.38</b>	-0.1	<b>-0.44</b>	0.2	0.0	0.0	0.1	<b>0.97</b>	-0.2	-0.1	0.1	<b>-0.41</b>	0.1	<b>0.30</b>	-0.24	0.0	0.0	0.1	<b>-0.57</b>	<b>0.63</b>	0.1
Sb	0.1	0.1	<b>0.41</b>	<b>0.51</b>	-0.21	<b>-0.52</b>	<b>-0.46</b>	-0.1	<b>-0.38</b>	<b>0.62</b>	0.1	<b>-0.45</b>	<b>0.48</b>	<b>0.22</b>	-0.25	0.1	-0.1	0.1	-0.2	<b>0.58</b>	-0.1	0.0
Sc	-0.1	-0.1	<b>0.60</b>	<b>0.55</b>	-0.1	<b>-0.52</b>	<b>-0.49</b>	-0.1	0.0	<b>0.28</b>	-0.26	-0.25	<b>0.24</b>	0.1	-0.1	0.0	0.0	-0.1	-0.1	<b>0.49</b>	<b>0.24</b>	<b>0.22</b>
Sm	<b>0.35</b>	<b>0.39</b>	<b>-0.33</b>	<b>-0.38</b>	<b>0.78</b>	0.0	0.0	<b>0.31</b>	<b>0.20</b>	-0.1	<b>0.20</b>	<b>0.42</b>	<b>-0.20</b>	0.2	<b>0.65</b>	-0.1	<b>0.74</b>	<b>0.44</b>	<b>0.80</b>	<b>-0.31</b>	0.0	<b>0.75</b>
Sr	<b>-0.46</b>	<b>-0.45</b>	<b>-0.40</b>	<b>-0.28</b>	0.0	<b>0.43</b>	<b>0.88</b>	-0.1	-0.1	<b>-0.41</b>	-0.1	<b>0.28</b>	-0.2	-0.1	0.1	-0.1	0.1	<b>-0.29</b>	-0.1	<b>-0.37</b>	0.1	<b>-0.21</b>
Th	<b>-0.58</b>	<b>-0.59</b>	0.1	0.0	-0.2	<b>0.29</b>	<b>0.47</b>	0.0	0.0	-0.2	<b>-0.25</b>	-0.1	0.1	-0.1	0.1	-0.1	0.1	<b>-0.35</b>	-0.2	-0.1	<b>0.21</b>	<b>-0.34</b>
V	<b>-0.34</b>	<b>-0.44</b>	<b>0.46</b>	<b>0.97</b>	-0.21	<b>-0.48</b>	<b>-0.30</b>	<b>-0.31</b>	<b>-0.41</b>	<b>0.27</b>	-0.1	<b>-0.34</b>	<b>0.69</b>	-0.1	-0.2	0.1	0.0	<b>-0.24</b>	-0.1	<b>0.76</b>	0.0	0.0
W	0.0	0.1	0.1	0.1	-0.1	<b>-0.30</b>	0.0	<b>-0.29</b>	<b>0.25</b>	0.2	<b>-0.24</b>	<b>-0.29</b>	0.0	0.1	-0.1	<b>-0.28</b>	-0.1	-0.1	-0.1	-0.1	<b>0.45</b>	0.1
Y	<b>0.51</b>	<b>0.43</b>	0.0	-0.24	<b>0.40</b>	-0.22	-0.20	<b>0.35</b>	0.0	<b>0.52</b>	<b>0.28</b>	0.1	0.0	<b>0.37</b>	<b>0.27</b>	-0.1	<b>0.39</b>	<b>0.57</b>	<b>0.40</b>	-0.2	0.0	<b>0.43</b>
Yb	-0.1	0.1	-0.1	-0.2	<b>0.37</b>	0.0	0.1	<b>0.28</b>	-0.22	<b>0.30</b>	0.1	0.1	0.1	0.0	<b>0.31</b>	0.1	<b>0.44</b>	<b>0.28</b>	<b>0.38</b>	-0.1	0.1	<b>0.38</b>
Zn	<b>0.60</b>	<b>0.60</b>	<b>-0.41</b>	<b>-0.45</b>	<b>0.30</b>	0.1	-0.1	<b>0.56</b>	<b>0.23</b>	-0.1	<b>0.57</b>	<b>0.34</b>	<b>-0.33</b>	0.1	0.1	0.1	0.1	<b>0.62</b>	<b>0.33</b>	<b>-0.29</b>	-0.1	<b>0.39</b>
Zr	0.0	-0.1	<b>0.62</b>	0.1	-0.22	<b>-0.33</b>	-0.2	0.0	-0.1	<b>0.81</b>	-0.1	<b>-0.27</b>	<b>0.37</b>	0.1	-0.1	0.0	-0.1	0.1	-0.23	0.1	0.1	<b>-0.28</b>

Name	Eu	Ga	Ge	Hf	La	Lu	Nb	Ni	Pb	Rb	Sb	Sc	Sm	Sr	Th	V	W	Y	Yb	Zn	Zr
Depth	0.24	-0.1	0.30	0.0	0.0	0.37	0.1	0.48	-0.1	0.1	0.1	-0.1	0.35	-0.46	-0.58	-0.34	0.0	0.51	-0.1	0.60	0.0
SiO <sub>2</sub>	0.35	-0.26	0.1	-0.2	0.0	0.22	0.0	0.53	0.21	0.38	0.1	-0.1	0.39	-0.45	-0.59	-0.44	0.1	0.43	0.1	0.60	-0.1
Al <sub>2</sub> O <sub>3</sub>	-0.27	0.92	0.35	0.55	-0.27	0.1	0.33	-0.39	-0.26	-0.1	0.41	0.60	-0.33	-0.40	0.1	0.46	0.1	0.0	-0.1	-0.41	0.62
Fe <sub>2</sub> O <sub>3</sub>	-0.25	0.60	0.25	0.32	-0.25	-0.1	0.1	-0.27	-0.2	-0.44	0.51	0.55	-0.38	-0.28	0.0	0.97	0.1	-0.24	-0.2	-0.45	0.1
MnO	0.77	-0.31	0.0	-0.26	0.71	0.21	-0.2	0.40	0.1	0.2	-0.21	-0.1	0.78	0.0	-0.2	-0.21	-0.1	0.40	0.37	0.30	-0.22
MgO	-0.1	-0.60	-0.39	-0.36	0.21	-0.24	-0.29	0.0	0.0	0.0	-0.52	-0.52	0.0	0.43	0.29	-0.48	-0.30	-0.22	0.0	0.1	-0.33
CaO	0.0	-0.41	-0.35	-0.19	0.20	-0.1	-0.1	-0.20	0.1	0.0	-0.46	-0.49	0.0	0.88	0.47	-0.30	0.0	-0.20	0.1	-0.1	-0.2
Na <sub>2</sub> O	0.2	-0.2	0.0	-0.1	0.20	0.2	-0.23	0.47	-0.2	0.1	-0.1	-0.1	0.31	-0.1	0.0	-0.31	-0.29	0.35	0.28	0.56	0.0
K <sub>2</sub> O	0.1	-0.2	-0.1	-0.2	0.2	-0.2	0.0	0.22	0.30	0.97	-0.38	0.0	0.20	-0.1	0.0	-0.41	0.25	0.0	-0.22	0.23	-0.1
TiO <sub>2</sub>	0.0	0.51	0.34	0.75	-0.20	0.53	0.58	-0.2	-0.28	-0.2	0.62	0.28	-0.1	-0.41	-0.2	0.27	0.2	0.52	0.30	-0.1	0.81
P <sub>2</sub> O <sub>5</sub>	0.1	-0.2	-0.1	-0.22	0.0	0.23	-0.1	0.46	-0.27	-0.1	0.1	-0.26	0.20	-0.1	-0.25	-0.1	-0.24	0.28	0.1	0.57	-0.1
S	0.36	-0.40	0.2	-0.31	0.27	0.2	-0.21	0.30	-0.1	0.1	-0.45	-0.25	0.42	0.28	-0.1	-0.34	-0.29	0.1	0.1	0.34	-0.27
As	-0.1	0.33	0.2	0.56	0.0	0.2	0.28	-0.21	-0.1	-0.41	0.48	0.24	-0.20	-0.2	0.1	0.69	0.0	0.0	0.1	-0.33	0.37
Au	0.1	0.0	0.0	0.1	0.1	0.28	0.1	0.1	0.29	0.1	0.22	0.1	0.2	-0.1	-0.1	-0.1	0.1	0.37	0.0	0.1	0.1
Ba	0.64	-0.23	0.0	-0.2	0.72	0.1	-0.1	0.23	0.2	0.30	-0.25	-0.1	0.65	0.1	0.1	-0.2	-0.1	0.27	0.31	0.1	-0.1
Br	0.0	0.1	0.2	-0.1	-0.2	0.1	-0.19	0.1	-0.29	-0.24	0.1	0.0	-0.1	-0.1	-0.1	0.1	-0.28	-0.1	0.1	0.1	0.0
Ce	0.74	-0.1	0.0	-0.1	0.84	0.26	-0.2	0.28	0.2	0.0	-0.1	0.0	0.74	0.1	0.1	0.0	-0.1	0.39	0.44	0.1	-0.1
Cl	0.37	-0.1	0.31	0.0	0.1	0.57	0.0	0.48	-0.25	0.0	0.1	-0.1	0.44	-0.29	-0.35	-0.24	-0.1	0.57	0.28	0.62	0.1
Co	0.79	-0.28	0.0	-0.25	0.71	0.25	-0.2	0.45	0.1	0.1	-0.2	-0.1	0.80	-0.1	-0.2	-0.1	-0.1	0.40	0.38	0.33	-0.23
Cr	-0.20	0.54	0.31	0.30	-0.24	0.0	0.0	-0.1	-0.22	-0.57	0.58	0.49	-0.31	-0.37	-0.1	0.76	-0.1	-0.2	-0.1	-0.29	0.1
Cs	0.1	0.2	-0.21	0.1	0.1	0.0	0.0	-0.1	0.2	0.63	-0.1	0.24	0.0	0.1	0.21	0.0	0.45	0.0	0.1	-0.1	0.1
Cu	0.77	-0.19	0.1	-0.29	0.52	0.31	-0.28	0.51	0.22	0.1	0.0	0.22	0.75	-0.21	-0.34	0.0	0.1	0.43	0.38	0.39	-0.28
Eu	1	-0.32	0.1	-0.1	0.74	0.55	-0.1	0.58	0.2	0.1	-0.1	-0.1	0.94	-0.1	-0.21	-0.2	0.0	0.69	0.54	0.56	-0.1
Ga	-0.32	1	0.30	0.57	-0.25	0.1	0.33	-0.42	-0.26	-0.2	0.49	0.52	-0.37	-0.38	0.2	0.62	0.2	0.0	-0.1	-0.45	0.58
Ge	0.1	0.30	1	0.21	-0.2	0.29	0.23	-0.1	-0.20	-0.21	0.2	0.28	0.0	-0.31	-0.32	0.23	0.1	0.2	0.1	0.0	0.2
Hf	-0.1	0.57	0.21	1	-0.1	0.37	0.54	-0.31	-0.20	-0.2	0.41	0.2	-0.2	-0.1	0.30	0.35	0.2	0.28	0.27	-0.21	0.83
La	0.74	-0.25	-0.2	-0.1	1	0.32	-0.1	0.37	0.1	0.2	-0.2	-0.22	0.82	0.2	0.25	-0.2	-0.20	0.51	0.45	0.31	0.0
Lu	0.55	0.1	0.29	0.37	0.32	1	0.1	0.26	-0.2	-0.22	0.27	0.0	0.56	-0.2	-0.2	0.0	0.1	0.82	0.61	0.32	0.43
Nb	-0.1	0.33	0.23	0.54	-0.1	0.1	1	-0.30	-0.25	0.0	0.32	0.0	-0.1	-0.1	0.1	0.1	0.0	0.21	0.0	-0.2	0.59
Ni	0.58	-0.42	-0.1	-0.31	0.37	0.26	-0.30	1	0.0	0.1	0.0	-0.1	0.63	-0.23	-0.41	-0.23	-0.2	0.38	0.1	0.90	-0.35
Pb	0.2	-0.26	-0.20	-0.20	0.1	-0.2	-0.25	0.0	1	0.31	-0.1	0.0	0.1	0.0	0.0	-0.2	0.27	-0.1	-0.1	-0.1	-0.23
Rb	0.1	-0.2	-0.21	-0.2	0.2	-0.22	0.0	0.1	0.31	1	-0.40	0.0	0.1	0.0	0.1	-0.42	0.23	0.0	-0.2	0.1	0.0
Sb	-0.1	0.49	0.2	0.41	-0.2	0.27	0.32	0.0	-0.1	-0.40	1	0.45	-0.1	-0.43	-0.25	0.59	0.0	0.27	0.1	-0.1	0.36
Sc	-0.1	0.52	0.28	0.2	-0.22	0.0	0.0	-0.1	0.0	0.0	0.45	1	-0.2	-0.43	-0.23	0.57	0.25	0.0	-0.1	-0.30	0.1
Sm	0.94	-0.37	0.0	-0.2	0.82	0.56	-0.1	0.63	0.1	0.1	-0.1	-0.2	1	0.0	-0.2	-0.29	-0.1	0.72	0.54	0.63	-0.1
Sr	-0.1	-0.38	-0.31	-0.1	0.2	-0.2	-0.1	-0.23	0.0	0.0	-0.43	-0.43	0.0	1	0.56	-0.29	-0.1	-0.22	0.1	-0.1	-0.1
Th	-0.21	0.2	-0.32	0.30	0.25	-0.2	0.1	-0.41	0.0	0.1	-0.25	-0.23	-0.2	0.56	1	0.0	-0.2	-0.26	0.1	-0.35	0.39
V	-0.2	0.62	0.23	0.35	-0.2	0.0	0.1	-0.23	-0.2	-0.42	0.59	0.57	-0.29	-0.29	0.0	1	0.2	-0.1	0.0	-0.43	0.2
W	0.0	0.2	0.1	0.2	-0.20	0.1	0.0	-0.2	0.27	0.23	0.0	0.25	-0.1	-0.1	-0.2	0.2	1	0.1	0.0	-0.1	0.0
Y	0.69	0.0	0.2	0.28	0.51	0.82	0.21	0.38	-0.1	0.0	0.27	0.0	0.72	-0.22	-0.26	-0.1	0.1	1	0.63	0.46	0.34
Yb	0.54	-0.1	0.1	0.27	0.45	0.61	0.0	0.1	-0.1	-0.2	0.1	-0.1	0.54	0.1	0.1	0.0	0.0	0.63	1	0.23	0.29
Zn	0.56	-0.45	0.0	-0.21	0.31	0.32	-0.2	0.90	-0.1	0.1	-0.1	-0.30	0.63	-0.1	-0.35	-0.43	-0.1	0.46	0.23	1	-0.24
Zr	-0.1	0.58	0.2	0.83	0.0	0.43	0.59	-0.35	-0.23	0.0	0.36	0.1	-0.1	-0.1	0.39	0.2	0.0	0.34	0.29	-0.24	1

**Appendix 4B: Correlation Coefficients for Data Set 2: all Samples in the top 5 m.**

Number of samples=15                      0.441   0.592   0.760  
 Degrees of Freedom=13                    95%    99%    99.9%

	Minimum	Maximum	Median	Mean	Std Dev
Depth	1	5	3	3	1
SiO <sub>2</sub>	19	46	31	30	8
Al <sub>2</sub> O <sub>3</sub>	4	21	10	10	5
Fe <sub>2</sub> O <sub>3</sub>	6	36	21	20	11
MnO	0.01	0.32	0.05	0.08	0.08
MgO	1	31	6	9	8
CaO	0	21	7	9	8
Na <sub>2</sub> O	0.08	1.14	0.41	0.42	0.23
K <sub>2</sub> O	0.08	0.33	0.22	0.19	0.08
TiO <sub>2</sub>	0.18	0.97	0.52	0.53	0.22
P <sub>2</sub> O <sub>5</sub>	0.007	0.041	0.014	0.017	0.008
S	0.03	0.67	0.20	0.21	0.19
As	7	50	21	22	13
Au	0.008	0.423	0.07	0.10	0.11
Ba	11	387	92	122	104
Br	6.1	17.5	13.9	12.9	2.9
Ce	12	47	17	19	8
Cl	110	1770	1100	978	467
Co	30	192	72	86	51
Cr	768	6080	2520	2995	1737
Cs	0.5	2.6	0.5	0.9	0.6
Cu	33	187	93	100	44
Eu	0.25	0.86	0.25	0.45	0.24
Ga	6	27	14	14	7
Ge	0.0	3.0	0.0	0.4	0.8
Hf	0.5	2.7	1.5	1.5	0.6
La	2	14	6	7	4
Lu	0.10	0.26	0.10	0.13	0.06
Nb	0.0	4.0	2.0	1.5	1.3
Ni	225	1642	607	682	410
Pb	2.0	10.0	5.0	5.4	2.4
Rb	1	16	7	7	4
Sb	0.5	2.4	1.3	1.3	0.6
Sc	13	68	31	35	19
Sm	0.9	3.1	1.7	1.8	0.8
Sr	28	672	188	243	212
Th	0.9	4.0	2.2	2.3	0.8
V	103	555	324	338	166
W	1	24	1	7	9
Y	7	21	11	12	3
Yb	0.72	1.82	1.10	1.16	0.27
Zn	10	122	33	39	33
Zr	36	71	47	50	10

Oxides and S in %, all other elements in mg/kg

	Depth	SiO2	Al2O3	Fe2O3	MnO	MgO	CaO	Na2O	K2O	TiO2	P2O5	S	As	Au	Ba	Br	Ce	Cl	Co	Cr	Cs	Cu
Depth	1	0.0	0.58	0.4	-0.4	0.1	<b>-0.78</b>	0.0	<b>-0.44</b>	0.3	<b>-0.61</b>	0.0	0.4	-0.4	-0.2	0.1	0.3	0.3	0.2	<b>0.48</b>	0.1	<b>0.51</b>
SiO2	0.0	1	0.46	0.2	<b>0.52</b>	<b>-0.47</b>	-0.4	<b>0.71</b>	0.0	<b>0.53</b>	<b>0.58</b>	-0.2	0.2	-0.2	-0.1	<b>0.80</b>	0.2	0.4	<b>0.74</b>	0.2	0.0	<b>0.51</b>
Al2O3	0.58	0.46	1	<b>0.71</b>	-0.3	<b>-0.62</b>	<b>-0.68</b>	0.1	<b>-0.48</b>	<b>0.85</b>	0.0	-0.2	<b>0.51</b>	0.0	-0.2	0.3	-0.2	0.2	0.3	<b>0.79</b>	0.4	<b>0.91</b>
Fe2O3	0.4	0.2	<b>0.71</b>	1	-0.50	<b>-0.71</b>	<b>-0.48</b>	-0.2	<b>-0.67</b>	<b>0.56</b>	0.0	-0.4	<b>0.86</b>	0.2	0.0	0.0	-0.3	0.0	0.2	<b>0.97</b>	0.3	<b>0.76</b>
MnO	-0.4	<b>0.52</b>	-0.3	-0.50	1	0.3	0.0	<b>0.80</b>	<b>0.45</b>	-0.1	<b>0.57</b>	0.0	-0.4	-0.4	0.0	<b>0.53</b>	<b>0.46</b>	0.3	<b>0.49</b>	<b>-0.49</b>	-0.2	-0.2
MgO	0.1	<b>-0.47</b>	<b>-0.62</b>	<b>-0.71</b>	0.3	1	0.0	0.0	0.2	<b>-0.59</b>	-0.4	0.3	<b>-0.48</b>	-0.4	0.0	-0.1	0.4	0.2	-0.2	<b>-0.64</b>	-0.3	<b>-0.57</b>
CaO	<b>-0.78</b>	-0.4	<b>-0.68</b>	<b>-0.48</b>	0.0	0.0	1	-0.4	<b>0.54</b>	<b>-0.53</b>	0.2	0.2	<b>-0.53</b>	0.4	0.2	-0.4	-0.2	<b>-0.59</b>	<b>-0.47</b>	<b>-0.59</b>	-0.1	<b>-0.73</b>
Na2O	0.0	<b>0.71</b>	0.1	-0.2	<b>0.80</b>	0.0	-0.4	1	0.1	0.3	<b>0.55</b>	0.1	-0.1	-0.4	0.1	<b>0.73</b>	0.2	0.3	<b>0.47</b>	-0.1	0.0	0.2
K2O	<b>-0.44</b>	0.0	<b>-0.48</b>	<b>-0.67</b>	<b>0.45</b>	0.2	<b>0.54</b>	0.1	1	-0.3	0.2	0.2	<b>-0.66</b>	-0.1	0.1	-0.1	0.4	0.0	0.0	<b>-0.71</b>	0.2	<b>-0.47</b>
TiO2	0.3	<b>0.53</b>	<b>0.85</b>	<b>0.56</b>	-0.1	<b>-0.59</b>	<b>-0.53</b>	0.3	-0.3	1	0.3	-0.4	0.2	0.1	-0.3	0.3	-0.1	0.4	0.2	<b>0.58</b>	<b>0.55</b>	<b>0.77</b>
P2O5	<b>-0.61</b>	<b>0.58</b>	0.0	0.0	<b>0.57</b>	-0.4	0.2	<b>0.55</b>	0.2	0.3	1	-0.3	-0.2	0.2	-0.2	0.3	-0.2	-0.1	0.2	-0.1	0.2	0.1
S	0.0	-0.2	-0.2	-0.4	0.0	0.3	0.2	0.1	0.2	-0.4	-0.3	1	-0.2	-0.4	0.4	0.1	0.0	-0.2	-0.3	-0.3	-0.2	-0.4
As	0.4	0.2	<b>0.51</b>	<b>0.86</b>	-0.4	<b>-0.48</b>	<b>-0.53</b>	-0.1	<b>-0.66</b>	0.2	-0.2	-0.2	1	0.0	0.2	0.2	-0.1	0.1	0.4	<b>0.88</b>	-0.1	<b>0.65</b>
Au	-0.4	-0.2	0.0	0.2	-0.4	-0.4	0.4	-0.4	-0.1	0.1	0.2	-0.4	0.0	1	-0.2	-0.2	-0.3	-0.1	-0.4	0.1	0.0	0.0
Ba	-0.2	-0.1	-0.2	0.0	0.0	0.0	0.2	0.1	0.1	-0.3	-0.2	0.4	0.2	-0.2	1	0.1	-0.1	-0.2	0.1	0.1	-0.2	-0.1
Br	0.1	<b>0.80</b>	0.3	0.0	<b>0.53</b>	-0.1	-0.4	<b>0.73</b>	-0.1	0.3	0.3	0.1	0.2	-0.2	0.1	1	0.2	<b>0.60</b>	<b>0.71</b>	0.1	-0.3	0.3
Ce	0.3	0.2	-0.2	-0.3	<b>0.46</b>	0.4	-0.2	0.2	0.4	-0.1	-0.2	0.0	-0.1	-0.3	-0.1	0.2	1	<b>0.51</b>	0.3	-0.3	-0.1	-0.2
Cl	0.3	0.4	0.2	0.0	0.3	0.2	<b>-0.59</b>	0.3	0.0	0.4	-0.1	-0.2	0.1	-0.1	-0.2	<b>0.60</b>	<b>0.51</b>	1	<b>0.51</b>	0.1	-0.1	0.3
Co	0.2	<b>0.74</b>	0.3	0.2	<b>0.49</b>	-0.2	<b>-0.47</b>	<b>0.47</b>	0.0	0.2	0.2	-0.3	0.4	-0.4	0.1	<b>0.71</b>	0.3	<b>0.51</b>	1	0.3	-0.3	<b>0.46</b>
Cr	<b>0.48</b>	0.2	<b>0.79</b>	<b>0.97</b>	<b>-0.49</b>	<b>-0.64</b>	<b>-0.59</b>	-0.1	<b>-0.71</b>	<b>0.58</b>	-0.1	-0.3	<b>0.88</b>	0.1	0.1	0.1	-0.3	0.1	0.3	1	0.2	<b>0.83</b>
Cs	0.1	0.0	0.4	0.3	-0.2	-0.3	-0.1	0.0	0.2	<b>0.55</b>	0.2	-0.2	-0.1	0.0	-0.2	-0.3	-0.1	-0.1	-0.3	0.2	1	0.3
Cu	<b>0.51</b>	<b>0.51</b>	<b>0.91</b>	<b>0.76</b>	-0.2	<b>-0.57</b>	<b>-0.73</b>	0.2	<b>-0.47</b>	<b>0.77</b>	0.1	-0.4	<b>0.65</b>	0.0	-0.1	0.3	-0.2	0.3	<b>0.46</b>	<b>0.83</b>	0.3	1
Eu	-0.4	0.3	<b>-0.50</b>	<b>-0.60</b>	<b>0.86</b>	0.4	0.2	<b>0.47</b>	<b>0.68</b>	-0.3	0.4	0.0	<b>-0.48</b>	-0.4	-0.1	0.2	<b>0.55</b>	0.2	0.4	<b>-0.63</b>	-0.1	-0.3
Ga	<b>0.44</b>	0.3	<b>0.90</b>	<b>0.87</b>	-0.4	<b>-0.72</b>	<b>-0.55</b>	0.0	<b>-0.49</b>	<b>0.77</b>	0.1	-0.4	<b>0.61</b>	0.2	-0.3	0.0	-0.3	0.0	0.1	<b>0.84</b>	<b>0.51</b>	<b>0.88</b>
Ge	0.1	-0.2	0.2	0.4	-0.3	-0.2	-0.1	-0.1	-0.3	0.1	-0.2	0.2	<b>0.47</b>	-0.1	<b>0.60</b>	0.0	-0.3	-0.1	0.0	<b>0.50</b>	0.2	0.3
Hf	0.2	0.4	<b>0.66</b>	0.4	-0.1	<b>-0.53</b>	-0.3	0.1	0.1	<b>0.81</b>	0.2	-0.2	0.1	0.2	-0.2	0.1	0.1	0.3	0.1	0.4	<b>0.62</b>	<b>0.64</b>
La	-0.4	0.0	<b>-0.71</b>	<b>-0.68</b>	<b>0.61</b>	0.4	<b>0.45</b>	0.2	<b>0.79</b>	<b>-0.62</b>	0.1	0.3	-0.4	-0.2	0.1	0.0	<b>0.67</b>	0.0	0.1	<b>-0.72</b>	-0.2	<b>-0.62</b>
Lu	0.1	0.0	<b>0.51</b>	0.3	-0.4	-0.4	-0.1	-0.2	0.1	<b>0.45</b>	0.1	-0.3	0.0	0.2	-0.4	<b>-0.50</b>	-0.2	-0.2	-0.2	0.3	<b>0.59</b>	<b>0.49</b>
Nb	<b>-0.60</b>	-0.1	<b>-0.56</b>	<b>-0.49</b>	0.1	0.0	<b>0.71</b>	-0.1	0.3	<b>-0.48</b>	0.4	0.3	-0.4	0.3	-0.1	-0.1	-0.2	-0.4	-0.3	<b>-0.60</b>	-0.3	<b>-0.58</b>
Ni	0.1	<b>0.67</b>	0.3	0.3	0.3	-0.3	-0.4	0.3	-0.1	0.3	0.1	-0.3	<b>0.46</b>	-0.3	0.2	<b>0.66</b>	0.1	0.4	<b>0.95</b>	0.4	-0.2	<b>0.53</b>
Pb	0.1	-0.1	0.0	0.1	0.0	0.0	0.0	-0.1	0.1	0.2	0.1	-0.4	0.0	0.4	-0.4	-0.2	<b>0.45</b>	0.2	-0.2	-0.1	0.2	0.0
Rb	-0.4	0.0	<b>-0.54</b>	<b>-0.79</b>	<b>0.50</b>	0.3	<b>0.53</b>	0.2	<b>0.94</b>	-0.4	0.2	0.3	<b>-0.76</b>	-0.2	0.1	0.0	0.4	0.0	-0.1	<b>-0.82</b>	0.1	<b>-0.62</b>
Sb	0.3	0.3	<b>0.74</b>	<b>0.92</b>	-0.4	<b>-0.68</b>	<b>-0.50</b>	0.0	<b>-0.61</b>	<b>0.63</b>	0.1	-0.4	<b>0.80</b>	0.2	0.1	0.1	-0.3	0.0	0.2	<b>0.93</b>	0.2	<b>0.84</b>
Sc	<b>0.61</b>	<b>0.45</b>	<b>0.94</b>	<b>0.84</b>	-0.3	<b>-0.60</b>	<b>-0.74</b>	0.1	<b>-0.59</b>	<b>0.72</b>	-0.1	-0.2	<b>0.74</b>	-0.1	0.0	0.3	-0.2	0.2	0.4	<b>0.92</b>	0.3	<b>0.93</b>
Sm	<b>-0.52</b>	0.3	<b>-0.61</b>	<b>-0.68</b>	<b>0.83</b>	0.3	0.4	0.4	<b>0.79</b>	-0.4	<b>0.45</b>	0.1	<b>-0.53</b>	-0.2	0.0	0.2	<b>0.56</b>	0.2	0.2	<b>-0.73</b>	-0.1	<b>-0.48</b>
Sr	<b>-0.49</b>	<b>-0.50</b>	<b>-0.56</b>	<b>-0.53</b>	-0.1	0.2	<b>0.81</b>	-0.2	0.4	<b>-0.47</b>	-0.1	<b>0.56</b>	<b>-0.53</b>	0.1	<b>0.48</b>	-0.2	-0.2	<b>-0.49</b>	<b>-0.56</b>	<b>-0.55</b>	-0.1	<b>-0.75</b>
Th	-0.2	0.0	-0.4	<b>-0.67</b>	<b>0.46</b>	0.4	0.3	0.2	<b>0.80</b>	-0.4	0.0	<b>0.48</b>	<b>-0.48</b>	-0.2	0.3	0.1	<b>0.56</b>	0.1	0.0	<b>-0.61</b>	-0.1	-0.4
V	0.4	0.2	<b>0.71</b>	<b>0.99</b>	<b>-0.46</b>	<b>-0.72</b>	<b>-0.48</b>	-0.2	<b>-0.61</b>	<b>0.56</b>	0.0	<b>-0.45</b>	<b>0.83</b>	0.2	-0.1	0.0	-0.2	-0.1	0.2	<b>0.94</b>	0.3	<b>0.76</b>
W	0.0	-0.2	0.4	<b>0.45</b>	<b>-0.49</b>	-0.4	0.0	-0.4	-0.1	<b>0.58</b>	0.1	<b>-0.48</b>	0.0	0.4	-0.4	<b>-0.53</b>	-0.3	-0.1	-0.4	0.3	<b>0.70</b>	0.3
Y	-0.4	<b>0.51</b>	0.0	-0.3	<b>0.73</b>	0.0	0.0	<b>0.64</b>	<b>0.48</b>	0.4	<b>0.74</b>	-0.3	<b>-0.49</b>	0.0	-0.3	0.3	0.3	0.3	0.2	-0.4	0.3	0.0
Yb	-0.2	<b>0.74</b>	0.2	-0.1	<b>0.73</b>	-0.2	-0.2	<b>0.78</b>	0.4	<b>0.48</b>	<b>0.63</b>	-0.1	-0.2	-0.3	-0.1	<b>0.54</b>	0.3	<b>0.45</b>	<b>0.53</b>	-0.1	0.3	0.4
Zn	<b>-0.50</b>	<b>0.61</b>	-0.3	-0.4	<b>0.89</b>	0.1	0.1	<b>0.72</b>	0.4	0.0	<b>0.64</b>	-0.1	-0.3	-0.3	0.1	<b>0.63</b>	0.2	0.3	<b>0.60</b>	-0.4	-0.2	-0.1
Zr	0.2	<b>0.57</b>	<b>0.62</b>	0.1	0.2	-0.3	-0.4	<b>0.50</b>	0.2	<b>0.75</b>	0.2	0.0	-0.1	-0.2	-0.1	0.4	0.2	<b>0.45</b>	0.4	0.2	<b>0.45</b>	<b>0.55</b>

	Eu	Ga	Ge	Hf	La	Lu	Nb	Ni	Pb	Rb	Sb	Sc	Sm	Sr	Th	V	W	Y	Yb	Zn	Zr
Depth	-0.4	<b>0.44</b>	0.1	0.2	-0.4	0.1	<b>-0.60</b>	0.1	0.1	-0.4	0.3	<b>0.61</b>	<b>-0.52</b>	<b>-0.49</b>	-0.2	0.4	0.0	-0.4	-0.2	<b>-0.50</b>	0.2
SiO <sub>2</sub>	0.3	0.3	-0.2	0.4	0.0	0.0	-0.1	<b>0.67</b>	-0.1	0.0	0.3	<b>0.45</b>	0.3	<b>-0.50</b>	0.0	0.2	-0.2	<b>0.51</b>	<b>0.74</b>	<b>0.61</b>	<b>0.57</b>
Al <sub>2</sub> O <sub>3</sub>	<b>-0.50</b>	<b>0.90</b>	0.2	<b>0.66</b>	<b>-0.71</b>	0.51	<b>-0.56</b>	0.3	0.0	<b>-0.54</b>	<b>0.74</b>	<b>0.94</b>	<b>-0.61</b>	<b>-0.56</b>	-0.4	<b>0.71</b>	0.4	0.0	0.2	-0.3	<b>0.62</b>
Fe <sub>2</sub> O <sub>3</sub>	<b>-0.60</b>	<b>0.87</b>	0.4	0.4	<b>-0.68</b>	0.3	<b>-0.49</b>	0.3	0.1	<b>-0.79</b>	<b>0.92</b>	<b>0.84</b>	<b>-0.68</b>	<b>-0.53</b>	<b>-0.67</b>	<b>0.99</b>	<b>0.45</b>	-0.3	-0.1	-0.4	0.1
MnO	<b>0.86</b>	-0.4	-0.3	-0.1	<b>0.61</b>	-0.4	0.1	0.3	0.0	<b>0.50</b>	-0.4	-0.3	<b>0.83</b>	-0.1	<b>0.46</b>	<b>-0.46</b>	<b>-0.49</b>	<b>0.73</b>	<b>0.73</b>	<b>0.89</b>	0.2
MgO	0.4	<b>-0.72</b>	-0.2	<b>-0.53</b>	0.4	-0.4	0.0	-0.3	0.0	0.3	<b>-0.68</b>	<b>-0.60</b>	0.3	0.2	0.4	<b>-0.72</b>	-0.4	0.0	-0.2	0.1	-0.3
CaO	0.2	<b>-0.55</b>	-0.1	-0.3	<b>0.45</b>	-0.1	<b>0.71</b>	-0.4	0.0	<b>0.53</b>	<b>-0.50</b>	<b>-0.74</b>	0.4	<b>0.81</b>	0.3	<b>-0.48</b>	0.0	0.0	-0.2	0.1	-0.4
Na <sub>2</sub> O	<b>0.47</b>	0.0	-0.1	0.1	0.2	-0.2	-0.1	0.3	-0.1	0.2	0.0	0.1	0.4	-0.2	0.2	-0.2	-0.4	<b>0.64</b>	<b>0.78</b>	<b>0.72</b>	<b>0.50</b>
K <sub>2</sub> O	<b>0.68</b>	<b>-0.49</b>	-0.3	0.1	<b>0.79</b>	0.1	0.3	-0.1	0.1	<b>0.94</b>	<b>-0.61</b>	<b>-0.59</b>	<b>0.79</b>	0.4	<b>0.80</b>	<b>-0.61</b>	-0.1	<b>0.48</b>	0.4	0.4	0.2
TiO <sub>2</sub>	-0.3	<b>0.77</b>	0.1	<b>0.81</b>	<b>-0.62</b>	<b>0.45</b>	<b>-0.48</b>	0.3	0.2	-0.4	<b>0.63</b>	<b>0.72</b>	-0.4	<b>-0.47</b>	-0.4	<b>0.56</b>	<b>0.58</b>	0.4	<b>0.48</b>	0.0	<b>0.75</b>
P <sub>2</sub> O <sub>5</sub>	0.4	0.1	-0.2	0.2	0.1	0.1	0.4	0.1	0.1	0.2	0.1	-0.1	<b>0.45</b>	-0.1	0.0	0.0	0.1	<b>0.74</b>	<b>0.63</b>	<b>0.64</b>	0.2
S	0.0	-0.4	0.2	-0.2	0.3	-0.3	0.3	-0.3	-0.4	0.3	-0.4	-0.2	0.1	<b>0.56</b>	<b>0.48</b>	<b>-0.45</b>	<b>-0.48</b>	-0.3	-0.1	-0.1	0.0
As	<b>-0.48</b>	<b>0.61</b>	<b>0.47</b>	0.1	-0.4	0.0	-0.4	<b>0.46</b>	0.0	<b>-0.76</b>	<b>0.80</b>	<b>0.74</b>	<b>-0.53</b>	<b>-0.53</b>	<b>-0.48</b>	<b>0.83</b>	0.0	<b>-0.49</b>	-0.2	-0.3	-0.1
Au	-0.4	0.2	-0.1	0.2	-0.2	0.2	0.3	-0.3	0.4	-0.2	0.2	-0.1	-0.2	0.1	-0.2	0.2	0.4	0.0	-0.3	-0.3	-0.2
Ba	-0.1	-0.3	<b>0.60</b>	-0.2	0.1	-0.4	-0.1	0.2	-0.4	0.1	0.1	0.0	0.0	<b>0.48</b>	0.3	-0.1	-0.4	-0.3	-0.1	0.1	-0.1
Br	0.2	0.0	0.0	0.1	0.0	<b>-0.50</b>	-0.1	<b>0.66</b>	-0.2	0.0	0.1	0.3	0.2	-0.2	0.1	0.0	<b>-0.53</b>	0.3	<b>0.54</b>	<b>0.63</b>	0.4
Ce	<b>0.55</b>	-0.3	-0.3	0.1	<b>0.67</b>	-0.2	-0.2	0.1	<b>0.45</b>	0.4	-0.3	-0.2	<b>0.56</b>	-0.2	<b>0.56</b>	-0.2	-0.3	0.3	0.3	0.2	0.2
Cl	0.2	0.0	-0.1	0.3	0.0	-0.2	-0.4	0.4	0.2	0.0	0.0	0.2	0.2	<b>-0.49</b>	0.1	-0.1	-0.1	0.3	<b>0.45</b>	0.3	<b>0.45</b>
Co	0.4	0.1	0.0	0.1	0.1	-0.2	-0.3	<b>0.95</b>	-0.2	-0.1	0.2	0.4	0.2	<b>-0.56</b>	0.0	0.2	-0.4	0.2	<b>0.53</b>	<b>0.60</b>	0.4
Cr	<b>-0.63</b>	<b>0.84</b>	<b>0.50</b>	0.4	<b>-0.72</b>	0.3	<b>-0.60</b>	0.4	-0.1	<b>-0.82</b>	<b>0.93</b>	<b>0.92</b>	<b>-0.73</b>	<b>-0.55</b>	<b>-0.61</b>	<b>0.94</b>	0.3	-0.4	-0.1	-0.4	0.2
Cs	-0.1	<b>0.51</b>	0.2	<b>0.62</b>	-0.2	<b>0.59</b>	-0.3	-0.2	0.2	0.1	0.2	0.3	-0.1	-0.1	-0.1	0.3	<b>0.70</b>	0.3	0.3	-0.2	<b>0.45</b>
Cu	-0.3	<b>0.88</b>	0.3	<b>0.64</b>	<b>-0.62</b>	<b>0.49</b>	<b>-0.58</b>	<b>0.53</b>	0.0	<b>-0.62</b>	<b>0.84</b>	<b>0.93</b>	<b>-0.48</b>	<b>-0.75</b>	-0.4	<b>0.76</b>	0.3	0.0	0.4	-0.1	<b>0.55</b>
Eu	1	<b>-0.50</b>	-0.3	0.0	<b>0.79</b>	-0.2	0.2	0.2	0.1	<b>0.66</b>	<b>-0.53</b>	<b>-0.51</b>	<b>0.94</b>	0.0	<b>0.58</b>	<b>-0.54</b>	-0.3	<b>0.68</b>	<b>0.63</b>	<b>0.74</b>	0.2
Ga	<b>-0.50</b>	1	0.2	<b>0.65</b>	<b>-0.68</b>	<b>0.63</b>	<b>-0.49</b>	0.2	0.1	<b>-0.60</b>	<b>0.83</b>	<b>0.88</b>	<b>-0.60</b>	<b>-0.63</b>	<b>-0.54</b>	<b>0.89</b>	<b>0.61</b>	0.0	0.1	-0.4	0.4
Ge	-0.3	0.2	1	0.2	-0.3	0.0	-0.3	0.2	-0.2	<b>-0.44</b>	<b>0.54</b>	0.4	-0.4	0.0	-0.2	0.4	0.1	-0.4	-0.1	-0.2	0.0
Hf	0.0	<b>0.65</b>	0.2	1	-0.2	<b>0.61</b>	-0.4	0.1	0.4	0.0	<b>0.51</b>	<b>0.52</b>	-0.1	-0.3	0.1	<b>0.45</b>	<b>0.61</b>	0.4	<b>0.54</b>	-0.1	<b>0.83</b>
La	<b>0.79</b>	<b>-0.68</b>	-0.3	-0.2	1	-0.3	0.4	-0.1	0.2	<b>0.81</b>	<b>-0.65</b>	<b>-0.69</b>	<b>0.90</b>	0.3	<b>0.81</b>	<b>-0.63</b>	<b>-0.47</b>	0.3	0.3	0.4	-0.1
Lu	-0.2	<b>0.63</b>	0.0	<b>0.61</b>	-0.3	1	-0.2	-0.2	0.3	0.0	0.4	0.4	-0.2	-0.3	0.0	0.4	<b>0.72</b>	0.2	0.2	-0.4	0.4
Nb	0.2	<b>-0.49</b>	-0.3	-0.4	0.4	-0.2	1	-0.3	0.1	0.4	<b>-0.53</b>	<b>-0.63</b>	0.4	<b>0.50</b>	0.2	<b>-0.48</b>	-0.3	0.1	-0.1	0.2	-0.4
Ni	0.2	0.2	0.2	0.1	-0.1	-0.2	-0.3	1	-0.4	-0.3	0.3	<b>0.49</b>	0.1	<b>-0.51</b>	-0.2	0.3	-0.3	0.1	0.4	<b>0.54</b>	0.3
Pb	0.1	0.1	-0.2	0.4	0.2	0.3	0.1	-0.4	1	0.0	0.1	-0.1	0.2	-0.2	0.1	0.1	0.4	0.4	0.1	-0.2	0.1
Rb	<b>0.66</b>	<b>-0.60</b>	<b>-0.44</b>	0.0	<b>0.81</b>	0.0	0.4	-0.3	0.0	1	<b>-0.75</b>	<b>-0.68</b>	<b>0.79</b>	<b>0.50</b>	<b>0.83</b>	<b>-0.73</b>	-0.2	<b>0.44</b>	0.3	0.4	0.2
Sb	<b>-0.53</b>	<b>0.83</b>	<b>0.54</b>	<b>0.51</b>	<b>-0.65</b>	0.4	<b>-0.53</b>	0.3	0.1	<b>-0.75</b>	1	<b>0.85</b>	<b>-0.60</b>	<b>-0.51</b>	<b>-0.50</b>	<b>0.90</b>	0.4	-0.2	0.1	-0.3	0.3
Sc	<b>-0.51</b>	<b>0.88</b>	0.4	<b>0.52</b>	<b>-0.69</b>	0.4	<b>-0.63</b>	<b>0.49</b>	-0.1	<b>-0.68</b>	<b>0.85</b>	1	<b>-0.64</b>	<b>-0.62</b>	<b>-0.47</b>	<b>0.83</b>	0.3	-0.2	0.2	-0.2	<b>0.47</b>
Sm	<b>0.94</b>	<b>-0.60</b>	-0.4	-0.1	<b>0.90</b>	-0.2	0.4	0.1	0.2	<b>0.79</b>	<b>-0.60</b>	<b>-0.64</b>	1	0.2	<b>0.70</b>	<b>-0.63</b>	-0.4	<b>0.66</b>	<b>0.56</b>	<b>0.70</b>	0.1
Sr	0.0	<b>-0.63</b>	0.0	-0.3	0.3	-0.3	<b>0.50</b>	<b>-0.51</b>	-0.2	<b>0.50</b>	<b>-0.51</b>	<b>-0.62</b>	0.2	1	0.4	<b>-0.56</b>	-0.1	-0.2	-0.3	-0.1	-0.2
Th	<b>0.58</b>	<b>-0.54</b>	-0.2	0.1	<b>0.81</b>	0.0	0.2	-0.2	0.1	<b>0.83</b>	<b>-0.50</b>	<b>-0.47</b>	<b>0.70</b>	0.4	1	<b>-0.64</b>	-0.4	0.3	0.3	0.3	0.3
V	<b>-0.54</b>	<b>0.89</b>	0.4	<b>0.45</b>	<b>-0.63</b>	0.4	<b>-0.48</b>	0.3	0.1	<b>-0.73</b>	<b>0.90</b>	<b>0.83</b>	<b>-0.63</b>	<b>-0.56</b>	<b>-0.64</b>	1	<b>0.48</b>	-0.3	-0.1	-0.4	0.1
W	-0.3	<b>0.61</b>	0.1	<b>0.61</b>	<b>-0.47</b>	<b>0.72</b>	-0.3	-0.3	0.4	-0.2	0.4	0.3	-0.4	-0.1	-0.4	<b>0.48</b>	1	0.1	0.0	<b>-0.47</b>	0.3
Y	<b>0.68</b>	0.0	-0.4	0.4	0.3	0.2	0.1	0.1	0.4	<b>0.44</b>	-0.2	-0.2	<b>0.66</b>	-0.2	0.3	-0.3	0.1	1	<b>0.84</b>	<b>0.65</b>	<b>0.51</b>
Yb	<b>0.63</b>	0.1	-0.1	<b>0.54</b>	0.3	0.2	-0.1	0.4	0.1	0.3	0.1	0.2	<b>0.56</b>	-0.3	0.3	-0.1	0.0	<b>0.84</b>	1	<b>0.72</b>	<b>0.73</b>
Zn	<b>0.74</b>	-0.4	-0.2	-0.1	0.4	-0.4	0.2	<b>0.54</b>	-0.2	0.4	-0.3	-0.2	<b>0.70</b>	-0.1	0.3	-0.4	<b>-0.47</b>	<b>0.65</b>	<b>0.72</b>	1	0.2
Zr	0.2	0.4	0.0	<b>0.83</b>	-0.1	0.4	-0.4	0.3	0.1	0.2	0.3	<b>0.47</b>	0.1	-0.2	0.3	0.1	0.3	<b>0.51</b>	<b>0.73</b>	0.2	1

**Appendix 4C: Correlation Coefficients for Data Set 2: all Bore Hole Samples below 5 m.**

Number of samples=59                      0.216   0.302   0.418  
 Degrees of Freedom=57                      95%   99%   99.9%

	Minimum	Maximum	Median	Mean	Std Dev
Depth	6	47	27	26	12
SiO <sub>2</sub>	25	69	47	48	12
Al <sub>2</sub> O <sub>3</sub>	5	30	14	15	6
Fe <sub>2</sub> O <sub>3</sub>	2	44	20	22	10
MnO	0.0	3.6	0.0	0.2	0.5
MgO	0	16	1	2	4
CaO	0.0	5.4	0.0	0.5	1.3
Na <sub>2</sub> O	0.16	0.84	0.40	0.42	0.15
K <sub>2</sub> O	0.0	1.7	0.2	0.4	0.4
TiO <sub>2</sub>	0.5	2.5	0.8	0.9	0.3
P <sub>2</sub> O <sub>5</sub>	0.003	0.077	0.015	0.021	0.016
S	0.04	0.48	0.20	0.22	0.11
As	3	103	18	22	18
Au	0.003	6.540	0.03	0.48	1.25
Ba	1	1576	39	108	229
Br	2	42	13	14	6
Ce	2	132	11	16	19
Cl	20	5990	1900	2428	1654
Co	17	3020	77	184	421
Cr	597	7430	3690	3966	1684
Cs	0.5	2.1	0.5	0.7	0.4
Cu	31	568	115	128	81
Eu	0.3	3.5	0.5	0.7	0.6
Ga	8	36	18	18	6
Ge	0.0	4.0	2.0	1.5	1.0
Hf	0.5	5.5	1.6	1.7	1.0
La	0	36	4	5	6
Lu	0.10	0.57	0.10	0.16	0.10
Nb	0.0	7.0	3.0	2.8	1.9
Ni	149	3160	762	1085	762
Pb	0	35	2	5	7
Rb	0	44	6	9	9
Sb	0.8	3.3	1.8	1.8	0.6
Sc	22	91	46	49	18
Sm	0.5	13.3	2.0	2.5	2.3
Sr	2	56	13	16	12
Th	0.3	5.5	0.6	0.7	0.8
V	89	685	367	369	139
W	1	18	6	7	5
Y	6	37	16	17	7
Yb	0.3	2.2	0.9	0.9	0.4
Zn	5	273	36	71	73
Zr	22	181	49	57	28

Oxides and S in %, all other elements in mg/kg

Name	Depth	SiO2	Al2O3	Fe2O3	MnO	MgO	CaO	Na2O	K2O	TiO2	P2O5	S	As	Au	Ba	Br	Ce	Cl	Co	Cr	Cs	Cu
Depth	1	0.53	-0.40	-0.69	0.0	0.41	0.30	0.67	0.2	0.1	0.55	0.42	-0.42	0.2	0.0	-0.1	-0.1	0.70	0.0	-0.57	-0.2	0.1
SiO2	0.53	1	-0.54	-0.78	0.2	0.0	-0.1	0.36	0.48	-0.1	0.28	0.2	-0.52	0.25	0.2	0.0	0.0	0.37	0.2	-0.65	0.1	0.32
Al2O3	-0.40	-0.54	1	0.39	-0.30	-0.59	-0.40	-0.27	-0.23	0.45	-0.35	-0.37	0.2	0.0	-0.2	0.1	-0.1	-0.2	-0.30	0.40	0.1	-0.34
Fe2O3	-0.69	-0.78	0.39	1	-0.30	-0.36	-0.35	-0.43	-0.50	0.1	-0.2	-0.28	0.68	-0.26	-0.27	0.1	-0.1	-0.40	-0.25	0.75	-0.2	-0.26
MnO	0.0	0.2	-0.30	-0.30	1	0.1	0.45	0.0	0.2	-0.26	-0.1	0.40	-0.22	0.0	0.92	-0.2	0.87	0.0	0.99	-0.31	0.2	0.84
MgO	0.41	0.0	-0.59	-0.36	0.1	1	0.75	0.33	0.1	-0.44	0.22	0.26	-0.2	-0.1	0.1	-0.2	0.0	0.1	0.1	-0.26	-0.2	0.0
CaO	0.30	-0.1	-0.40	-0.35	0.45	0.75	1	0.0	0.1	-0.33	0.0	0.35	-0.25	0.0	0.38	-0.24	0.33	0.0	0.42	-0.34	0.0	0.25
Na2O	0.67	0.36	-0.27	-0.43	0.0	0.33	0.0	1	0.2	-0.1	0.51	0.41	-0.33	0.1	0.0	0.1	0.0	0.74	0.0	-0.26	-0.1	0.1
K2O	0.2	0.48	-0.23	-0.50	0.2	0.1	0.1	0.2	1	-0.27	-0.1	0.1	-0.43	0.1	0.34	-0.28	0.0	0.0	0.2	-0.67	0.74	0.22
TiO2	0.1	-0.1	0.45	0.1	-0.26	-0.44	-0.33	-0.1	-0.27	1	0.0	-0.31	0.45	0.1	-0.25	0.0	-0.2	0.1	-0.26	0.1	-0.1	-0.30
P2O5	0.55	0.28	-0.35	-0.2	-0.1	0.22	0.0	0.51	-0.1	0.0	1	0.24	-0.25	-0.1	-0.2	0.2	-0.2	0.56	-0.1	-0.2	-0.22	0.1
S	0.42	0.2	-0.37	-0.28	0.40	0.26	0.35	0.41	0.1	-0.31	0.24	1	-0.2	-0.1	0.24	0.30	0.30	0.55	0.41	-0.2	-0.1	0.39
As	-0.42	-0.52	0.2	0.68	-0.22	-0.2	-0.25	-0.33	-0.43	0.45	-0.25	-0.2	1	-0.2	-0.2	0.0	0.0	-0.25	-0.2	0.62	-0.23	-0.34
Au	0.2	0.25	0.0	-0.26	0.0	-0.1	0.0	0.1	0.1	0.1	-0.1	-0.1	-0.2	1	0.0	0.0	0.0	0.1	0.0	-0.1	0.2	0.0
Ba	0.0	0.2	-0.2	-0.27	0.92	0.1	0.38	0.0	0.34	-0.25	-0.2	0.24	-0.2	0.0	1	-0.23	0.84	-0.1	0.90	-0.34	0.33	0.76
Br	-0.1	0.0	0.1	0.1	-0.2	-0.2	-0.24	0.1	-0.28	0.0	0.2	0.30	0.0	0.0	-0.23	1	-0.1	0.33	-0.1	0.40	-0.2	-0.1
Ce	-0.1	0.0	-0.1	-0.1	0.87	0.0	0.33	0.0	0.0	-0.2	-0.2	0.30	0.0	0.0	0.84	-0.1	1	0.0	0.88	-0.1	0.1	0.75
Cl	0.70	0.37	-0.2	-0.40	0.0	0.1	0.0	0.74	0.0	0.1	0.56	0.55	-0.25	0.1	-0.1	0.33	0.0	1	0.0	-0.24	-0.2	0.2
Co	0.0	0.2	-0.30	-0.25	0.99	0.1	0.42	0.0	0.2	-0.26	-0.1	0.41	-0.2	0.0	0.90	-0.1	0.88	0.0	1	-0.25	0.2	0.85
Cr	-0.57	-0.65	0.40	0.75	-0.31	-0.26	-0.34	-0.26	-0.67	0.1	-0.2	-0.2	0.62	-0.1	-0.34	0.40	-0.1	-0.24	-0.25	1	-0.34	-0.36
Cs	-0.2	0.1	0.1	-0.2	0.2	-0.2	0.0	-0.1	0.74	-0.1	-0.22	-0.1	-0.23	0.2	0.33	-0.2	0.1	-0.2	0.2	-0.34	1	0.24
Cu	0.1	0.32	-0.34	-0.26	0.84	0.0	0.25	0.1	0.22	-0.30	0.1	0.39	-0.34	0.0	0.76	-0.1	0.75	0.2	0.85	-0.36	0.24	1
Eu	0.2	0.32	-0.35	-0.25	0.78	0.0	0.2	0.2	0.1	-0.1	0.1	0.48	-0.1	0.1	0.69	0.0	0.77	0.33	0.80	-0.22	0.1	0.83
Ga	-0.41	-0.60	0.92	0.51	-0.37	-0.55	-0.41	-0.25	-0.25	0.43	-0.25	-0.42	0.29	0.0	-0.22	0.1	-0.1	-0.2	-0.36	0.43	0.1	-0.40
Ge	0.0	-0.1	0.27	0.2	-0.1	-0.32	-0.1	0.0	-0.28	0.2	-0.2	0.2	0.2	-0.1	-0.1	0.2	0.0	0.2	0.0	0.2	-0.28	0.0
Hf	-0.1	-0.30	0.55	0.30	-0.28	-0.39	-0.34	-0.2	-0.23	0.78	-0.26	-0.37	0.60	0.1	-0.2	-0.1	-0.1	0.0	-0.27	0.27	0.0	-0.38
La	0.1	0.1	-0.2	-0.2	0.74	0.2	0.26	0.22	0.2	-0.1	0.0	0.31	0.0	0.1	0.76	-0.2	0.86	0.2	0.76	-0.2	0.2	0.63
Lu	0.37	0.2	0.0	-0.2	0.22	-0.2	0.0	0.29	-0.2	0.52	0.22	0.31	0.2	0.27	0.1	0.1	0.30	0.59	0.25	-0.1	-0.1	0.28
Nb	-0.1	-0.2	0.39	0.1	-0.2	-0.31	-0.2	-0.30	-0.1	0.64	-0.22	-0.40	0.37	0.1	-0.1	-0.23	-0.1	-0.2	-0.2	0.0	0.1	-0.32
Ni	0.47	0.49	-0.61	-0.40	0.40	0.33	0.1	0.56	0.2	-0.33	0.47	0.48	-0.28	0.1	0.25	0.0	0.31	0.44	0.44	-0.25	0.0	0.49
Pb	-0.1	0.30	-0.29	-0.2	0.2	0.0	0.1	-0.2	0.33	-0.31	-0.29	0.0	-0.2	0.30	0.2	-0.29	0.2	-0.26	0.1	-0.24	0.2	0.24
Rb	0.1	0.41	-0.1	-0.43	0.2	0.0	0.0	0.1	0.98	-0.22	-0.2	0.0	-0.39	0.1	0.32	-0.26	0.0	0.0	0.1	-0.62	0.80	0.2
Sb	-0.26	-0.23	0.25	0.41	-0.28	-0.35	-0.36	-0.2	-0.53	0.55	0.1	-0.55	0.46	0.2	-0.31	0.0	-0.1	-0.1	-0.25	0.46	-0.2	-0.2
Sc	-0.47	-0.41	0.47	0.47	-0.1	-0.41	-0.27	-0.24	-0.1	0.1	-0.35	-0.28	0.2	0.0	-0.1	0.0	0.0	-0.22	-0.1	0.33	0.30	0.1
Sm	0.36	0.39	-0.40	-0.39	0.78	0.1	0.27	0.34	0.2	-0.1	0.2	0.55	-0.2	0.1	0.69	-0.1	0.77	0.43	0.81	-0.34	0.1	0.80
Sr	0.41	0.1	-0.28	-0.48	0.48	0.60	0.66	0.38	0.46	-0.26	0.1	0.34	-0.32	0.0	0.58	-0.28	0.45	0.24	0.46	-0.51	0.27	0.35
Th	-0.32	-0.46	0.61	0.29	-0.2	-0.2	-0.2	-0.2	0.1	0.2	-0.27	-0.36	0.27	0.0	0.1	-0.1	0.1	-0.2	-0.2	0.2	0.27	-0.32
V	-0.64	-0.74	0.38	0.96	-0.23	-0.39	-0.36	-0.37	-0.48	0.2	-0.1	-0.29	0.67	-0.2	-0.2	0.1	0.0	-0.34	-0.2	0.71	-0.1	-0.2
W	-0.1	0.2	0.0	0.0	0.0	-0.23	-0.1	-0.2	0.36	0.1	-0.36	-0.1	0.0	0.1	0.0	-0.28	-0.1	-0.2	-0.1	-0.35	0.30	0.1
Y	0.45	0.32	-0.1	-0.29	0.39	-0.1	0.0	0.35	0.0	0.47	0.23	0.26	0.0	0.36	0.32	-0.1	0.44	0.52	0.39	-0.23	0.0	0.44
Yb	0.23	0.2	0.0	-0.1	0.43	-0.27	0.0	0.2	-0.2	0.49	0.1	0.25	0.1	0.0	0.35	0.1	0.46	0.45	0.45	0.0	0.0	0.46
Zn	0.68	0.60	-0.55	-0.51	0.28	0.25	0.1	0.61	0.2	-0.2	0.56	0.48	-0.34	0.1	0.1	0.0	0.2	0.61	0.32	-0.36	-0.1	0.40
Zr	0.0	-0.2	0.65	0.1	-0.24	-0.42	-0.29	-0.1	-0.1	0.86	-0.2	-0.36	0.41	0.1	-0.1	-0.1	-0.1	0.0	-0.25	0.1	0.1	-0.34

Name	Eu	Ga	Ge	Hf	La	Lu	Nb	Ni	Pb	Rb	Sb	Sc	Sm	Sr	Th	V	W	Y	Yb	Zn	Zr
Depth	0.2	-0.41	0.0	-0.1	0.1	0.37	-0.1	<b>0.47</b>	-0.1	0.1	-0.26	<b>-0.47</b>	0.36	0.41	-0.32	<b>-0.64</b>	-0.1	<b>0.45</b>	0.23	<b>0.68</b>	0.0
SiO <sub>2</sub>	0.32	<b>-0.60</b>	-0.1	<b>-0.30</b>	0.1	0.2	-0.2	<b>0.49</b>	0.30	0.41	-0.23	<b>-0.41</b>	0.39	0.1	<b>-0.46</b>	<b>-0.74</b>	0.2	0.32	0.2	<b>0.60</b>	-0.2
Al <sub>2</sub> O <sub>3</sub>	-0.35	<b>0.92</b>	0.27	<b>0.55</b>	-0.2	0.0	0.39	<b>-0.61</b>	-0.29	-0.1	0.25	<b>0.47</b>	<b>-0.40</b>	-0.28	<b>0.61</b>	0.38	0.0	-0.1	0.0	<b>-0.55</b>	<b>0.65</b>
Fe <sub>2</sub> O <sub>3</sub>	-0.25	<b>0.51</b>	0.2	<b>0.30</b>	-0.2	-0.2	0.1	<b>-0.40</b>	-0.2	<b>-0.43</b>	0.41	<b>0.47</b>	<b>-0.39</b>	<b>-0.48</b>	0.29	<b>0.96</b>	0.0	-0.29	-0.1	<b>-0.51</b>	0.1
MnO	<b>0.78</b>	<b>-0.37</b>	-0.1	<b>-0.28</b>	<b>0.74</b>	0.22	-0.2	<b>0.40</b>	0.2	0.2	-0.28	-0.1	<b>0.78</b>	<b>0.48</b>	0.29	<b>0.96</b>	0.0	0.39	<b>0.43</b>	0.28	-0.24
MgO	0.0	<b>-0.55</b>	-0.32	<b>-0.39</b>	0.2	-0.2	<b>-0.31</b>	0.33	0.0	0.0	-0.35	<b>-0.41</b>	0.1	<b>0.60</b>	-0.2	<b>-0.23</b>	0.0	0.39	<b>0.43</b>	0.28	-0.24
CaO	0.2	<b>-0.41</b>	-0.1	<b>-0.34</b>	0.26	0.0	-0.2	0.1	0.1	0.0	<b>-0.36</b>	<b>-0.27</b>	0.27	<b>0.66</b>	-0.2	<b>-0.36</b>	-0.1	0.0	0.0	0.1	-0.29
Na <sub>2</sub> O	0.2	-0.25	0.0	-0.2	0.22	0.29	-0.30	<b>0.56</b>	-0.2	0.1	-0.2	-0.24	0.34	0.38	-0.2	<b>-0.37</b>	-0.2	0.35	0.2	<b>0.61</b>	-0.1
K <sub>2</sub> O	0.1	-0.25	-0.28	-0.23	0.2	-0.2	-0.1	0.2	0.33	<b>0.98</b>	<b>-0.53</b>	-0.1	0.2	<b>0.46</b>	0.1	<b>-0.48</b>	0.36	0.0	-0.2	0.2	-0.1
TiO <sub>2</sub>	-0.1	<b>0.43</b>	0.2	<b>0.78</b>	-0.1	<b>0.52</b>	<b>0.64</b>	<b>-0.33</b>	<b>-0.31</b>	-0.22	<b>0.55</b>	0.1	-0.1	-0.26	0.2	0.2	0.1	<b>0.47</b>	<b>0.49</b>	-0.2	<b>0.86</b>
P <sub>2</sub> O <sub>5</sub>	0.1	-0.25	-0.2	-0.26	0.0	0.22	-0.22	<b>0.47</b>	-0.29	-0.2	0.1	<b>-0.35</b>	0.2	0.1	-0.27	-0.1	<b>-0.36</b>	0.23	0.1	<b>0.56</b>	-0.2
S	<b>0.48</b>	<b>-0.42</b>	0.2	<b>-0.37</b>	0.31	0.31	<b>-0.40</b>	<b>0.48</b>	0.0	0.0	<b>-0.55</b>	<b>-0.28</b>	<b>0.55</b>	0.34	<b>-0.36</b>	<b>-0.29</b>	-0.1	0.26	0.25	<b>0.48</b>	<b>-0.36</b>
As	-0.1	0.29	0.2	<b>0.60</b>	0.0	0.2	0.37	-0.28	-0.2	<b>-0.39</b>	<b>0.46</b>	0.2	-0.2	<b>-0.32</b>	0.27	<b>0.67</b>	0.0	0.0	0.1	<b>-0.34</b>	0.41
Au	0.1	0.0	-0.1	0.1	0.1	0.27	0.1	0.1	0.30	0.1	0.2	0.0	0.1	0.0	0.0	-0.2	0.1	0.36	0.0	0.1	0.1
Ba	<b>0.69</b>	-0.22	-0.1	-0.2	<b>0.76</b>	0.1	-0.1	0.25	0.2	0.32	<b>-0.31</b>	-0.1	<b>0.69</b>	<b>0.58</b>	0.1	-0.2	0.0	0.32	0.35	0.1	-0.1
Br	0.0	0.1	0.2	-0.1	-0.2	0.1	-0.23	0.0	-0.29	-0.26	0.0	0.0	-0.1	-0.28	-0.1	0.1	-0.28	-0.1	0.1	0.0	-0.1
Ce	<b>0.77</b>	-0.1	0.0	-0.1	<b>0.86</b>	0.30	-0.1	0.31	0.2	0.0	-0.1	0.0	<b>0.77</b>	<b>0.45</b>	0.1	0.0	-0.1	<b>0.44</b>	<b>0.46</b>	0.2	-0.1
Cl	0.33	-0.2	0.2	0.0	0.2	<b>0.59</b>	-0.2	<b>0.44</b>	-0.26	0.0	-0.1	-0.22	<b>0.43</b>	0.24	-0.2	<b>-0.34</b>	-0.2	<b>0.52</b>	<b>0.45</b>	<b>0.61</b>	0.0
Co	<b>0.80</b>	<b>-0.36</b>	0.0	-0.27	<b>0.76</b>	0.25	-0.2	<b>0.44</b>	0.1	0.1	-0.25	-0.1	<b>0.81</b>	<b>0.46</b>	-0.2	-0.2	-0.1	0.39	<b>0.45</b>	0.32	-0.25
Cr	-0.22	<b>0.43</b>	0.2	0.27	-0.2	-0.1	0.0	-0.25	-0.24	<b>-0.62</b>	<b>0.46</b>	0.33	<b>-0.34</b>	<b>-0.51</b>	0.2	<b>0.71</b>	<b>-0.35</b>	-0.23	0.0	<b>-0.36</b>	0.1
Cs	0.1	0.1	-0.28	0.0	0.2	-0.1	0.1	0.0	0.2	<b>0.80</b>	-0.2	0.30	0.1	0.27	0.27	-0.1	0.30	0.0	0.0	-0.1	0.1
Cu	<b>0.83</b>	<b>-0.40</b>	0.0	<b>-0.38</b>	<b>0.63</b>	0.28	<b>-0.32</b>	<b>0.49</b>	0.24	0.2	-0.2	0.1	<b>0.80</b>	0.35	<b>-0.32</b>	-0.2	0.1	<b>0.44</b>	<b>0.46</b>	0.40	<b>-0.34</b>
Eu	1	<b>-0.38</b>	0.0	-0.1	<b>0.77</b>	<b>0.58</b>	-0.2	<b>0.59</b>	0.2	0.0	-0.1	-0.1	<b>0.94</b>	0.36	-0.2	-0.2	0.1	<b>0.68</b>	<b>0.64</b>	<b>0.54</b>	-0.1
Ga	-0.38	1	0.23	<b>0.57</b>	-0.2	0.0	<b>0.43</b>	<b>-0.61</b>	<b>-0.31</b>	-0.1	0.36	0.38	<b>-0.42</b>	<b>-0.27</b>	<b>0.69</b>	<b>0.54</b>	0.0	-0.1	-0.1	<b>-0.55</b>	<b>0.63</b>
Ge	0.0	0.23	1	0.2	-0.1	0.27	0.2	-0.26	-0.2	-0.28	-0.1	0.1	0.0	-0.2	0.0	0.2	0.1	0.1	0.28	-0.1	0.1
Hf	-0.1	<b>0.57</b>	0.2	1	-0.1	0.34	<b>0.62</b>	<b>-0.38</b>	-0.23	-0.2	0.40	0.1	-0.2	-0.2	<b>0.52</b>	0.34	0.1	0.25	0.29	-0.24	<b>0.84</b>
La	<b>0.77</b>	-0.2	-0.1	-0.1	1	0.39	-0.1	<b>0.44</b>	0.1	0.1	-0.1	-0.1	<b>0.85</b>	<b>0.62</b>	0.2	-0.1	-0.2	<b>0.57</b>	<b>0.47</b>	0.33	0.0
Lu	<b>0.58</b>	0.0	0.27	0.34	0.39	1	0.1	0.26	-0.2	-0.25	0.22	-0.1	<b>0.59</b>	0.1	-0.1	0.0	0.0	<b>0.86</b>	<b>0.75</b>	0.34	<b>0.42</b>
Nb	-0.2	<b>0.43</b>	0.2	<b>0.62</b>	-0.1	0.1	1	<b>-0.40</b>	-0.26	0.0	0.37	0.0	-0.2	-0.1	0.38	0.2	0.2	0.1	0.1	-0.26	<b>0.66</b>
Ni	<b>0.59</b>	<b>-0.61</b>	-0.26	<b>-0.38</b>	<b>0.44</b>	0.26	<b>-0.40</b>	1	0.1	0.1	-0.2	<b>-0.32</b>	<b>0.65</b>	0.27	<b>-0.39</b>	<b>-0.35</b>	-0.2	0.35	0.2	<b>0.92</b>	<b>-0.42</b>
Pb	0.2	<b>-0.31</b>	-0.2	-0.23	0.1	-0.2	-0.26	0.1	1	0.32	-0.2	0.0	0.1	0.1	-0.1	-0.2	0.32	-0.1	-0.1	0.0	-0.24
Rb	0.0	-0.1	-0.28	-0.2	0.1	-0.25	0.0	0.1	0.32	1	<b>-0.46</b>	0.0	0.1	0.42	0.2	<b>-0.42</b>	0.36	-0.1	-0.2	0.1	0.0
Sb	-0.1	0.36	-0.1	0.40	-0.1	0.22	0.37	-0.2	-0.2	<b>-0.46</b>	1	0.27	-0.2	<b>-0.44</b>	0.1	<b>0.52</b>	-0.1	0.22	0.23	-0.23	0.37
Sc	-0.1	0.38	0.1	0.1	-0.1	-0.1	0.0	<b>-0.32</b>	0.0	0.0	0.27	1	-0.22	-0.29	0.0	<b>0.50</b>	0.28	0.0	0.0	<b>-0.42</b>	0.1
Sm	<b>0.94</b>	<b>-0.42</b>	0.0	-0.2	<b>0.85</b>	<b>0.59</b>	-0.2	<b>0.65</b>	0.1	0.1	-0.2	-0.22	1	<b>0.50</b>	-0.2	-0.30	0.0	<b>0.72</b>	<b>0.62</b>	<b>0.62</b>	-0.1
Sr	0.36	-0.27	-0.2	-0.2	<b>0.62</b>	0.1	-0.1	0.27	0.1	0.42	<b>-0.44</b>	-0.29	<b>0.50</b>	1	0.24	<b>-0.45</b>	-0.1	0.22	0.1	0.27	0.0
Th	-0.2	<b>0.69</b>	0.0	<b>0.52</b>	0.2	-0.1	0.38	-0.39	-0.1	0.2	0.1	0.0	-0.2	0.24	1	0.27	-0.2	-0.1	-0.2	<b>-0.37</b>	<b>0.63</b>
V	-0.2	<b>0.54</b>	0.2	0.34	-0.1	0.0	0.2	<b>-0.35</b>	-0.2	<b>-0.42</b>	<b>0.52</b>	<b>0.50</b>	-0.30	<b>-0.45</b>	0.27	1	0.0	-0.1	0.0	<b>-0.49</b>	0.2
W	0.1	0.0	0.1	0.1	-0.2	0.0	0.2	-0.2	0.32	0.36	-0.1	0.28	0.0	-0.1	-0.2	0.0	1	0.1	0.0	-0.1	0.0
Y	<b>0.68</b>	-0.1	0.1	0.25	<b>0.57</b>	<b>0.86</b>	0.1	0.35	-0.1	-0.1	0.22	0.0	<b>0.72</b>	0.22	-0.1	-0.1	0.1	1	<b>0.79</b>	0.41	0.33
Yb	<b>0.64</b>	-0.1	0.28	0.29	<b>0.47</b>	<b>0.75</b>	0.1	0.2	-0.1	-0.2	0.23	0.0	<b>0.62</b>	0.1	-0.2	0.0	0.0	<b>0.79</b>	1	0.28	0.31
Zn	<b>0.54</b>	<b>-0.55</b>	-0.1	-0.24	0.33	0.34	-0.26	<b>0.92</b>	0.0	0.1	-0.23	<b>-0.42</b>	<b>0.62</b>	0.27	<b>-0.37</b>	<b>-0.49</b>	-0.1	0.41	0.28	1	-0.28
Zr	-0.1	<b>0.63</b>	0.1	<b>0.84</b>	0.0	<b>0.42</b>	<b>0.66</b>	<b>-0.42</b>	-0.24	0.0	0.37	0.1	-0.1	0.0	<b>0.63</b>	0.2	0.0	0.33	0.31	-0.28	1

**Appendix 4D: Correlation Coefficients for Data Set 4: MC500, Mn-rich Samples.**

Number of samples=7                      0.669   0.833   0.951  
 Degrees of Freedom=5                      95%   99%   99.9%

	Minimum	Maximum	Median	Mean	Std Dev
Depth	22	32	27	26	4
SiO <sub>2</sub>	47	69	66	62	8
Al <sub>2</sub> O <sub>3</sub>	6.9	11.1	9.6	9.5	1.6
Fe <sub>2</sub> O <sub>3</sub>	10.9	19.6	13.7	13.9	2.7
MnO	0.1	3.6	0.9	1.1	1.2
MgO	0.5	4.0	1.6	1.8	1.2
CaO	0.0	5.1	0.2	1.0	1.8
Na <sub>2</sub> O	0.26	0.51	0.38	0.37	0.09
K <sub>2</sub> O	0.56	1.11	0.71	0.76	0.20
TiO <sub>2</sub>	0.48	0.79	0.62	0.62	0.10
P <sub>2</sub> O <sub>5</sub>	0.003	0.028	0.014	0.015	0.010
S	0.13	0.48	0.25	0.29	0.12
As	6.4	12.8	9.0	9.1	2.3
Au	0.125	4.640	0.46	1.46	1.77
Ba	148	1576	258	482	521
Br	7	15	10	10	3
Ce	15	132	28	45	40
Cl	790	3720	1740	1986	974
Co	57	3020	643	883	1004
Cr	1770	3410	2160	2401	557
Cs	0.5	1.7	1.1	1.0	0.5
Cu	149	568	242	266	141
Eu	0.6	3.5	1.6	1.7	0.9
Ga	8.0	16.0	11.0	11.4	2.6
Ge	0.0	2.0	1.0	1.0	0.8
Hf	0.5	1.9	1.1	1.0	0.5
La	3	36	11	14	11
Lu	0.10	0.37	0.10	0.19	0.11
Nb	0.0	3.0	1.0	1.6	1.4
Ni	613	2867	1954	1881	882
Pb	1	35	22	18	14
Rb	12	24	17	17	4
Sb	1.06	1.79	1.42	1.40	0.29
Sc	26	50	46	42	9
Sm	2	13	5	6	4
Sr	11	52	18	22	13
Th	0.25	0.87	0.25	0.34	0.23
V	184	398	232	261	71
W	3	13	8	9	3
Y	14	37	18	22	8
Yb	0.6	2.2	0.8	1.0	0.6
Zn	20	230	135	124	74
Zr	28	56	36	37	9

Oxides and S in %, all other elements in mg/kg

Name	Depth	SiO2	Al2O3	Fe2O3	MnO	MgO	CaO	Na2O	K2O	TiO2	P2O5	S	As	Au	Ba	Br	Ce	Cl	Co	Cr	Cs	Cu
Depth	1	-0.2	-0.2	0.5	-0.2	0.5	-0.1	0.3	0.4	0.4	0.81	0.2	0.4	0.3	-0.3	0.7	-0.1	0.5	-0.2	0.6	0.0	-0.2
SiO2	-0.2	1	-0.6	-0.3	-0.67	-0.88	-0.77	-0.5	-0.1	-0.5	-0.1	-0.69	0.2	-0.2	-0.7	-0.3	-0.74	-0.5	-0.67	-0.3	-0.6	-0.7
Al2O3	-0.2	-0.6	1	0.6	0.0	0.2	0.2	0.5	0.5	0.6	-0.3	0.0	0.0	0.6	0.2	0.0	0.1	0.3	0.0	0.4	0.70	0.0
Fe2O3	0.5	-0.3	0.6	1	-0.4	0.1	-0.3	0.74	0.85	0.86	0.5	0.0	0.6	0.82	-0.4	0.6	-0.4	0.72	-0.4	0.91	0.6	-0.4
MnO	-0.2	-0.67	0.0	-0.4	1	0.72	0.93	0.0	-0.6	-0.2	-0.2	0.73	-0.5	-0.6	0.94	0.0	0.97	0.1	1.00	-0.4	0.1	1.00
MgO	0.5	-0.88	0.2	0.1	0.72	1	0.81	0.3	-0.1	0.3	0.3	0.78	-0.2	0.0	0.6	0.4	0.81	0.4	0.72	0.1	0.3	0.71
CaO	-0.1	-0.77	0.2	-0.3	0.93	0.81	1	0.0	-0.5	-0.1	-0.3	0.69	-0.6	-0.4	0.90	-0.1	0.98	0.0	0.93	-0.4	0.2	0.94
Na2O	0.3	-0.5	0.5	0.74	0.0	0.3	0.0	1	0.76	0.90	0.6	0.5	0.7	0.6	-0.1	0.77	0.0	0.89	0.1	0.7	0.84	0.0
K2O	0.4	-0.1	0.5	0.85	-0.6	-0.1	-0.5	0.76	1	0.86	0.5	0.0	0.70	0.93	-0.6	0.6	-0.5	0.6	-0.6	0.77	0.70	-0.6
TiO2	0.4	-0.5	0.6	0.86	-0.2	0.3	-0.1	0.90	0.86	1	0.6	0.4	0.70	0.75	-0.3	0.77	-0.2	0.71	-0.2	0.87	0.77	-0.2
P2O5	0.81	-0.1	-0.3	0.5	-0.2	0.3	-0.3	0.6	0.5	0.6	1	0.4	0.78	0.2	-0.4	0.93	-0.2	0.6	-0.1	0.69	0.1	-0.2
S	0.2	-0.69	0.0	0.0	0.73	0.78	0.69	0.5	0.0	0.4	0.4	1	0.2	-0.2	0.5	0.6	0.73	0.5	0.77	0.0	0.5	0.72
As	0.4	0.2	0.0	0.6	-0.5	-0.2	-0.6	0.7	0.70	0.70	0.78	0.2	1	0.4	-0.6	0.82	-0.5	0.5	-0.4	0.73	0.3	-0.5
Au	0.3	-0.2	0.6	0.82	-0.6	0.0	-0.4	0.6	0.93	0.75	0.2	-0.2	0.4	1	-0.5	0.3	-0.5	0.5	-0.6	0.7	0.71	-0.6
Ba	-0.3	-0.7	0.2	-0.4	0.94	0.6	0.90	-0.1	-0.6	-0.3	-0.4	0.5	-0.6	-0.5	1	-0.3	0.92	0.0	0.92	-0.5	0.0	0.94
Br	0.7	-0.3	0.0	0.6	0.0	0.4	-0.1	0.77	0.6	0.77	0.93	0.6	0.82	0.3	-0.3	1	0.0	0.69	0.0	0.75	0.4	0.0
Ce	-0.1	-0.74	0.1	-0.4	0.97	0.81	0.98	0.0	-0.5	-0.2	-0.2	0.73	-0.5	-0.5	0.92	0.0	1	0.1	0.96	-0.4	0.1	0.97
Cl	0.5	-0.5	0.3	0.72	0.1	0.4	0.0	0.89	0.6	0.71	0.6	0.5	0.5	0.5	0.0	0.69	0.1	1	0.1	0.6	0.6	0.1
Co	-0.2	-0.67	0.0	-0.4	1.00	0.72	0.93	0.1	-0.6	-0.2	-0.1	0.77	-0.4	-0.6	0.92	0.0	0.96	0.1	1	-0.4	0.1	1.00
Cr	0.6	-0.3	0.4	0.91	-0.4	0.1	-0.4	0.7	0.77	0.87	0.69	0.0	0.73	0.7	-0.5	0.75	-0.4	0.6	-0.4	1	0.4	-0.4
Cs	0.0	-0.6	0.70	0.6	0.1	0.3	0.2	0.84	0.70	0.77	0.1	0.5	0.3	0.71	0.0	0.4	0.1	0.6	0.1	0.4	1	0.0
Cu	-0.2	-0.7	0.0	-0.4	1.00	0.71	0.94	0.0	-0.6	-0.2	-0.2	0.72	-0.5	-0.6	0.94	0.0	0.97	0.1	1.00	-0.4	0.0	1
Eu	0.0	-0.70	0.0	-0.2	0.93	0.73	0.80	0.3	-0.4	0.0	0.1	0.81	-0.2	-0.5	0.83	0.3	0.87	0.4	0.94	-0.2	0.1	0.92
Ga	0.3	-0.4	0.72	0.87	-0.3	0.2	-0.1	0.77	0.89	0.96	0.4	0.2	0.6	0.87	-0.3	0.6	-0.2	0.6	-0.3	0.84	0.78	-0.3
Ge	-0.76	-0.2	0.3	-0.3	0.6	0.0	0.4	-0.2	-0.5	-0.3	-0.6	0.1	-0.3	-0.5	0.70	-0.4	0.4	-0.2	0.6	-0.4	-0.1	0.6
Hf	0.2	-0.1	0.5	0.86	-0.5	-0.2	-0.5	0.72	0.84	0.68	0.4	-0.2	0.6	0.77	-0.4	0.4	-0.5	0.73	-0.5	0.6	0.6	-0.5
La	0.0	-0.80	0.1	-0.2	0.96	0.83	0.89	0.3	-0.4	0.1	0.1	0.85	-0.2	-0.4	0.86	0.2	0.94	0.4	0.96	-0.2	0.2	0.95
Lu	0.3	-0.91	0.4	0.3	0.67	0.85	0.7	0.71	0.2	0.6	0.4	0.86	0.1	0.1	0.6	0.6	0.69	0.75	0.69	0.3	0.6	0.6
Nb	0.2	-0.1	0.1	0.6	0.0	0.0	-0.3	0.5	0.3	0.4	0.6	0.0	0.6	0.1	-0.1	0.5	-0.2	0.7	0.0	0.6	0.1	-0.1
Ni	0.77	-0.5	-0.2	0.3	0.3	0.69	0.2	0.6	0.2	0.5	0.86	0.71	0.5	0.0	0.1	0.86	0.3	0.70	0.3	0.5	0.2	0.3
Pb	-0.3	0.6	0.1	-0.1	-0.69	-0.67	-0.5	-0.6	0.1	-0.3	-0.5	-0.81	-0.2	0.2	-0.5	-0.6	-0.6	-0.73	-0.70	-0.1	-0.3	-0.6
Rb	0.2	0.0	0.5	0.82	-0.70	-0.3	-0.6	0.7	0.98	0.80	0.4	-0.2	0.69	0.91	-0.69	0.4	-0.7	0.4	-0.67	0.74	0.6	-0.71
Sb	0.76	0.4	-0.6	0.0	-0.5	0.0	-0.4	-0.2	0.1	0.0	0.5	-0.2	0.2	0.1	-0.6	0.3	-0.4	-0.2	-0.4	0.3	-0.4	-0.4
Sc	-0.5	-0.4	0.93	0.4	0.0	-0.1	0.1	0.3	0.3	0.4	-0.4	-0.1	-0.1	0.4	0.3	-0.2	0.0	0.2	0.0	0.2	0.5	0.1
Sm	0.1	-0.73	0.0	-0.2	0.94	0.81	0.84	0.3	-0.4	0.1	0.2	0.88	-0.1	-0.5	0.80	0.3	0.90	0.4	0.95	-0.1	0.2	0.93
Sr	-0.1	-0.79	0.2	-0.3	0.97	0.81	0.97	0.0	-0.5	-0.1	-0.2	0.69	-0.5	-0.4	0.95	0.0	0.98	0.1	0.96	-0.3	0.1	0.97
Th	0.68	-0.4	0.4	0.92	-0.3	0.3	-0.2	0.68	0.76	0.76	0.6	0.1	0.4	0.79	-0.3	0.6	-0.2	0.79	-0.3	0.80	0.5	-0.3
V	0.4	-0.78	0.74	0.82	0.1	0.6	0.2	0.80	0.7	0.85	0.3	0.4	0.3	0.71	0.1	0.5	0.2	0.78	0.1	0.70	0.79	0.1
W	-0.1	0.6	0.0	0.2	-0.72	-0.68	-0.68	-0.4	0.1	-0.1	-0.1	-0.87	0.1	0.1	-0.6	-0.3	-0.75	-0.5	-0.73	0.3	-0.5	-0.68
Y	0.2	-0.93	0.4	0.2	0.78	0.86	0.78	0.6	0.0	0.4	0.1	0.80	-0.1	0.0	0.73	0.4	0.80	0.7	0.78	0.1	0.6	0.75
Yb	-0.2	-0.73	0.2	-0.3	0.97	0.68	0.89	0.2	-0.5	0.0	-0.2	0.74	-0.3	-0.5	0.94	0.1	0.92	0.2	0.98	-0.3	0.2	0.97
Zn	0.74	-0.2	-0.4	0.2	0.2	0.5	0.1	0.5	0.1	0.4	0.89	0.7	0.5	-0.1	-0.1	0.84	0.2	0.5	0.3	0.4	0.1	0.2
Zr	0.6	-0.5	0.6	0.94	-0.3	0.3	-0.1	0.79	0.84	0.94	0.6	0.2	0.6	0.82	-0.3	0.70	-0.2	0.72	-0.2	0.92	0.7	-0.3

Name	Eu	Ga	Ge	Hf	La	Lu	Nb	Ni	Pb	Rb	Sb	Sc	Sm	Sr	Th	V	W	Y	Yb	Zn	Zr
Depth	0.0	0.3	-0.76	0.2	0.0	0.3	0.2	0.77	-0.3	0.2	0.76	-0.5	0.1	-0.1	0.68	0.4	-0.1	0.2	-0.2	0.74	0.6
SiO <sub>2</sub>	-0.70	-0.4	-0.2	-0.1	-0.80	-0.91	-0.1	-0.5	0.6	0.0	0.4	-0.4	-0.73	-0.79	-0.4	-0.78	0.6	-0.93	-0.73	-0.2	-0.5
Al <sub>2</sub> O <sub>3</sub>	0.0	0.72	0.3	0.5	0.1	0.4	0.1	-0.2	0.1	0.5	-0.6	0.93	0.0	0.2	0.4	0.74	0.0	0.4	0.2	-0.4	0.6
Fe <sub>2</sub> O <sub>3</sub>	-0.2	0.87	-0.3	0.86	-0.2	0.3	0.6	0.3	-0.1	0.82	0.0	0.4	-0.2	-0.3	0.92	0.82	0.2	0.2	-0.3	0.2	0.94
MnO	0.93	-0.3	0.6	-0.5	0.96	0.67	0.0	0.3	-0.69	-0.70	-0.5	0.0	0.94	0.97	-0.3	0.1	-0.72	0.78	0.97	0.2	-0.3
MgO	0.73	0.2	0.0	-0.2	0.83	0.85	0.0	0.69	-0.67	-0.3	0.0	-0.1	0.81	0.81	0.3	0.6	-0.68	0.86	0.68	0.5	0.3
CaO	0.80	-0.1	0.4	-0.5	0.89	0.7	-0.3	0.2	-0.5	-0.6	-0.4	0.1	0.84	0.97	-0.2	0.2	-0.68	0.78	0.89	0.1	-0.1
Na <sub>2</sub> O	0.3	0.77	-0.2	0.72	0.3	0.71	0.5	0.6	-0.6	0.7	-0.2	0.3	0.3	0.0	0.68	0.80	-0.4	0.6	0.2	0.5	0.79
K <sub>2</sub> O	-0.4	0.89	-0.5	0.84	-0.4	0.2	0.3	0.2	0.1	0.98	0.1	0.3	-0.4	-0.5	0.76	0.7	0.1	0.0	-0.5	0.1	0.84
TiO <sub>2</sub>	0.0	0.96	-0.3	0.68	0.1	0.6	0.4	0.5	-0.3	0.80	0.0	0.4	0.1	-0.1	0.76	0.85	-0.1	0.4	0.0	0.4	0.94
P <sub>2</sub> O <sub>5</sub>	0.1	0.4	-0.6	0.4	0.1	0.4	0.6	0.86	-0.5	0.4	0.5	-0.4	0.2	-0.2	0.6	0.3	-0.1	0.1	-0.2	0.89	0.6
S	0.81	0.2	0.1	-0.2	0.85	0.86	0.0	0.71	-0.81	-0.2	-0.2	-0.1	0.88	0.69	0.1	0.4	-0.87	0.80	0.74	0.7	0.2
As	-0.2	0.6	-0.3	0.6	-0.2	0.1	0.6	0.5	-0.2	0.69	0.2	-0.1	-0.1	-0.5	0.4	0.3	0.1	-0.1	-0.3	0.5	0.6
Au	-0.5	0.87	-0.5	0.77	-0.4	0.1	0.1	0.0	0.2	0.91	0.1	0.4	-0.5	-0.4	0.79	0.71	0.1	0.0	-0.5	-0.1	0.82
Ba	0.83	-0.3	0.70	-0.4	0.86	0.6	-0.1	0.1	-0.5	-0.69	-0.6	0.3	0.80	0.95	-0.3	0.1	-0.6	0.73	0.94	-0.1	-0.3
Br	0.3	0.6	-0.4	0.4	0.2	0.6	0.5	0.86	-0.6	0.4	0.3	-0.2	0.3	0.0	0.6	0.5	-0.3	0.4	0.1	0.84	0.70
Ce	0.87	-0.2	0.4	-0.5	0.94	0.69	-0.2	0.3	-0.6	-0.7	-0.4	0.0	0.90	0.98	-0.2	0.2	-0.75	0.80	0.92	0.2	-0.2
Cl	0.4	0.6	-0.2	0.73	0.4	0.75	0.7	0.70	-0.73	0.4	-0.2	0.2	0.4	0.1	0.79	0.78	-0.5	0.7	0.2	0.5	0.72
Co	0.94	-0.3	0.6	-0.5	0.96	0.69	0.0	0.3	-0.70	-0.67	-0.4	0.0	0.95	0.96	-0.3	0.1	-0.73	0.78	0.98	0.3	-0.2
Cr	-0.2	0.84	-0.4	0.6	-0.2	0.3	0.6	0.5	-0.1	0.74	0.3	0.2	-0.1	-0.3	0.80	0.70	0.3	0.1	-0.3	0.4	0.92
Cs	0.1	0.78	-0.1	0.6	0.2	0.6	0.1	0.2	-0.3	0.6	-0.4	0.5	0.2	0.1	0.5	0.79	-0.5	0.6	0.2	0.1	0.7
Cu	0.92	-0.3	0.6	-0.5	0.95	0.6	-0.1	0.3	-0.6	-0.71	-0.4	0.1	0.93	0.97	-0.3	0.1	-0.68	0.75	0.97	0.2	-0.3
Eu	1	-0.2	0.5	-0.3	0.98	0.81	0.3	0.6	-0.88	-0.5	-0.4	0.0	0.99	0.89	-0.1	0.2	-0.74	0.85	0.95	0.5	-0.1
Ga	-0.2	1	-0.3	0.7	-0.1	0.4	0.2	0.3	0.0	0.85	0.0	0.5	-0.1	-0.2	0.77	0.85	0.0	0.3	-0.2	0.1	0.94
Ge	0.5	-0.3	1	-0.3	0.4	0.1	0.1	-0.4	-0.1	-0.5	-0.81	0.5	0.4	0.5	-0.5	-0.2	0.0	0.3	0.7	-0.4	-0.4
Hf	-0.3	0.7	-0.3	1	-0.3	0.2	0.6	0.1	-0.1	0.83	-0.2	0.4	-0.3	-0.4	0.76	0.6	0.1	0.1	-0.3	0.0	0.70
La	0.98	-0.1	0.4	-0.3	1	0.85	0.1	0.5	-0.83	-0.5	-0.4	0.1	0.99	0.95	0.0	0.3	-0.78	0.91	0.96	0.4	0.0
Lu	0.81	0.4	0.1	0.2	0.85	1	0.3	0.72	-0.86	0.0	-0.3	0.2	0.83	0.71	0.4	0.74	-0.75	0.97	0.74	0.5	0.5
Nb	0.3	0.2	0.1	0.6	0.1	0.3	1	0.4	-0.5	0.3	-0.2	0.2	0.2	-0.1	0.5	0.4	0.1	0.2	0.1	0.4	0.4
Ni	0.6	0.3	-0.4	0.1	0.5	0.72	0.4	1	-0.78	0.0	0.3	-0.4	0.6	0.3	0.5	0.5	-0.5	0.6	0.3	0.96	0.5
Pb	-0.88	0.0	-0.1	-0.1	-0.83	-0.86	-0.5	-0.78	1	0.2	0.3	0.1	-0.87	-0.6	-0.2	-0.4	0.78	-0.83	-0.72	-0.69	-0.2
Rb	-0.5	0.85	-0.5	0.83	-0.5	0.0	0.3	0.0	0.2	1	0.1	0.4	-0.5	-0.6	0.7	0.6	0.3	-0.2	-0.6	0.0	0.77
Sb	-0.4	0.0	-0.81	-0.2	-0.4	-0.3	-0.2	0.3	0.3	0.1	1	-0.74	-0.3	-0.4	0.2	-0.2	0.3	-0.4	-0.6	0.5	0.1
Sc	0.0	0.5	0.5	0.4	0.1	0.2	0.2	-0.4	0.1	0.4	-0.74	1	-0.1	0.1	0.2	0.5	0.2	0.3	0.2	-0.6	0.3
Sm	0.99	-0.1	0.4	-0.3	0.99	0.83	0.2	0.6	-0.87	-0.5	-0.3	-0.1	1	0.90	-0.1	0.3	-0.78	0.86	0.93	0.5	0.0
Sr	0.89	-0.2	0.5	-0.4	0.95	0.71	-0.1	0.3	-0.6	-0.6	-0.4	0.1	0.90	1	-0.1	0.2	-0.7	0.83	0.95	0.2	-0.1
Th	-0.1	0.77	-0.5	0.76	0.0	0.4	0.5	0.5	-0.2	0.7	0.2	0.2	-0.1	-0.1	1	0.85	0.0	0.3	-0.2	0.3	0.92
V	0.2	0.85	-0.2	0.6	0.3	0.74	0.4	0.5	-0.4	0.6	-0.2	0.5	0.3	0.2	0.85	1	-0.3	0.67	0.2	0.2	0.90
W	-0.74	0.0	0.0	0.1	-0.78	-0.75	0.1	-0.5	0.78	0.3	0.3	0.2	-0.78	-0.7	0.0	-0.3	1	-0.78	-0.68	-0.5	0.0
Y	0.85	0.3	0.3	0.1	0.91	0.97	0.2	0.6	-0.83	-0.2	-0.4	0.3	0.86	0.83	0.3	0.67	-0.78	1	0.83	0.4	0.3
Yb	0.95	-0.2	0.7	-0.3	0.96	0.74	0.1	0.3	-0.72	-0.6	-0.6	0.2	0.93	0.95	-0.2	0.2	-0.68	0.83	1	0.2	-0.1
Zn	0.5	0.1	-0.4	0.0	0.4	0.5	0.4	0.96	-0.69	0.0	0.5	-0.6	0.5	0.2	0.3	0.2	-0.5	0.4	0.2	1	0.3
Zr	-0.1	0.94	-0.4	0.70	0.0	0.5	0.4	0.5	-0.2	0.77	0.1	0.3	0.0	-0.1	0.92	0.90	0.0	0.3	-0.1	0.3	1

# Appendix 5: Mulgarrie Groundwater Data.

All elements in mg/L (ppm), unless otherwise noted.

Site	Mul1	Mul2	Mul3	Mul4	Mul5	Mul6	Mul7
Easting (m)	nd	10010	10125	10065	10065	10090	10035
Northing (m)	8200	10745	10565	10640	10655	10620	10660
Water Table	18 m	-	29 m	26 m	27 m	27 m	28 m
Hole Bottom	24 m	-	45 m	30 m	31 m	32 m	33 m
Sample Depth	22 m	36 m	40 m	29 m	29 m	-	-
pH	3.47	7.67	7.15	6.38	6.43	6.66	6.71
Eh (mV)	325	286	137	179	177	163	162
Na	13280	13350	11500	11720	11870	11570	11800
Mg	2510	2350	2140	2150	2150	2120	2170
Ca	224	479	522	486	482	497	511
K	147	159	181	169	169	180	160
Cl <sup>-</sup>	25800	24600	21600	22100	22300	21500	22800
SO <sub>4</sub> <sup>2-</sup>	4080	4820	4260	4080	4330	4360	4130
Br <sup>-</sup>	69	74	68	65	67	67	62
HCO <sub>3</sub> <sup>-</sup>	0	441	451	361	319	433	385
TDS	46100	46000	40400	40900	41500	40500	41800
Al	24	0	0	0.24	0	0	0
Si	42	16.8	6.1	12.4	11	11.6	11.5
V	0.032	<0.002	<0.002	<0.002	<0.002	<0.002	<0.002
Cr	0.006	0.061	<0.002	0.047	0.046	0.033	<0.002
Mn	3.4	0.33	20	0.41	1.38	0.15	1.04
Fe	0.14	0	0.055	0.13	0.028	0	0.03
Co	0.38	<0.005	0.26	0.024	0.061	0.008	0.012
Ni	0.27	0.02	0.36	0.12	0.12	0.11	0.13
Cu	0.57	0.03	0.015	0.007	0.003	0.024	0.045
Zn	0.81	0.035	0.04	0.015	0.027	0.05	0.03
As	<0.02	<0.02	<0.02	<0.02	<0.02	<0.02	<0.02
Sr	8.5	8.9	8.1	8.3	8.4	7.9	8.6
Ag	0.003	<0.002	0.002	<0.002	<0.002	0.003	<0.002
Cd	<0.005	0.003	0.001	0.002	0.001	0.002	0.003
Sb	0.0009	<0.0003	<0.0003	<0.0003	<0.0003	<0.0003	<0.0003
I <sup>-</sup>	0.33	0.14	1.45	0.26	0.26	0.14	0.51
Ba	0.052	0.009	0.194	0.021	0.014	0.015	0.065
Hg	<0.002	<0.002	<0.002	<0.002	<0.002	<0.002	<0.002
Pb	0.42	0.004	0.004	0.018	0.006	0.005	0.005
Bi	<0.002	<0.002	<0.002	<0.002	<0.002	<0.002	<0.002
Au (µg/L)	0.028	0.046	0.058	0.019	0.038	0.109	0.01